FATIGUE RELIABILITY ASSESSMENT OF STEEL BRIDGES INSTRUMENTED WITH STRUCTURAL HEALTH MONITORING SYSTEM

Xiao-Wei YE

Ph.D.

THE HONG KONG POLYTECHNIC UNIVERSITY

2010

The Hong Kong Polytechnic University

Department of Civil and Structural Engineering

FATIGUE RELIABILITY ASSESSMENT OF STEEL BRIDGES INSTRUMENTED WITH STRUCTURAL HEALTH MONITORING SYSTEM

Xiao-Wei YE

A thesis submitted in partial fulfilment of the requirements for the degree of

Doctor of Philosophy

July 2010

To my parents

CERTIFICATE OF ORIGINALITY

I hereby declare that this thesis is my own work and that, to the best of my knowledge and belief, it reproduces no material previously published or written, nor material that has been accepted for the award of any other degree or diploma, except where due acknowledgement has been made in the text.

_____ (Signed)

_____ (Name of student)

ABSTRACT

Fatigue is among the most critical forms of damage potentially occurring in steel structures, and therefore it is essential to assess the fatigue damage status as well as the remaining fatigue life of steel bridges. As a paradigm of integrating structural health monitoring (SHM) data into practical structural condition assessment, the continuously measured dynamic strain data from a long-term SHM system are significantly useful in assessing the fatigue life and reliability of steel bridges. The research presented in this dissertation has been devoted to investigating fatigue life assessment and reliability analysis of welded connections of steel bridges using long-term monitoring data from the permanently installed bridge health monitoring system (BHMS).

A monitoring-based stress-life fatigue evaluation method is firstly developed for deterministic fatigue life assessment of steel bridges by use of long-term measured dynamic strain data from an on-line SHM system. The proposed method takes the benefits of resemblance and consistence in daily stress spectra obtained under normal traffic (highway and railway) and wind conditions, and accounts for predominant factors which affects the prediction of fatigue life, such as the diversity of daily strain data subjected to diurnal and seasonal traffic variations and the typhoon effect. With the continuously measured dynamic strain data from the instrumented Tsing Ma

Bridge (TMB), the proposed method is exemplified to evaluate the fatigue life of the failure-critical welded details of the bridge.

A combined method of finite mixture distributions and hybrid mixture parameter estimation is proposed to formulate the multi-modal probability density function (PDF) of the stress spectrum acquired from the monitoring data. This method is capable of modeling complex probability distributions and enables the statistical modeling of random variables with multi-modal behavior where a simple parametric model fails to adequately represent the characteristics of observations. The rainflow counting algorithm is utilized to obtain the rainflow stress matrix including the information such as stress range, mean stress, and number of cycles. The method of finite mixture distributions is applied to formulate the PDF of the stress range, while the joint PDF of the stress range and the mean stress is derived by means of a mixture of multivariate Weibull-normal distributions. The formulated PDF fits the measurement data fairly well and thus provides a crucial basis for fatigue reliability evaluation.

The determination of stress concentration factor (SCF) and its stochastic characteristics for a typical welded bridge T-joint is perceived by conducting full-scale model experiments of a railway beam section of the TMB. The strain data at the pre-allocated measuring points are acquired and the hot spot strain at the weld toe is determined by a linear regression method. The SCF is then calculated as a ratio

between the hot spot strain and the nominal strain which is obtained directly from the strain gauge. To fully account for the effect of predominant factors on the scatter of SCF, the experiments have been carried out under different moving load conditions. The statistical properties and probability distribution of SCF are achieved, which reveals that the SCF for the welded steel bridge T-joint conforms to a normal distribution.

Two reliability-based fatigue life assessment methods are proposed. In the first method, the stress cycle of specific stress range is treated as a random variable. The statistics obtained for all concerned stress ranges is combined with the *S-N* relationship along with the Miner's damage cumulative rule to conduct a probabilistic fatigue life assessment. In the second method, a fatigue reliability model integrated with the probability distribution of hot spot stress range is formulated based on the *S-N* relationship. The joint PDF of the hot spot stress range is constructed from the obtained probability distributions of the stress range and the SCF. The two methods have been applied for probabilistic fatigue life assessment of critical welded details at the TMB by use of the long-term monitoring data, and the mean value and the standard deviation of the fatigue life as well as the failure probability and reliability index versus fatigue life are achieved.

In summary, the research addressed in this dissertation chiefly contributes to the development of a systematic framework for *S-N* approach-based fatigue reliability

assessment of welded joints of steel bridges making use of long-term monitoring data. Aiming to narrow the gap currently existing between SHM technologies and structural condition assessment practices, the approach developed in this PhD study is capable of performing fatigue life and reliability evaluation with taking into account uncertainty and randomness inherent in the nature of fatigue phenomenon and measurement data. Following this approach, reliable fatigue condition assessment can be achieved for instrumented steel bridges and rational strategies on bridge inspection and maintenance can be executed in accordance with the correlativity between reliability indices and predefined inspection and/or maintenance actions.

LIST OF PUBLICATIONS

Journal Articles

Y. Q. Ni, X. W. Ye, and J. M. Ko (2010), "Monitoring-based fatigue reliability assessment of steel bridges: analytical model and application", accepted to *Journal of Structural Engineering*, ASCE, Vol. 136, No. 12 (proofs available).

Y. Q. Ni, P. Zhang, X. W. Ye, K. C. Lin, and W. Y. Liao (2010), "Modeling of temperature distribution in a reinforced concrete supertall structure based on structural health monitoring data", accepted to *Computers and Concrete*, in press.

X. W. Ye, Y. Q. Ni, K. Y. Wong, and J. M. Ko (2009), "Statistical analysis of stress spectra for fatigue life assessment of steel bridges with structural health monitoring data", submitted to *Computers and Structures*, in review.

Y. Q. Ni, X. W. Ye, and J. M. Ko (2009), "Modeling of stress spectrum using long-term monitoring data and finite mixture distributions", submitted to *Journal of Engineering Mechanics*, ASCE, in review.

X. W. Ye, Y. Q. Ni, and J. M. Ko (2009), "Full-scale model experiments for determining SCF and its stochastic characteristics of welded steel bridge T-joints", submitted to *Journal of Constructional Steel Research*, in review.

Y. Q. Ni, X. W. Ye, and J. M. Ko (2006), "Fatigue reliability analysis of a suspension bridge using long-term monitoring data", *Key Engineering Materials*, Vol. 321-323, 223-229.

Conference Papers

X. W. Ye, Y. Q. Ni, J. M. Ko, and K. Y. Wong (2010), "A method for stress concentration factor determination of welded steel bridge T-joints under moving load", *Proceedings of the 5th International Conference on Bridge Maintenance, Safety and Management*, 11-15 July 2010, Philadelphia, USA, 2670-2676.

X. W. Ye, Y. Q. Ni, and J. M. Ko (2009), "SHM-based fatigue reliability evaluation of steel bridges: methodology, experiment, and application", *Proceedings of the 6th International Conference on Advances in Steel Structures*, 16-18 December 2009, Hong Kong, China, 377-386.

Y. Q. Ni, X. W. Ye, and J. M. Ko (2009), "Theoretical and experimental investigation on probabilistic fatigue life assessment of steel bridges instrumented with structural health monitoring system", *Proceedings of the 5th International Workshop on Advanced Smart Materials and Smart Structures Technology*, 29 July - 1 August 2009, Boston, USA, 65-73.

X. W. Ye, Y. Q. Ni, and J. M. Ko (2009), "Fatigue reliability assessment of steel bridges with structural health monitoring system: methodology, experiment, and application", *2009 NSF Civil, Mechanical and Manufacturing Innovation Grantees and Research Conference*, 22-25 June 2009, Honolulu, USA (poster presentation).

Y. Q. Ni, P. Zhang, X. W. Ye, K. C. Lin, and W. Y. Liao (2009), "Temperature-induced deformations of reinforced concrete core of a supertall structure: integrating field monitoring data into finite element analysis", *Proceedings of the 1st International Conference on Computational Technologies in Concrete Structures*, 24-27 May 2009, Jeju, Korea, 327-

339.

X. W. Ye, Y. Q. Ni, and J. M. Ko (2007), “Hot spot stress approach for fatigue life assessment in welded bridge connections using monitoring data and FEM analysis”, *Proceedings of the 3rd International Conference on Structural Health Monitoring of Intelligent Infrastructure*, 13-16 November 2007, Vancouver, Canada (CD-ROM).

X. W. Ye, Y. Q. Ni, and J. M. Ko (2007), “Monitoring-based fatigue life assessment of a suspension bridge accounting for both traffic and typhoon effects”, *Proceedings of the 4th Cross-Strait Conference on Structural and Geotechnical Engineering*, 24-26 April 2007, Hangzhou, China, 832-843.

X. W. Ye, Y. Q. Ni, and J. M. Ko (2006), “Probability-based fatigue life assessment of a suspension bridge using long-term monitoring data”, *Proceedings of the 1st Faculty Postgraduate Research Conference*, 4 November 2006, Hong Kong, China, 9-16.

Y. Q. Ni, G. Chen, X. W. Ye, and J. M. Ko (2006), “Fatigue life assessment of a suspension bridge using long-term monitoring data”, *Proceedings of the 4th World Conference on Structural Control and Monitoring*, 11-13 July 2006, San Diego, USA (CD-ROM).

ACKNOWLEDGEMENTS

I owe my deepest gratitude and will forever be indebted to my chief supervisor, Prof. Y. Q. Ni, for his enlightening guidance and constructive advice, high sense of responsibility, and detailed comments and insight throughout my study and preparation of the thesis. Without his consistent and illuminating instruction, the completion of this thesis is unachievable. I benefit greatly from his zealousness in scientific research, his meticulous work attitude, and his rigorous scholarship. I would also like to thank my co-supervisor, Prof. J. M. Ko, for his generous support and constant encouragement in the course of my PhD project.

In addition, I would like to express my heartfelt thanks to Dr. K. Y. Wong in the Highways Department of the Hong Kong Special Administrative Region Government for providing invaluable structural health monitoring data. I want to express my sincerest gratitude to Prof. M. Nagode for bringing me into the area of finite mixture modeling and hybrid mixture parameter estimation. I am also grateful to all of my friends and colleagues in Department of Civil and Structural Engineering, The Hong Kong Polytechnic University, particularly Dr. X. G. Hua, Dr. Y. F. Duan, Dr. J. Y. Wang, Dr. Z. Fang, Dr. L. J. Su, Dr. J. H. Tang, Dr. G. M. Chen, Dr. H. H. Zhu, Dr. W. B. Wei, Mr. G. Chen, and Mr. H. W. Xia for their very precious discussions and suggestions on the thesis.

Furthermore, I gratefully acknowledge the financial supports from The Hong Kong Polytechnic University for providing me such a golden opportunity to undertake this

research project. Special thanks must also go to staff in the university library, research office, finance office, and general office and laboratory of Department of Civil and Structural Engineering, The Hong Kong Polytechnic University for their kind help and assistance during my stay at the university.

Finally, I dedicate this thesis to my beloved parents with gratitude for their everlasting love, encouragement, and support.

TABLE OF CONTENTS

LIST OF FIGURES

LIST OF TABLES

LIST OF ABBREVIATIONS

Abbreviation	Description
AASHTO	American Association of State Highway and Transportation Officials
ADTT	Average daily truck traffic
AIC	Akaike's information criterion
API	American Petroleum Institute
ASCE	American Society of Civil Engineers
ASTM	American Society for Testing and Materials
AWS	American Welding Society
BHMS	Bridge health monitoring system
BMMS	Bridge management and maintenance system
BSI	British Standards Institution
CDF	Cumulative distribution function
CDM	Continuum damage mechanics
CEN	European Committee for Standardization
CHS	Circular hollow section
COV	Coefficient of variation
DATS	Data acquisition and transmission system
DPCS	Data processing and control system
ECCS	European Convention for Constructional Steelwork
EM	Expectation maximization
FEM	Finite element method
FORM	First-order reliability method
GPS	Global positioning system

HCF	High-cycle fatigue
HSWC	Hong Kong – Shenzhen Western Corridor
IIW	International Institute of Welding
IMS	Inspection and maintenance system
IPB	In-plane bending
KSMB	Kap Shui Mun Bridge
LCF	Low-cycle fatigue
LEFM	Linear elastic fracture mechanics
MCS	Monte Carlo simulation
NDE	Non-destructive evaluation
NIST	National Institute of Standards and Technology
OPB	Out-of-plane bending
PDF	Probability density function
RMS	Root mean square
SCB	Stonecutters Bridge
SCF	Stress concentration factor
SHDMS	Structural health data management system
SHES	Structural health evaluation system
SHM	Structural health monitoring
SHS	Square hollow section
SORM	Second-order reliability method
SS	Sensory system
TKB	Ting Kau Bridge
TMB	Tsing Ma Bridge
WASHMS	Wind and structural health monitoring system
WIM	Weigh-in-motion

LIST OF SYMBOLS

Symbol	Description
Chapter 1	
S	Stress range
N	Number of cycles to failure
Chapter 2	
ϵ	Strain range
T	Plate thickness
m, A	Empirical material constants
F_l	Fatigue limit stress
R_s	Stress ratio
S_m	Mean stress
S_q	Equivalent stress
C	Constant parameter
L	Fatigue load
R	Fatigue resistance
n	Stress cycle
Chapter 3	
D	Fatigue damage accumulation index
n_i	Number of cycles for the ith stress range S_i
N_i	Number of cycles to failure for the ith stress range S_i
S_0	Fatigue limit

λ_i	Reducing factor
m	Inverse slope of the mean-line log$S$-log$N$ curve
K_0	Constant relating to the mean-line log$S$-log$N$ curve
Δ	Reciprocal of the anti-log of the standard deviation of log$N$
d	Number of standard deviations below the mean-line log$S$-log$N$ curve; also called probability factor
F	Fatigue life

Chapter 4

$\mathbf{y}$	Independent scalar or vector observations
c	Number of components or groups
$\mathbf{w}$	Weight vector
$\boldsymbol{\theta}$	Parameter vector
$\boldsymbol{\theta}_l$	Component parameters
l	Component index
w_l	Component weights
μ_l	Mean values of normal mixture parameters
σ_l	Standard deviations of normal mixture parameters
β_l, θ_l	Weibull shape parameters
$\Phi(\cdot)$	Standard normal cumulative distribution function
R_j	The jth bin region
V_j	The jth bin volume
$\mathbf{y}_j$	Independent observation inside the jth bin
n	Total number of independent scalar or vector observations
k_j	Fraction of observations falling into R_j
p	Dimension of independent scalar or vector observations
$\mathbf{h}_j$	Side length of the jth bin

$\boldsymbol{y}_0$	An arbitrary origin
k	Number of bins
q	Global mode index
$\mathbf{y}_q$	Independent observation where empirical density takes on a maximum value
f_{lq}	Empirical density of component l in a global mode
f_{lj}	Empirical density of component l in the jth bin
k_{lj}	Observation frequencies of component l in the jth bin
n_l	Number of observations in component l
m_l	Component mean
V_l	Component variance
$\Gamma(\cdot)$	Gamma function
$w_{\min}$	Critical component weight
$D_{\min}$	Critical absolute relative deviation
Q	Number of parameters in the statistical model
$L(\cdot)$	Maximized value of the likelihood function
D	Total of the absolute relative deviations
K	Number of equally spaced classes
M	Total number of the data samples
$\lceil\ \rceil$	Ceiling operator, i.e., taking the closest integer above the calculated value
$\mathbf{s}$	Stress matrix
$f(\mathbf{s})$	Joint PDF of rainflow stress matrix
s_r	Rainflow stress range
s_m	Mean stress
$f_l(\mathbf{s})$	The lth joint component PDF of rainflow stress matrix
$f_l(s_r)$	PDF of stress range corresponding to the lth joint component distribution
$f_l(s_m)$	PDF of mean stress corresponding to the lth joint component distribution

$F_l(s_r)$ CDF of stress range corresponding to the lth joint component distribution

$F_l(s_m)$ CDF of mean stress corresponding to the lth joint component distribution

Chapter 5

ε_{hot} Hot spot strain

ε_{nom} Nominal strain

ε Strain value along the bottom flange of the steel beam

δ Distance from the weld toe at the bottom flange of the steel beam

α_0, α_1 Regression coefficients

$S_{\delta\delta}$ Variance of δ

$S_{\varepsilon\delta}$ Covariance between ε and δ

$\bar{\varepsilon}$ Mean of ε

$\bar{\delta}$ Mean of δ

R^2 Coefficient of determination

ε_i Observed data of ε

$\hat{\varepsilon}_i$ Estimator of ε_i

$F_0(x)$ Specified theoretical CDF of a continuous variate X

H_0 Null hypothesis

$F_n(x)$ True CDF of the continuous variate X

D_n Maximum absolute difference

H_1 Alternative hypothesis

Chapter 6

$f_S(s)$ PDF of the stress range S

ΔS Width of stress block

N_T Total number of stress cycles in time T

$E(\cdot)$ Expected value

Δ	Critical fatigue damage accumulation index
g	Limit-state function
p_f	Probability of fatigue failure
D_T	Fatigue damage at time T
S_{re}	Effective stress range
S_{ri}	Midwidth of the ith stress interval in a histogram
α_i	Fraction of stress range cycles within an interval
B	Constant parameter
Y_e	Expected or desired design life
Y_f	Remaining safe fatigue life
T_a	Estimated lifetime average daily truck volume
C	Number of cycles per truck passage
Y_a	Age of the bridge
K	Constant depending on the structural detail
f	Factor to account for the difference between the mean and allowable S-N curve
R_s	Reliability factor
μ_F	Mean value of fatigue life
D_F	Variance of fatigue life
μ_{ni}	Mean of random variable n_i
D_{ni}	Variance of random variable n_i
F_e	Expected fatigue life
β	Reliability index
$\sigma_{\max}$	Maximum stress in one stress cycle
$\sigma_{\min}$	Minimum stress in one stress cycle
S_h	Hot spot stress range
$f(h)$	Joint PDF of hot spot stress range

$f(s)$	PDF of stress range
$f(t)$	PDF of SCF
n_{tot}	Total number of cycles
N_f	Stress cycles at failure
D_f	Fatigue damage at failure
σ_{hot}	Hot spot stress
σ_{nom}	Nominal stress

CHAPTER 1

INTRODUCTION

1.1 Research Background

Fatigue is a progressive and localized process in which structural damage accumulates continuously due to the repetitive application of external loadings such as vehicles for steel bridges, winds for high-rise buildings, waves for offshore platforms, and temperature for turbine engines; while these applied loadings may be well below the structural resistance capacity. This kind of process is extraordinarily dangerous because a single application of the load would not create any abnormal effects, whereas a conventional structural stress analysis might lead to a conclusion of safety that does not exist. In a pervasive perspective of metal fatigue, the fatigue process is deemed to initiate from an internal or surface flaw where the stresses are concentrated, and originally consists of shear flow along slip planes. Suffering from an amount of cycles, this slip generates intrusions and extrusions and ultimately results in forming into a crack. With the propagation of cracks, it will eventually lead to fatigue failure in the structural components.

The most important failure modes for steel structures with welded connections are primarily classified as strength failure, including fracture due to overload or excessive plastic deformation; serviceability failure, such as large vibration and deflection under service-load conditions; and fatigue failure. Over a long period of time, the strength and serviceability modes of failure have been well investigated and understood in the professional engineering communities. As one of the most critical forms of damage and principal failure modes for steel structures, fatigue phenomenon is still less understood. It is therefore essential to seek novel methodologies and develop advanced technologies for seizing the fatigue mechanisms and conducting reliable assessment of fatigue damage status of steel bridges which serve as vital components in the transportation infrastructure of a nation.

Two approaches are commonly employed for fatigue damage evaluation and life prediction of bridge structures. The first approach is the traditional *S*-*N* curve method, in which the relationship of the constant-amplitude stress range, *S*, and the number of cycles to failure, *N*, is determined by appropriate fatigue experiments and described by an *S*-*N* curve. The Palmgren-Miner linear damage hypothesis, also called Miner's rule (Miner 1945), extends this approach to variable-amplitude loading. The second method is the fracture mechanics approach which is dominantly dedicated in exploring the features and disciplines of crack initiation and growth in consideration of stress field at the crack tip. In general, the two approaches are applied sequentially,

with the *S-N* curve method being used at the bridge design stage or preliminary evaluation of fatigue life and the fracture mechanics approach for more refined crack-based remaining fatigue life assessment or effective decision-making on inspection/maintenance strategies (Chryssanthopoulos and Righiniotis 2006).

There have been a lot of investigations and applications on bridge fatigue damage evaluation and fatigue life prediction using the traditional *S-N* method (Schilling *et al*. 1978; Moses *et al*. 1987; Laman and Nowak 1996; DeWolf *et al*. 1997; Mohammadi *et al*. 1998; Connor and Fisher 2001; Peil *et al*. 2001; Li *et al*. 2003; Chan *et al*. 2005; Al-Rubaie 2008) or the fracture mechanics approach (Fisher 1984; Zhao and Haldar 1996; Agerskov and Nielsen 1999; Lukic and Cremona 2001; Kiss and Dunai 2002; Righiniotis and Chryssanthopoulos 2003; Park *et al*. 2005; Ibrahim *et al*. 2006a, b; MacDougall *et al*. 2006; Xiao *et al*. 2006; Imam *et al*. 2008; Ghidini and Dalle Donne 2009). Some specifications (BSI 1980; AASHTO 1990; CEN 1992) adopt the traditional *S-N* method to guide bridge fatigue design or evaluation. According to these specifications, the fatigue life prediction of stochastically loaded structures is to determine the correlation between the fatigue life, the stress spectra and the material endurance. The material endurance is generally given in the form of *S-N* curves for constant-amplitude loading. The stress spectra are generally unknown and need to be evaluated by means of experiments or simulations. In the process of fatigue life prediction, the stress spectrum is obtained by extracting the stress cycles from a measured or simulated stress time history with a suitable cycle counting method.

Next, a proper fatigue damage accumulative rule is chosen and the fatigue damage caused by individual stress cycle is calculated. The total fatigue damage equals the sum of damage resulting from individual stress cycle. One of the most widely used damage accumulative rules is the Miner's linear damage accumulative rule, and a rainflow cycle counting method is generally used for extracting the stress cycles from the stress time histories.

The nature of fatigue process and uncertainties associated with the load histories and the estimation of future loads require field inspection as a necessary tool for fatigue damage detection and prevention. The fatigue damage condition and fatigue crack growth in bridge components are then assessed with data and information collected from regular field inspection. Inspection may involve the visual examination of structural components and/or the use of a variety of non-destructive evaluation (NDE) techniques, such as dynamic testing method, radiographic inspection, electric inspection method, sonic and ultrasonic method, acoustic emission method, and dye penetration (Achenbach 2000). They are conducted typically after observing deterioration and damage such as fatigue cracking in local areas and often expensive, time-consuming, and labor intensive to execute on large-scale bridges. When visual inspections without NDE techniques are used, the effectiveness of the inspection program primarily depends on the inspector's experience and the type of damage observed in generic classes of structures inspected. In cases where NDE techniques are used, the effectiveness of the inspection process, to a great extent, depends on the

reliability of the selected technique in damage detection. These tests may reveal a snapshot of the operating loads and the corresponding response of the bridge to assess fatigue life at fatigue-sensitive (especially at fracture-critical) details. However, some of the tests will restrict normal operation of bridges.

Recently, long-term structural health monitoring (SHM) of bridges has been one of the major attentions for researchers and engineers in civil, mechanical, material, and computer science fields (Balageas *et al*. 2006). Design and implementation of such a system is an integration of analytical skills, instrumentation and information technologies with the knowledge and experience in bridge design, construction, management and maintenance. On-line SHM system is able to provide reliable information pertaining to the integrity, durability, and reliability of bridges. The information can then be incorporated into bridge management and maintenance system (BMMS) for optimizing the maintenance actions and to improve design standards, specifications, codes, and guidelines. SHM is, in fact, an augment but not a substitute of current practice in bridge maintenance and management, not only through the use of advanced technologies in sensing, data acquisition, computing, communication, and data and information management, but also through effective integration of these technologies into an intelligent system. An accurate estimation of the actual situation in fatigue and remaining life of the critical components is an important task of the SHM system, which can be achieved by use of the continuously measured dynamic strain/stress data from the long-term SHM system.

The nominal stress approach is widely used for fatigue evaluation because most design specifications and codes for steel structures contain a standard procedure for fatigue analysis based on this approach. However, the nominal stress approach is not suitable for the structural joint if the object detail is complicated and incomparable to any classified joints, or the loadings are complex to make it difficult or impossible to determine the nominal stress (Xiao and Yamada 2004). Moreover, it has an obvious drawback in that it largely ignores the actual dimensional variations of a specific structural detail (Poutiainen *et al*. 2004). Therefore, the fatigue life predicted using nominal stress may be unreliable. An alternative method for the fatigue analysis of complicated welded steel joints is the hot spot stress approach which is more reasonable and accurate than nominal stress approach (Han and Shin 2000). The advantage of the hot spot stress method is that all kinds of details are related to the same hot spot *S*-*N* curve determined by the stress concentration factor (SCF) to estimate fatigue strength, rather than using numerous curves corresponding to welded joint categories of welded structures (Lotsberg and Landet 2005).

Fatigue performance of steel bridges depends on a number of factors such as material characteristics, stress history, and environment, and all these factors exhibit uncertainty and randomness during the service life of the bridge. On the other hand, when the field measurement data are used for fatigue condition assessment, the uncertainties related to the field-measured data and the inaccuracies due to data processing techniques are subsistent and hardly avoidable. In view of these facts, it is

more appropriate to conduct fatigue life assessment in a probabilistic way than deterministic procedures.

1.2 Research Objectives

The aim of this PhD study is to investigate fatigue life assessment and reliability analysis of steel bridges by using long-term monitoring data. The specific objectives of this research are:

(1) To develop a deterministic method for evaluating fatigue life of steel bridges based on the stress-life (*S*-*N*) approach by making use of long-term monitoring data from an on-line SHM system.

(2) To propose a procedure for modeling the probability density function (PDF) of stress range and the joint PDF of stress matrix after rainflow cycle counting using the method of finite mixture distributions in conjunction with a hybrid mixture parameter estimation approach.

(3) To experimentally investigate the determination of SCF and its probability distribution and stochastic properties for fatigue reliability analysis through full-scale model experiments of a typical welded bridge T-joint.

(4) To propose a method for probability-based fatigue life assessment by use of long-term monitoring data. In this method, the stress cycle for a specific

rainflow-counted stress range is treated as a random variable with a probability distribution.

(5) To develop a fatigue reliability model which integrates the probability distribution of hot spot stress range with a continuous probabilistic formulation of Miner's damage cumulative rule for fatigue life and reliability evaluation of steel bridges with long-term monitoring data.

1.3 Thesis Organization

There are seven chapters in this thesis. A brief description of the chapters is given in the following.

Chapter 1 introduces the background of this research and the research objectives to be pursued in this PhD study.

Chapter 2 contains a review of the literature on fatigue analysis methods and fatigue reliability models, particularly the research on fatigue life and reliability assessment based on the field measured data. After a brief introduction of the fundamentals of fatigue, classical fatigue analysis methods including stress-life method, strain-life method, and fracture mechanics approach are introduced. Then, the research efforts pertaining to the NDE-based and SHM-based fatigue life assessment as well as the investigations on fatigue analysis accounting for stress concentration are reviewed. Subsequently, the existing fatigue reliability models and studies on the reliability

analysis for fatigue damage and life assessment based on the *S-N* curve method are surveyed. These models include fatigue resistance models, fatigue load models, and other *S-N* approach-based probabilistic models. Finally, a discussion on critical issues and existent problems related to the existing method of fatigue life assessment and reliability analysis is provided.

In Chapter 3, a monitoring-based method for fatigue life assessment of steel bridges is proposed. This method is based on the strain measurement data from the SHM system instrumented on the bridge. The daily stress spectra at a specific location are attained using field-measured strain time histories and rainflow counting algorithm. After examining the stress spectra obtained in different days under normal traffic and wind conditions as well as typhoon conditions, a standard daily stress spectrum is derived by combining proportionally the strain data under different conditions. The optimal number of daily strain data for derivation of a standard daily stress spectrum is determined by analyzing the significant factors influencing the predicted fatigue life. Making use of one-year monitoring data from the suspension Tsing Ma Bridge (TMB), the proposed method is used to predict the fatigue life of the fatigue-prone welded details according to the procedure stipulated in BS5400 specification.

Chapter 4 focuses on how to exploit the long-term monitoring data for modeling of rainflow-counted stress spectra that contain the stress range and mean stress, which is achieved by making use of the method of finite mixture distributions in conjunction with a hybrid mixture parameter estimation algorithm. First, the method of finite

mixture distributions which is widely used for PDF generation and a hybrid mixture parameter estimation method are briefly introduced. Second, the original measured strain data are preprocessed to eliminate the temperature effect by using a wavelet-based filtering method. The obtained stress spectra and predicted fatigue life by using the original measured and filtered strain data are also compared. Then, a representative sample of stress spectrum data is constructed accounting for both traffic and typhoon effects. At last, the multi-modal modeling of the stress range is performed by use of finite mixed normal, lognormal, and Weibull distributions; the joint PDF of stress matrix are also estimated by means of a mixture of multivariate distributions.

Chapter 5 explores the method of determination of SCF and its stochastic properties for fatigue reliability assessment, and it is pursued by conducting an experimental investigation of a typical welded bridge T-joint. A full-scale test model is designed and fabricated, which holds a uniform profile with the railway beam section of the TMB in the geometrical dimension and material property as well as the weld detail of the welded joint. The strain data of the pre-allocated measuring points are acquired and the hot stop strain at the weld toe is determined by using linear regression method. The SCF is then calculated as the ratio between the hot spot strain and the nominal strain which is derived from the measured data at the location of desired strain gauge. Test cases are carried out under moving loading conditions with a combination of three load weight grades, two velocities of moving load, and two axle-distances of the test bogie. The statistical properties and probability distribution

of the SCF for the typical welded T-joint are achieved.

In Chapter 6, two reliability-based fatigue life assessment methods are proposed. In the first approach, the stress cycle of specific stress range is treated as a random variable. The statistics obtained for all concerned stress ranges is combined with the *S-N* relationships stipulated in specifications to conduct a probabilistic assessment of fatigue life with the use of the Miner's rule, from which the mean value and standard deviation of the fatigue life as well as the failure probability and reliability index versus fatigue life are obtained. In the second method, a fatigue reliability model is formulated in a continuous probabilistic formulation of Miner's rule by considering both the nominal stress range obtained by measurements and the corresponding SCF as random variables. The developed probabilistic model is then illustrated using the long-term strain monitoring data from the TMB for evaluating fatigue life and failure probability with the aid of structural reliability theory. The global and local finite element models (FEMs) of the bridge are developed for numerically calculating the SCFs at fatigue-susceptible locations, and the joint PDF of hot spot stress range is obtained using the procedure for modeling the PDF of the stress range as addressed in Chapter 4 and the results of the statistical distribution of SCF presented in Chapter 5. The failure probability and reliability index versus fatigue life are accomplished from the obtained joint PDF of the hot spot stress range in terms of the nominal stress range and SCF random variables.

Chapter 7 summarizes the conclusions achieved from the theoretical, numerical, and

experimental studies in this PhD study. Recommendations for future work are also presented.

CHAPTER 2

LITERATURE REVIEW

2.1 Basic Aspects of Fatigue

As a well-known phenomenon in metallic structures, fatigue failures in service were already observed in the 19th century. The word “fatigue” was introduced in the 1840s and 1850s to describe failures occurring from repeated loads. The first noteworthy investigation on fatigue is generally dated from the engineering research work of August Wöhler, a technologist in the German railroad system in the early 1850s. Wöhler was concerned by the failure of railroad axles after various times in service at loads considerably less than the static strength of the structures and undertook the first systematic study of fatigue by performing many laboratory fatigue tests under cyclic stresses. However, in the 19th century, fatigue was thought to be a mysterious phenomenon in the material of an engineering structure because fatigue damage could not be seen and failure apparently occurred without any early warning. In the 20th century, it has been observed that repeated load applications can start a fatigue mechanism in the engineering material leading to nucleation of a microcrack, crack growth, and ultimately to complete failure of a structure.

The history of fatigue covering a time span from 1837 to 1994 was reviewed in a survey paper by Schütz (Schütz 1996). Mann (Mann 1970, 1978, 1983, 1990) compiled 21,075 literature sources about fatigue problems on engineering materials, components, and structures covering the period from 1838 to 1990 in four books with an index on subjects, authors, and years. A comprehensive survey of the historical development of the contributions to fatigue on metallic materials, nonmetallic materials, and composites can also be found in Suresh (1998). Cui (2002) carried out a state-of-the-art review of metal fatigue with particular emphasis on the latest developments in fatigue life prediction methods.

2.1.1 Significance of Fatigue

Fatigue is one of the main causes involved in fatal mechanical failures of a wide range of structures and infrastructures, such as aircrafts, ships, vehicles, offshore structures, pipelines, machinery, pressure vessels, cranes, power turbines, transmission tower, bridges, or other engineering structures of high visibility. Such devastating events occur suddenly and result in heavy losses of life and property. Even though no exact percentage is available on the mechanical failures due to fatigue, many studies have suggested that 50 to 90 percent of all mechanical failures are fatigue failures (Stephens *et al*. 2001). American Society of Civil Engineers (ASCE) Committee on Fatigue and Fracture Reliability stated that about 80 ~ 90% of failures in metallic structures are related to fatigue fracture (ASCE Committee on

Fatigue and Fracture Reliability 1982a, b, c, d).

The fact that most mechanical failures are associated with fatigue is also testified by the results of an extensive study reported in 1983 by Battelle Columbus Laboratories in conjunction with the National Bureau of Standards (currently NIST, National Institute of Standards and Technology) (Reed *et al*. 1983). As illustrated in **Table 2.1**, it is clear that 141 out of the 230 failures (nearly 61%) were associated with fatigue and three main causes of fatigue are improper maintenance, fabrication defects, and design deficiencies. The investigation also emphasized that the cost of fatigue-induced fracture could be dramatically reduced by using proper fatigue analysis methods and technologies. However, fatigue failure of metal materials, components, and structures is very recondite and not well understood, nor readily predicted, by designers and engineers due to the complex nature of the fatigue mechanism.

2.1.2 Mechanism of Metal Fatigue

The mechanisms of the fatigue process are quite complicated and controversial which are still only partially understood. However, understanding the fatigue mechanism is a prerequisite for considering various factors which affect fatigue life and fatigue crack growth, such as the material surface quality, residual stress, and environmental influence. This knowledge is essential for the analysis of fatigue

properties of an engineering structure. Generally, fatigue is understood as a crack initiation process followed by a crack growth period, as shown in **Figure 2.1**. Fatigue cracks caused by the repeated application of loads, which individually would be too small to cause failure, usually initiate from the surface of a structural component where fatigue damage initiates as microscopic shear cracks on crystallographic slip planes as intrusions and extrusions, which is the first stage called crack initiation (stage I). The crack may then propagate from the localized plastic deformation to a macroscopic size in a direction perpendicular to the applied load, which is a crack propagation process (stage II). Finally the crack becomes unstable and the component may fracture. Usually, it is difficult to make an exact description and distinction of the transition between two phases of the fatigue process since this distinction depends upon many factors, such as component size, material, and the methods used to detect cracks.

Typically, the crack initiation period accounts for most of the fatigue life of a component made of steels, particularly in the high-cycle fatigue (HCF) regime (approximately larger than 10,000 cycles). In the low-cycle fatigue (LCF) regime (approximately less than 10,000 cycles), most of the fatigue life is spent on crack propagation. Modern fatigue theories provide separate analyses for each phase of the fatigue process. Crack initiation theories are based on the assumption that fatigue cracks are initiated by the local strains and stresses concentrating on the surface of a structural component due to geometric shapes such as holes, discontinuities, and

fillet radii. Crack propagation and final failure stages are analyzed by relating crack growth to the stresses in the component using fracture mechanics.

2.1.3 Classical Fatigue Analysis Methods

Fatigue process is a very progressive and complicated metallurgical process which is difficult to describe accurately and model precisely on the microscopic level. Despite these complexities, fatigue analysis methods have been developed for fatigue damage assessment for the design of components and structures. Historically two overriding considerations have promoted the development of fatigue analysis methods. The first has been the need to provide designers and engineers with methods that are practical, easily implemented, and cost effective. The second consideration has been the need to reconcile these analytical approaches with physical observations. One of the most important physical observations is that the fatigue process can generally be broken into two distinct phases: initiation life and propagation life. Three primary fatigue analysis methods are presented in this section, including the stress-life (S-N) approach, the strain-life (ϵ-N) approach, and the fracture mechanics approach. These methods have their own region of application with some degree of overlap between them.

Stress-life approach is used mainly for long life applications where stresses and strains are elastic. This method is best suited for HCF. It does not distinguish

between initiation and propagation, but deals with a total life or the life to failure of a component. The current stress-life approaches can be divided into different categories depending on the type of stress analysis performed on the structural details, mainly including the nominal stress approach, hot spot stress approach, and notch stress approach (Fricke 2003; Radaj *et al*. 2006). The strain-life method developed in the 1960s is usually considered an initiation approach. It is used when the strain is no longer totally elastic, but has a plastic component. Short fatigue lives in LCF generally occur under these conditions. The fracture mechanics method is based upon linear elastic fracture mechanics (LEFM) principles which are adapted for fluctuating loading. This method is used to predict propagation life from an initial crack or defect and it is also used in combination with the strain-life approach to predict a total life.

2.2 Fatigue Condition Assessment Based on Field Data

When the stress-life approach is adopted for bridge fatigue damage evaluation and fatigue life prediction, the engineer must have the most realistic and precise load and resistance information to make an accurate fatigue assessment, particularly when the live load stresses are used in cubic equations (Sartor *et al*. 1999). In this type of analysis, a small variation in live load stress range will induce drastically different fatigue assessment results. Analysis using computational models of load and structure cannot attempt to mimic the variation in stress range that a typical structural

element will experience. Additionally, it would be extremely time-consuming and almost impossible to attempt to account for all of the variables in a conventional simulation analysis. The only way to obtain precise information that accounts for these variables is through field measurement, where sensors are attached to the bridge elements and the actual stresses and distribution of stresses that the structural element experiences can be measured and recorded. Consequently, it is considered that the field-measured data would provide the simplest and most accurate basis for fatigue assessment. This section provides a comprehensive overview of fatigue analysis of bridge structures based on field-measured data from load-controlled diagnostic load testing and short-term in-service monitoring using NDE techniques and long-term monitoring strategy dominated by SHM technologies.

2.2.1 NDE-Based Fatigue Assessment

As the traffic volume and truck weight continue to increase, and as bridge conditions continue to deteriorate, a lot of existing steel bridges need to be strengthened, repaired, or reconstructed to insure an acceptable level of safety considering present and future traffic conditions (Zhao and Haldar 1996). Furthermore, because of lack of funds and the high cost of reconstruction, NDE technology has been developed to improve the accuracy of bridge condition evaluation (Russo *et al*. 2000; Shenton *et al*. 2003). Among the methods, diagnostic load testing with controlled loadings and short-term in-service monitoring under normal traffic loadings currently are mainly

used and the fatigue condition of bridges is then assessed with the obtained data and information from the deployed sensors and data acquisition systems.

The load-controlled diagnostic load testing has the advantages of using known loadings, which allows relatively accurate quantification of bridge response and the determination of a fairly comprehensive baseline model for a bridge. The limitation to this type of testing, as opposed to in-service monitoring, is that one must use some level of traffic control during testing. The time used for setup is longer, and the response represents only a snapshot in time. The short-term in-service monitoring, on the other hand, has the advantages of not requiring traffic control during monitoring; having a very rapid setup time; recording the response due to ambient traffic, thereby providing statistical information about actual responses; and allowing the response to be tracked over time. The limitation of in-service monitoring is that the weight and the classification of the truck loadings are not specifically known, and the limited data will not allow bridge parameters to be evaluated explicitly (Chajes *et al*. 2000).

Some investigations on bridge fatigue analysis through use of NDE techniques have been made in recent years. For example, Hahin *et al*. (1993), and Mohammadi *et al*. (1998) presented the application of field strain data to condition assessment and prediction of fatigue life of fifteen highway bridges located in Illinois, and the results were further used to study the significance of truck weight increase and traffic volume growth on fatigue life of the bridges. DeWolf *et al*. (1997, 2002), and

Bernard *et al*. (1997) evaluated fatigue life for a variety of bridges using field monitoring data by a portable computer-based strain gauge data acquisition system which has been extensively used in Connecticut to assist the Department of Transportation in the evaluation and renewal of the state's bridge infrastructure, and identified cost-effective maintenance, repair, and replacement strategies (Chakraborty and DeWolf 2006). Peil *et al*. (1997, 2000, 2001) studied the precision on life cycle prediction of steel bridges under live loading using strain monitoring at the real critical points.

Chajes and Mertz (2003) discussed the diagnostic load tests performed at various stages throughout the process on determining the circumstances leading up to the fatigue crack and its cause, and presented the temporary and permanent repair strategies. Zhou (2003, 2004, 2005, 2006) proved that the fatigue evaluation based on field-measured stress range histograms under actual traffic load was a more accurate and efficient method for existing bridges, and applied this approach in assessing the remaining fatigue life of aged riveted steel bridges. Ermopoulos and Spyrakos (2006) identified the structural components in need of strengthening or replacement for a 19th century railway bridge through static and dynamic field measurements as well as laboratory tests, and proposed the strengthening schemes and predicted the remaining fatigue life of the bridge in its present condition and after the suggested strengthening. Investigations into fatigue evaluation of steel bridges by use of NDE techniques were also reported by Moses *et al*. 1994, Roeder

et al. (2000), Abdou *et al*. (2003), Lund and Alampalli (2004), Spyrakos *et al*. (2004), Wang *et al*. (2005), Alampalli and Lund (2006), and Malm and Andersson (2006).

2.2.2 SHM-Based Fatigue Assessment

To secure structural and operational safety throughout the bridge life-cycles and issue early warnings on any deterioration or damage of bridges prior to costly repair or even catastrophic collapse, the significance of implementing long-term SHM systems for bridges has been increasingly recognized in USA (Pines and Aktan 2002; Chang *et al*. 2003; Peil 2005; Feng 2009), European (Casciati 2003; Brownjohn 2007; Matos *et al*. 2009), Japan (Mita 1999; Fujino 2002), Korea (Koh *et al*. 2003; Yun *et al*. 2003), Hong Kong (Ko 2004; Ko and Ni 2005; Wong 2007), Chinese mainland (Xiang 2000; Ou 2004; Zhang and Zhou 2007), Canada (Cheung *et al*. 1997; Mufti 2002; Desjardins *et al*. 2006), among others. A review of the literature indicates that there is a growing trend in incorporation of computer- and sensor-based long-term health monitoring systems into bridges especially for long-span bridges due to their large investments, their significant roles in economics, and innovative techniques used to design and construct such bridges.

An important function of SHM systems is to monitor structural health and performance, as well as accurately estimate the actual status in fatigue and remaining life of the bridge (Chan *et al*. 2001). It has become an important issue of high

research interest with the development of SHM systems for large complicated structures. However, little work on fatigue analysis and condition assessment of bridge structures based on long-term monitoring data has been made in the past decade because SHM is a relatively new technology for applications in civil engineering communities, and even a comprehensive definition of SHM and the system design guidelines have yet to be standardized; Another important reason is that such a complicated system has not been extensively installed in most of the bridges worldwide due to high cost.

However, investigations on fatigue condition assessment based on long-term monitoring data still can be found. Chan *et al*. (2001), and Li *et al*. (2001) developed a methodology and strategy for fatigue damage analysis and life prediction, and fatigue condition assessment of bridge-deck sections of the TMB was carried out taking full advantage of the on-line SHM data. Connor *et al*. (2003) developed and implemented an in-depth instrumentation, testing, and monitoring program on the Bronx-Whitestone Bridge as part of a comprehensive fatigue evaluation for the replacement orthotropic bridge deck. Ni *et al*. (2006a, b) presented a study on fatigue life assessment of the TMB using the standard daily stress spectrum method and also proposed a method for fatigue reliability analysis based on long-term monitoring data. Xu *et al*. (2009) developed a systematic framework for assessing long-term buffeting-induced fatigue damage to a long suspension bridge by integrating a few important wind/structural components with continuum damage mechanics

(CDM)-based fatigue damage assessment method.

2.3 Fatigue Analysis Accounting for Stress Concentration

Steel bridges are usually composed of lots of longitudinal and transverse plate-type structural members with welded joints at their intersections, for example, joints of main girders and floor beams, floor beams and stringers in plate girder bridges, and longitudinal ribs and transverse ribs in steel deck plates. Investigations on the fatigue behavior of welded joints as well as fundamentals of the fatigue strength assessment together with design rules and applications are numerous (e.g., Gurney 1979; van Delft 1981; Maddox 1991; Hobbacher 1996). The welded joints contain some form of geometrical or microstructural discontinuities, while the weld toes in welded joints are the positions with the maximum local stresses where fatigue cracks are most likely to occur. Hot spot stress is the value of the structural stress at the hot spot usually located at a weld toe, which can be calculated by multiplying the nominal stress by a SCF commonly obtained from the finite element analysis or experimental measurements using strain gauges or experiential formulae (Pilkey 2008).

2.3.1 Determination of SCF and Hot Spot Stress

Numerical analyses have the distinct advantage of giving the exact positions, directions and magnitudes of high stresses and the patterns of stress distribution in

the entire zone of the specific joint being considered. When using the finite element method to analyze the SCF, the structural behavior can be analyzed by a global FEM. A part of the structure including the studied detail is extracted for a more detailed analysis where is large enough to prevent boundary interaction on the stress distribution at the welded joint with adequate boundary conditions. This selected area should be newly modeled, in which the meshing is refined to obtain enough fine meshes at the welded connection provided with the boundary conditions from the global FEM calculation. The local stress concentrations at the weld toe are heavily dependent, in physical models, on the local weld profile and, in numerical analysis, on the mesh refinement (Morgan and Lee 1997). Therefore, it is necessary to find a compromise between the refinement of the meshing and the size in degrees of freedom of the numerical model.

When tests are performed and strain measurements are used to determine the SCF, an elaborate and reasonable instrumentation scheme of strain gauges is crucial. The selection of hot spot locations for instrumentation with strain gauges was improved and refined based on experience from a number of finite element analyses of the typical details such as rib-to-diaphragm, rib-to-bulkhead, rib-to-stiffener, and diaphragm-to-deck connections (Kaczinski *et al*. 1997; Barth and Bowman 2001; Tsakopoulos and Fisher 2002; Connor 2004; Al-Emrani 2005; Connor and Fisher 2006). The hot spot stress is calculated by extrapolation or regression of the stress distribution outside of the weld to the weld toe. For example, Puthli *et al*. (1988)

investigated strain/stress concentration factors numerically and experimentally on X, T, and K joints using square hollow steel sections and obtained parametric strain/stress concentration factor formulae using regression analyses. Fung *et al*. (2002) studied the SCFs of double plate reinforced tubular T-joints subjected to various types of basic loading such as axial tension, axial compression, and in-plane and out-of plane bending by using numerical and experimental methods. Similar investigations can also be found in Iida (1984), Karamanos *et al*. (2000), Gho *et al*. (2003), and Gao *et al*. (2007).

In general, the actual values for hot spot stress cannot be determined easily and accurately, alternatively it can be introduced as an estimated value calculated through the extrapolation of the stresses at adjacent points where the stresses can be determined easily. Numerous research efforts have been made on hot spot stress evaluation, and many suggestions given are based on the surface extrapolation technique and fewer on other techniques. The International Institute of Welding (IIW) recommendations for determining the structural hot spot stress are based on the principle of surface extrapolation. Niemi (1995), and Niemi *et al*. (2003) gave detailed recommendations concerning stress determination for the fatigue analysis of welded components and proposed distances of 0.4 and 1 times plate thickness T from the weld toe, also distances 0.5 and 1 times plate thickness for coarser meshes. Yagi *et al*. (1991) proposed a definition of hot spot stress for fatigue design of plate-type structures, and the hot spot stress should be obtained by means of the linear

extrapolation of the specific two points at $1.57\sqrt[4]{T^3}$ and $4.9\sqrt[4]{T^3}$ to the weld toe. Nonlinear extrapolation instead of the linear extrapolation is occasionally applied by considering that the structural stress increase in front of the welded joint occurs with various gradients and nonlinearities (van Wingerde *et al*. 1995).

The second method for determining structural hot spot stress is through thickness-at-weld-toe method. Radaj (1996) demonstrated that structural hot spot stress could be evaluated either by surface extrapolation or by linearization through the pate thickness. Dong (2001) proposed an alternative structural hot spot stress computation method combining the features of the surface extrapolation methods with those of the through thickness methods. Doerk *et al*. (2003) explained and compared various procedures for evaluating structural hot spot stress at different types of welded joints. Poutiainen *et al*. (2004) investigated the limits and accuracy of different methods for hot spot stress determination and compared them with finite element analysis results from simple 2D and precise 3D models. Xiao and Yamada (2004) proposed a new method of determining structural hot spot stress in welded constructions based on the computed stress 1 mm below the surface in the direction corresponding to the expected crack path. This method has an additional advantage of being able to account for the size and thickness effects observed in welded joints when compared to the surface extrapolation technique for structural hot spot stress evaluation.

A lot of research investigations have been carried out in the determination of SCF

and hot spot stress for welded tubular joints. Morgan and Lee (1998a, b) carried out an extensive parametric study of the distribution of SCF for the in-plane moment loading and out-of-plane moment loading cases in tubular K-joints commonly found in offshore platforms and proposed a new equation to determine SCF on the chord and brace. Gandhi and Berge (1998) conducted fatigue tests on seven different T-joints made of circular brace and rectangular chord in constant amplitude axial loading and compared the SCF measured experimentally with those by various existent parametric formulae.

Analytical expressions for SCFs of circumferential welds in tubular joints under consideration of fabrication tolerances were given by Lotsberg (1998). van Wingerde *et al*. (2001) presented simplified design formulae and graphs to facilitate the SCF-determination of K-shaped connections. Mashiri *et al*. (2002, 2004a, b) carried out fatigue tests to investigate the SCF and fatigue behavior of welded thin-walled T-joints made of circular hollow section (CHS) braces welded onto square hollow section (SHS) chords under in-plane bending (IPB). Bian and Lim (2003) determined experimentally hot spot stress and the SCF through the test on hollow section T-joint subjected to both axial and IPB loads. Chiew *et al*. (2004, 2007), and Lie *et al*. (2004) investigated experimentally and numerically the fatigue performance of a cracked tubular T-joint subjected to IPB only, a combination of IPB and out-of-plane bending (OPB), and a combination of axial loading, IPB and OPB, respectively. The hot spot stress distribution along the intersection of chord and brace was carried out by static

tests to determine the peak hot spot stress and its location when the joints were subjected to various load cases. Pang *et al*. (2009) described the determination of SCF of dragline tubular joints through laboratory testing of four full-size dragline tubular joints.

2.3.2 Fatigue Assessment Using Hot Spot Stress Method

Analysis and assessment of the hot spot stress with respect to fatigue has had a rather long history. Pioneering investigations were made in the 1960's by several researchers to relate the fatigue strength to local strain/stress measured at a certain point close to the weld toe (Radaj *et al*. 2006). In 1970's, the development of the hot spot stress approach with the definition of reference points for stress evaluation and extrapolation at certain distances away from the weld toe was reviewed by van Wingerde *et al*. (1995), which was particularly successful for the fatigue strength assessment of tubular joints. First attempts to apply the approach to welded joints at plates were seen in the early 1980's, and CEN (1992) extended the hot spot stress approach to plate-type structures due to the increasing demand although only limited guidance was provided (Poutiainen *et al*. 2004). Up to now, the hot spot stress approach has been well accepted and recommended by several national and international codes and standards (ECCS 1985; CEN 1992; API 1993; BSI 1993; AWS 1998; IIW 2000).

Little research has been performed on the application of the hot spot stress approach to fatigue damage evaluation of the welded plate joint of steel structures, especially for cable-supported steel bridge fatigue evaluation (Chan *et al*. 2005). Miki and Tateishi (1997) studied the fatigue strength and local stress for cope hole details existing in I-section beams by fatigue test, stress measurement and stress analysis and proposed a simple equation for estimation SCF based on the results of finite element analysis which was verified by experimental results and confirmed to be accurate. Savaidis and Vormwald (2000) investigated numerically and experimentally the hot spot stress and fatigue life of four different welded joints from the floor structure of city buses under bending and tensional cyclic loadings. Han and Shin (2000) derived a consistent and unified *S-N* curve by using the hot spot stress approach through a numerical and experimental analysis which can be applied for fatigue strength estimation and fatigue design for general welded steel structures. Chan *et al*. (2003, 2005) reported that the hot spot stress approach gave a more appropriate fatigue life prediction than the nominal stress approach for a steel suspension bridge.

2.4 Reliability-Based Fatigue Condition Assessment

In October, 1945, a paper entitled “The Safety of Structures” appeared in the Proceedings of the ASCE. This historical paper was written by A. M. Freudenthal, and its purpose was to analyze the safety factor in engineering structures in order to

establish a rational method of evaluating its magnitude. It was selected for inclusion with many discussions in the 1947 Transactions of the ASCE (Freudenthal 1947). The publication of this paper marked the beginning of structural reliability studies in the United States (ASCE Committee on Fatigue and Fracture Reliability 1982a). Over the past several decades, the concepts and methods of structural reliability have developed rapidly and become more widely understood and accepted. There have been a lot of studies and applications (Rackwitz and Fiessler 1978; Liu and Kiureghian 1991; Das 1998; Frangopol *et al*. 1998; Frangopol and Imai 2000; Imai and Frangopol 2000; Stewart 2001; Ang and DeLeon 2005) and comprehensive books (Benjamin 1970; Ang and Tang 1975; Thoft-Christensen and Baker 1982; Ang and Tang 1984; Kececioglu 1991a, b; Ditlevsen and Madsen 1996; Haldar and Mahadevan 2000a, b; Ayyub and McCuen 2003; Hurtado 2004) on reliability-based structure analysis.

Fatigue reliability evaluation is a very important task for the design and management of bridges. For highway and railway bridges, the techniques of fatigue reliability have been applied mainly in (Lukic and Cremona 2001): (i) condition assessment and estimation of the remaining lifetime of bridges, where probabilistic methods can be used to obtain estimates of the adequacy of the existing structure, need for increased inspection in the future to prevent failure, and approximate remaining fatigue lifetime based on projections of the future loads; and (ii) development of probability-based design stress ranges for fatigue-critical bridge components, where

accurate traffic load data can be acquired through weigh-in-motion (WIM) systems, from which an extensive amount of data are available showing distribution of load by its time of appearance, transversal position, speed, number of axles, gross weight of axles, and distance between axles.

Most of the research work on reliability-based fatigue analysis has focused on steel bridges. A comprehensive literature review on the existing fatigue reliability approaches for reassessment of steel structures, including railway and highway bridges, is available in Byers *et al*. (1997a, b). The general approach for analyzing reliability against fatigue failure is first to formulate a mathematical model, whether on the basis of mechanics or extensive observations of the phenomenon, which incorporates as many of the variables as practical that are known to affect fatigue behavior. The probabilistic and statistical analysis method then is performed within this provided analytical framework.

2.4.1 Fatigue Reliability Assessment from Field Data

Field monitoring has proven to be an effective method for the evaluation of integrity and estimation of fatigue reliability of structures. In most applications, it requires a complete live load history of the structure achieved through a comprehensive field data compilation for the reliability analysis of fatigue-critical structures. A continuous monitoring process used to compile load data and update the information

on fatigue reliability is costly and may not be easily applicable or economically viable for all types of structures. An alternative process will be a limited amount of data that can be assumed to represent the load population.

An effective method for computing fatigue damage to critical bridge components is through field stress range data. The data generally contain a reasonable pool of all potential stress ranges applied on the bridge which constitute a major component of fatigue reliability assessment process (Mohammadi and Polepeddi 2000). The installation of gauges at critical locations on steel girders of the bridge requires no alteration to the bridge and can be achieved without closing the bridge to the traffic. The strain data compiled can be converted into stress ranges and arranged in the form of frequency diagrams as the data acquisition process is in progress by means of a data compression and reduction process with a cycle counting technique. A major issue in compiling data to construct stress range frequency is the duration of the data acquisition process. In highway bridges, a two- or three-day period is satisfactory and five- to ten-day period for railway bridges (Mohammadi *et al*. 1998). During this period nearly all stress ranges, experienced by a critical component in a bridge, are captured.

Preferably, the data acquisition device should be left running continuously to capture the effect of day and night traffic, and empty and full trucks. To include seasonal changes in traffic patterns, the data acquisition process may have to be conducted in

several two- or three-day sessions at various times during a year. Longer periods of data compilation will be needed when a bridge is subject to frequent overload conditions. However, if the complied data are only for a limited number of days, fatigue damage estimation for a given period of time requires additional information pertinent to the bridge and roadway. The average daily traffic, annual traffic growth and distribution of trucks by lanes are among important information needed to complete the fatigue damage estimation.

Issues in conducting a fatigue reliability analysis from field data have been summarized as follows (Mohammadi 1995; Mohammadi 2001): (i) the method of fatigue damage estimation; (ii) the number of parameters for which data must be compiled; (iii) type of data needed; (iv) data processing method; and (v) the duration of data acquisition session. Although the live load stress data appears to be the most important parameter for which data must be compiled, fatigue reliability analysis can benefit from data on other parameters as well. With a careful planning, other structural parameters can also be included in a data acquisition process with a marginal additional cost and extra effort. A reliability-based inspection scheduling procedure can yield an optimal inspection schedule and can maintain a specified safety level for fracture-critical members in steel bridges through their planned service lives. This procedure is based, in sequence, on a stress range analysis, a fatigue reliability analysis, and an optimization analysis (Chung *et al*. 2003; Chung *et al*. 2006).

2.4.2 Stress-Life Fatigue Analysis Models

Fatigue data are obtained by cycling test specimens at constant-amplitude stress until visible cracking occurs. Such tests are repeated several times at different stress levels to establish the *S*-*N* curves. Running fatigue tests is an expensive and time-consuming process and curve fitting of fatigue data is also time-consuming. Fatigue analytical models can link theoretical ideas with the observed data to provide a good prediction of future observations. WÖhler was the pioneer researcher who tried to quantify fatigue strength based on the results of experiments on the endurance of metals, and investigated the fatigue failure in railroad axles for German Railway Industry. His work also led to the characterization of fatigue behavior as the applied stress versus the cycles to failure and to the concept of fatigue limit (Al-Rubaie 2008).

Basquin (1910) represented the finite life region of the WÖhler curve as log*N* on the abscissa and log*S* on the ordinate. The Basquin function can be represented mathematically as

$$NS^m = A \tag{2.1}$$

or

$$\log N = -m \log S + \log A \tag{2.2}$$

where m and A are positive empirical material constants. Obviously, log$A$ and m are the intercept on the log$N$ axis and constant slope of Equation (2.2), respectively.

Considering the existence of fatigue limit, Stromeyer (1914) modified Equation (2.2) by introducing an extra parameter F_l as

$$\log N = -m\log\left(S - F_l\right) + \log A \tag{2.3}$$

In cases where the optimum value of the parameter F_l is negative or insignificant, it should be omitted since F_l represents the fatigue limit stress.

To show the effect of stress ratio R_s or mean stress S_m on fatigue life, Walker (1970) proposed the equivalent stress S_q model which is given by

$$\log N = -m\log\left(S_q - F_l\right) + \log A \tag{2.4}$$

where

$$S_q = S(1 - R_s)^C \tag{2.5}$$

Since

$$S_m = \frac{S}{2}\left(1 + R_s\right) \tag{2.6}$$

substituting R_s in Equation (2.5) with S_m, gives

$$S_q = S(2 - \frac{2S_m}{S})^C \tag{2.7}$$

where C is a constant parameter.

2.4.3 Fatigue Reliability Assessment Using S-N Approach

Fatigue load and resistance are two main variables when the *S-N* method is chosen for developing fatigue reliability analytical models. The *S-N* curves are the most traditional way to define the fatigue strength of a material. There has always been a great deal of scatter in the data characterizing the fatigue strengths of various details. The scatter resulting from the experimental tests available allows statistical treatment of the results and helps propose the best-fit *S-N* curve for a required safety level. In the fatigue tests carried out under variable-amplitude stress increments, the Palgrem-Miner hypothesis may be used due to its simplicity although it may err in neglecting loading sequence. The failure happens when the final summation of the elementary damage reaches a determined value, which is a random variable and generally equal to unit as a deterministic value. The fatigue load is generally obtained by means of measurements or simulations. In the process of *S-N* curve-based fatigue life analysis, the stress spectrum is obtained by extracting the stress range and cycle from a measured or simulated stress time history with a suitable cycle counting method. **Figure 2.2** illustrates the fatigue reliability analysis framework based on the *S-N* curve method.

The fatigue load model should be determined not only by magnitude but also by

frequency of occurrence which can be obtained by WIM measurements (Wang *et al*. 2005; Chotickai and Bowman 2006), and resistance model should be derived from a lot of fatigue tests under varying amplitude loading (Nowak and Szerszen 1999; Szerszen *et al*. 1999). Usually, the lognormal distribution and the Weibull distribution are used for load and strength probability distribution (Wirsching and Yao 1970; Ellingwood 1982; Zheng *et al*. 1995; Yan *et al*. 2000; Jakubczak *et al*. 2006). Murty *et al*. (1995) proposed a method to deal with the derivation of the fatigue strength distribution as a function of number of cycles to failure. Zhao *et al*. (2000) developed an approach to determine an appropriate distribution from four possible assumed distributions of the fatigue life under limited data. Loren (2004) presented a model for calculating the fatigue limit distribution based on the inclusion size.

Research efforts have been devoted by a number of investigators for modeling the stress range data by using various single theoretical probability distributions. Based on 106 recorded stress range histograms, Yamada and Albrecht (1976) presented that the probability distribution of dimensionless stress range normalized by the maximum stress range could be expressed by a polynomial distribution. In order to select a single non-dimensional mathematical expression that can be used to represent the stress histogram of highway bridges, a continuous two-parameter Rayleigh curve was used to model the probability distribution of stress range in the fatigue test program (Schilling *et al*. 1978). Wirsching (1984) assumed that the

long-term stress range data were Weibull distributed and Madsen (1984) took the nominal stress range as a random variable with normal distribution. Beta distribution has been suggested as a theoretical stress range distribution model to describe the field data by Ang and Munse (1975) and Walker (1978). Park *et al*. (2005) successfully expressed that the stress range frequency distribution of 400 block loadings by a lognormal probability distribution.

There have been a number of studies on the reliability analysis for fatigue damage and life prediction of bridges (Crespo-Minguillon and Casas 1998; Cho *et al*. 2001; Kim *et al*. 2001; Pourzeynali and Datta 2005) and other types of structures (Ricles and Leger 1993; Zhao *et al*. 2000; Ang *et al*. 2001; Tovo 2001; Amanullah *et al*. 2002; Liu *et al*. 2008). Deoliya and Datta (2001) presented a reliability analysis of antenna towers against cumulative fatigue damage failure for the gustiness of wind by the *S*-*N* curve approach using the Miner's fatigue damage rule and the reliability against fatigue damage failure was obtained using both the first-order second-moment method and a full distribution procedure. Park and Tang (2006) developed an algorithm which combined the accumulated damage analysis with first-order reliability method (FORM) to evaluate fatigue reliability by determining a reliability factor using an inverse reliability analysis which could then be used to generate a reliability related *S*-*N* curve family for evaluating the relationship between mission life and desired reliability. Goode and van de Lindt (2007) presented the process and results for the development of a reliability-based design procedure for

high-mast lighting structural supports subjected to wind load. Imam *et al*. (2008) presented a probabilistic fatigue assessment methodology for riveted railway bridges and applied this method to a typical, short-span, riveted U.K. railway bridge under historical and present day train loading.

2.5 Identified Key Issues

Steel bridges are subjected to a large number of repetitive loadings of different magnitudes caused mainly by the passage of vehicles. They are expected to be vulnerable to fatigue-related damage and failure, and it is therefore essential to assess the fatigue behavior of structural components especially welded details in steel bridges. Among the current fatigue analysis methodologies, the nominal stress-life (*S-N*) approach has widely been used for fatigue-related design and evaluation of aircraft, offshore structures, and steel bridges (Schilling *et al*. 1978; Moses *et al*. 1987; Mohammadi *et al*. 1998; Connor and Fisher 2006; Albrecht and Lenwari 2009). When the nominal stress-life approach stipulated in specifications is adopted for bridge fatigue damage and life evaluation, it is necessary to know the stress spectra of welded details in critical locations and the *S-N* curves of the details.

The stress spectra can be acquired from a theoretical stress analysis by assuming a fatigue loading model and a structural model. Currently, most of the existent fatigue load models usually are assumed based on the specifications or obtained from the

measured data for a relatively short time, and seldom constructed according to the statistical treatment of the long-term measured data under actual traffic conditions. As to the structural model, the uncertainties in the material properties, geometrical configurations, and boundary conditions cannot be entirely considered although the finite element technique provides a powerful tool in structural modeling and analysis. Therefore, the accuracy of the simulated stress may be very limited and a significant discrepancy between the theoretical stress analysis results and field measured data is existing (Mohammadi and Polepeddi 2000). The consequence of inaccurate estimation of the stress spectra would be significant in view of the fact that the predicted fatigue life is inversely proportional to at least the cube of the stress range (Gurney 1992).

Experience from bridge engineering practices has indicated that fatigue analysis based on specification loads and distribution factors usually underestimates the remaining fatigue life of existing bridges by overestimating the live load stress ranges. Fatigue evaluation based on field-measured stress range histograms under actual traffic load proves to be a more accurate and efficient method for existing bridges. This can be achieved by using NDE technologies such as the load-controlled diagnostic load testing and short-term in-service monitoring. However, most of these strategies are encountered with the problems either in disturbing the normal operation of the tested bridge or only procuring limited data under normal traffic conditions with a designated time period. Particularly, the NDE technologies are

impossible to be performed and thus incapable of recording the field strain time history data under extreme conditions, such as typhoon, earthquake, and ship collision.

Long-term SHM has increasingly become an important tool for diagnosing and prognosing the structural health condition and safety evaluation of bridges. With an instrumented bridge health monitoring system (BHMS), the continuously field-measured dynamic strain data are attained and transferred into the stress spectra resulting from the actual traffic and environmental conditions. The achieved stress spectra will provide the most authentic and practical data for fatigue performance assessment especially for decision-making on bridge inspection and maintenance actions. Unfortunately, a review of the literature indicates that the research work on fatigue life assessment of bridges based on long-term monitoring data is limited.

After transforming the stress time histories into stress spectra, the fatigue damage can be estimated by use of the Miner's damage cumulative rule in combination with the inherent structural fatigue endurance if the recorded stress time histories are long enough so as to contain adequate stress cycles with high stress ranges. When relatively short stress time histories are exclusively available, it is necessary to model the distribution of the stress range in the rainflow domain with a continuous PDF in order to adequately represent the stochastic stress states and extrapolate to the region which was not covered by the measured data. Also, the development of stress range

distribution function is a fundamental requirement for conducting the structural reliability evaluation of the structural component under stochastic loadings, in particular in the fatigue reliability assessment by making use of a continuous probabilistic formulation of the Miner's rule. While the stress distribution function is not easily formulated due to the scatter of the data, a common theoretical distribution model is usually assumed (Ang and Munse 1975; Yamada and Albrecht 1976; Walker 1978; Madsen 1984; Wirsching 1984; Park *et al*. 2005). On the other hand, when the mean stress also needs to be considered in the estimation of the fatigue damage (Susmel *et al*. 2005), the extraction of the stress spectra from the stress time histories is performed with a two-parametric rainflow method and each stress cycle is then represented with two components: the stress range and the mean stress. Then, the stress spectrum is defined by the corresponding rainflow stress matrix with relative frequencies in the two-dimensional space, and a continuous multivariate PDF is needed to be explored for modeling the distribution of the extracted stress spectra.

Due to the limitation of sensor implementation techniques and specific in-situ conditions, however, the sensors for strain monitoring usually are not deployed at the most critical locations where fatigue cracks are expected to occur and thus only the nominal strain/stress is obtained. To handle such a critical problem, the hot spot stress approach which takes into account the dimensions and stress concentrating effects at the critical details has been well investigated. As a significant factor in fatigue design and life prediction of welded structures using the hot spot stress

method, a theoretical SCF is traditionally defined as the ratio of the hot spot strain/stress in the area of a discontinuity or other stress raiser to the corresponding nominal strain/stress, and it is an indication of the effect of stress concentrators on structural components and members. In the past years, a significant number of studies have been conducted on the determination of SCF and the derivation of its experiential formulae for different kinds of structural joints by means of the finite element analyses and experimental measurements, and most of which are focused upon the modeling and analysis of welded offshore tubular joints. Only little research has been devoted to investigating the properties of SCF for the welded plate joints of large-scale civil engineering structures, especially for cable-supported steel bridges.

Moreover, the determination of SCF is an extraordinarily complicated process involving considerable effects and sources of uncertainties such as geometrical and material parameters, weld irregularity and quality, and loading cases and combinations, so that the SCF has a nature of randomness subjected to the stochastic behavior of the complex operating conditions. Unfortunately, it is not a topic that has received a great deal of attention from the research community especially on the quantitative descriptions of the stochastic characteristics and distribution functions of SCF. Alternatively the SCF is presumed to be a random variable with an assumed probability distribution (Madsen 1984). Generally, its exact distribution can be obtained and verified by conducting FEM simulation and local laboratory model experiment or field test with a combination of a hot spot stress extrapolation or

regression procedure.

In recognition of uncertainty and randomness inherent in the nature of fatigue phenomenon and field measurement data, investigations for probabilistic assessment of fatigue life have been carried out and most of them have focused on the usage of the *S-N* curve procedure (Crespo-Minguillon and Casas 1998; Szerszen *et al*. 1999; Cho *et al*. 2001; Kim *et al*. 2001; Pourzeynali and Datta 2005). Only a very limited amount of research is available on monitoring-based fatigue reliability assessment. The lack of such studies is mainly due to the challenging nature that a continuous monitoring process for compiling external load and structural response data and updating the structural performance against fatigue is costly and may not be easily applicable or economically viable for all types of structures (Mohammadi 2001; Ni *et al*. 2006). Furthermore, most fatigue reliability probabilistic models catering for the *S-N* curve method have been developed on such as fatigue resistance, stress range, and stress cycle. However, the incorporation of SCF in fatigue reliability modeling for probabilistic fatigue life assessment has scarcely been addressed.

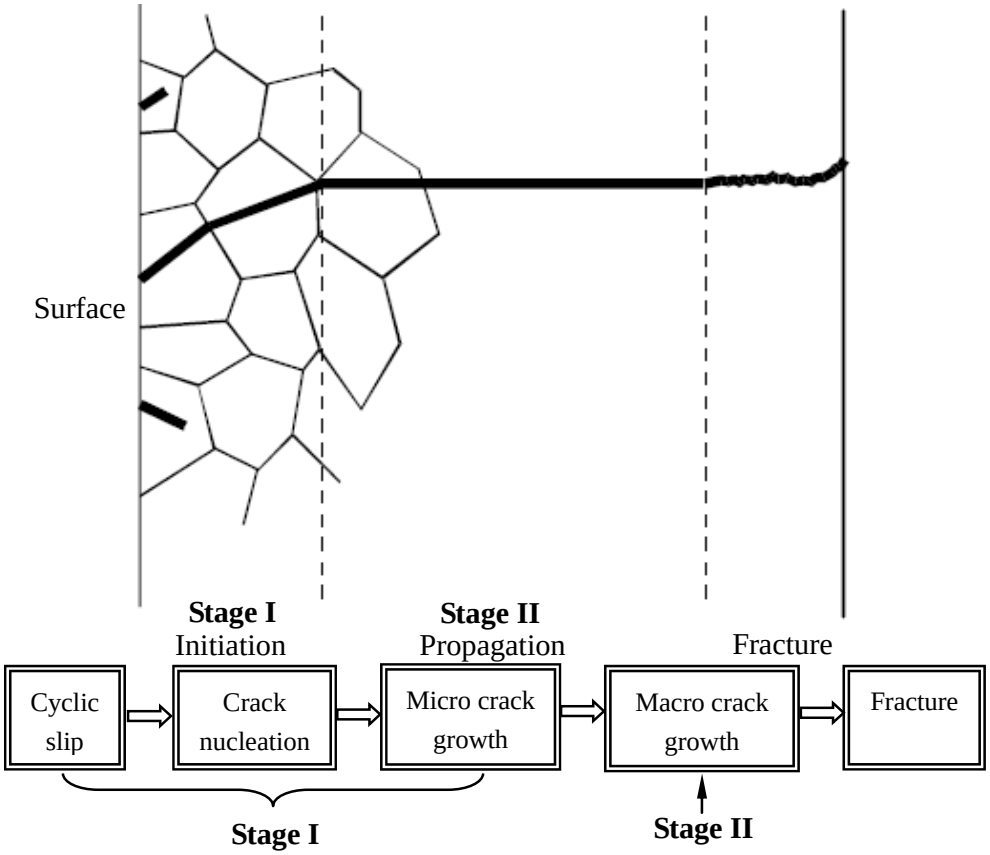

Figure 2.1 Illustration of the two-stage mechanism of fatigue failure

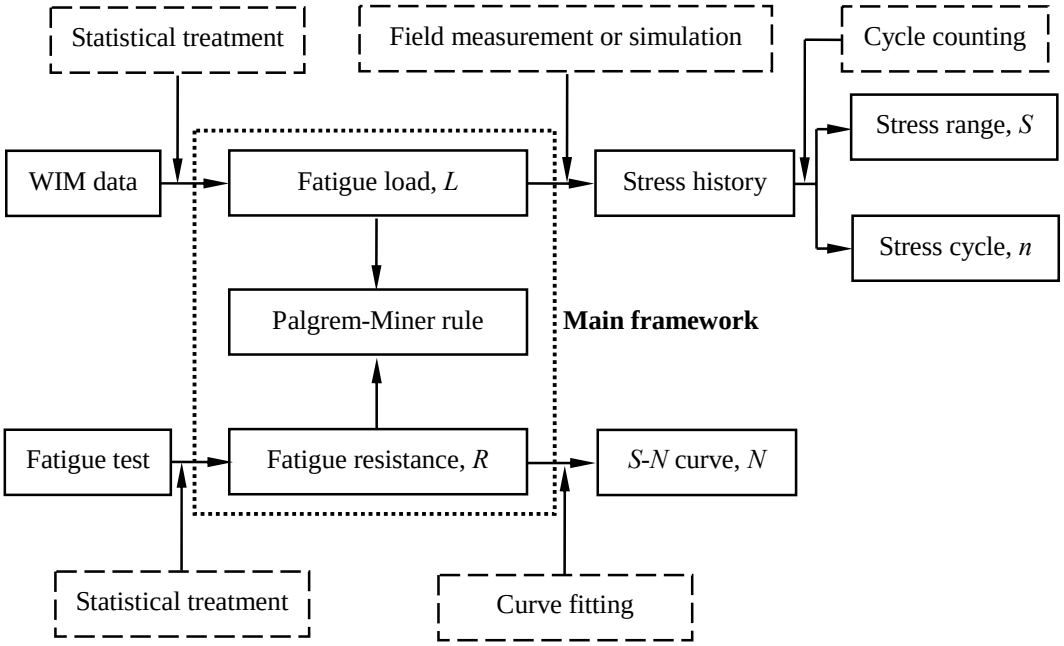

Figure 2.2 Framework for *S*-*N* curve-based fatigue reliability analysis

Table 2.1 Summary of type and number of failures of 230 failed components

Cause	Type of Failure							
	Fatigue	Overload	Stress corrosion or hydrogen embrittlement	Corrosion	Stress rupture	High-temperature oxidation	Wear or excessive deformation	Total
Improper maintenance	52	18	11	4	0	2	15	102
Fabrication defects	31	6	0	1	0	1	0	39
Design deficiencies	24	5	4	1	1	1	1	37
Defective material	10	3	1	0	0	0	1	15
Abnormal service	13	7	1	0	2	0	0	23
Undetermined	11	2	1	0	0	0	0	14
Total	141	41	18	6	3	4	17	230

CHAPTER 3

MONITORING-BASED FATIGUE LIFE ASSESSMENT OF STEEL BRIDGES ACCOUNTING FOR BOTH TRAFFIC AND TYPHOON EFFECTS

3.1 Introduction

In the past decade, a sophisticated long-term SHM system, named wind and structural health monitoring system (WASHMS) (Wong 2004; Wong and Ni 2009), has been devised and implemented by the Highways Department of the Hong Kong Special Administrative Region Government to monitor and evaluate the structural health conditions of five cable-supported bridges in Hong Kong, including the suspension TMB, the cable-stayed Kap Shui Mun Bridge (KSMB), the cable-stayed Ting Kau Bridge (TKB), the cable-stayed bridge on HSWC (Hong Kong – Shenzhen Western Corridor), and the cable-stayed Stonecutters Bridge (SCB).

This on-line monitoring system is devised based on modular architecture, and is composed of six functional modules, namely: (i) module 1 – sensory system (SS), (ii) module 2 – data acquisition and transmission system (DATS), (iii) module 3 – data

processing and control system (DPCS), (iv) module 4 – structural health evaluation system (SHES), (v) module 5 – structural health data management system (SHDMS), and (vi) module 6 – inspection and maintenance system (IMS).

The durability of a steel bridge is mainly dominated by fatigue behavior of its critical components since they are subjected to a large number of repetitive loadings of different magnitudes caused mainly by the passage of vehicles. Therefore, an accurate estimation of the actual status on fatigue damage and remaining life of the critical components of bridge structures is of vital importance, which is necessary for the bridge administration to make cost-effective decisions regarding inspection, maintenance, and repair. The instrumented SHM system on a bridge is capable of continuously providing huge amounts of monitoring data for reliably assessing the structural health and condition of the bridge. As a paradigm of integrating SHM data into structural condition evaluation practice, the measurement data of dynamic strain/stress are of great value in achieving the authentic field-based stress spectra for conducting fatigue life assessment of steel bridges.

In this chapter, long-term monitoring data from the instrumented TMB carrying both highway and railway traffic are used to carry out fatigue life assessment of the fatigue-prone welded details. The daily stress spectra at a specific location are procured using field-measured strain time history data and rainflow counting algorithm. It is found that the stress spectra obtained in different days under normal

traffic and wind conditions are similar, and thus a standard traffic-stress spectrum is obtained by averaging an appropriate number of daily stress spectra. A standard typhoon-stress spectrum is also derived using the field-measured data during typhoon periods. Then, a standard daily stress spectrum accounting for highway traffic, railway traffic, and typhoon effects is achieved by synthesizing the two kinds of stress spectra in accordance with the proportion of typhoon days in one year. The optimal number of daily strain data for derivation of a standard daily stress spectrum is determined by examining the effect of different influencing factors on the predicted fatigue life, including the number of daily strain data, weekend and workday traffic variations, and seasonal changes in traffic patterns. With such an obtained standard daily stress spectrum, the fatigue life of the welded detail in concern is evaluated according to the fatigue life assessment procedure stipulated in BS5400 specification.

3.2 TMB and its SHM System

The TMB, as shown in **Figure 3.1**, is a steel suspension bridge with a main span of 1377 m and an overall length of 2160 m. It carries a dual three-lane highway on its upper level of the bridge deck while two railway tracks and twin single-lane sheltered carriageways are located on the lower level within the bridge deck. As a combined highway and railway transport connection between Tsing Yi Island and Lantau Island, it forms a key part of the most essential transportation network linking

the Hong Kong International Airport to the urban areas.

After completing construction in 1997, a long-term monitoring system has been installed and operated on the TMB, which consists of 283 sensors in eight types, namely, anemometers, servo-type accelerometers, temperature sensors, dynamic strain gauges, global positioning systems (GPSs), displacement transducers, level sensors, and dynamic WIM sensors. As part of this monitoring system, 110 weldable foil-type strain gauges were installed to measure the change in strain of structural members under different loading conditions. As shown in **Figure 3.1**, the locations of strain gauges include the rail track section at Chainage (CH) 24662.5, bridge-deck trough section at CH24664.75, deck at tower and rocker bearing links at CH23623, and bridge-deck section at CH23488. Most of the strain gauges were attached to the fatigue-prone portions which were identified during the design of WASHMS (Flint and Neil Partnership 1998).

3.3 Strain Measurement Data from SHM System

In order to assess the fatigue condition of the whole bridge, one-year (the year of 1999) monitoring data of dynamic strain from all the 110 strain gauges have been acquired for strain-based fatigue and condition assessment. The fatigue life evaluation for the monitored detail by the strain gauge SSTLS13 on the rail track section at CH24662.5 is presented herein. **Figure 3.2** illustrates the location of the

strain gauge SSTLS13 which was installed under the bottom flange of the railway beam composed of two inverted T-beams welded to the top flange plate, denoted as Detail H in **Figure 3.2(a)**. **Figure 3.2(b)** shows the sectional view of Detail H.

3.3.1 Strain Measurement Data under Normal Traffic and Wind Conditions

The strain data were recorded continuously at a sample frequency of 51.2 Hz. **Figure 3.3** illustrates four typical daily strain time histories obtained from the strain gauge SSTLS13 under normal traffic and wind conditions. **Figure 3.4** shows one-hour strain data on September 24, 1999. By examining the measured data, the following observations are made:

(i) The amplitude of strain cycles is varying from time to time, indicating that the bridge is subject to variable-amplitude loadings during its service time. Each pulse in the strain-time curve corresponds to a stress cycle which will generate accumulative fatigue damage;

(ii) The daily strain-time curves exhibit some common characteristics in the shape of curves and magnitude of cycles, and there are almost no strain pulses from 1:30 am to 5:30 am since the airport railway ceases its daily service during this time period;

(iii) Many strain pulses with large amplitudes are observed in each daily strain time history, which are the strain responses caused by train traffic; and

(iv) The overall drift of the strain-time curve is significant, which is attributed to

the environmental factors such as temperature and solar radiation. This drift does not influence the calculation of stress range since the stress range depends only on the difference between the peak and the valley of each stress cycle.

3.3.2 Strain Measurement Data under Typhoon Conditions

The TMB is located at a region with typhoon wind climate. In 1999, totally five typhoons named “Leo”, “Maggie”, “Sam”, “York”, and “Dan” buffeted Hong Kong as illustrated in **Figure 3.5**. **Table 3.1** lists the typhoon warning signals in 1999 issued by the Hong Kong Observatory. The wind response data under typhoon conditions were measured by the digital ultrasonic anemometers which were deployed on the north and south sides of the bridge deck at the middle of the main span of the TMB. Each ultrasonic anemometer is able to measure three components of wind velocity simultaneously.

Figure 3.6 shows the 10-minute mean wind speed and direction, respectively, obtained from the north anemometer denoted as WITJN01 on August 22, 1999 during typhoon “Sam”. The wind direction is measured from east anti-clockwise. It is seen from **Figure 3.6** that the maximum 10-minute mean wind speed was 24.03 m/s at about 15:40, August 22, 1999 during typhoon “Sam”.

The strain time history data were recorded by the monitoring system for the bridge during typhoon attacks. These data are invaluable for the analysis of typhoon-induced fatigue because they are very limited up to now. It is difficult to carry out field testing when a typhoon passes over the bridge since usually all actions on the bridge have to be stopped during a typhoon. For the TMB, trains across the bridge to the Hong Kong Airport are still in service during a typhoon attacking Hong Kong.

Figure 3.7 gives typhoon "Sam" induced strain time history on August 22, 1999 at the location of the strain gauge SSTLS13. It is observed that the strain time history due to typhoon, when the road was closed, has a pattern different from that under normal traffic and wind conditions as shown in **Figure 3.3**. A further observation into **Figure 3.7** reveals that the strain values obtained during 12:30 ~ 16:00 are larger than others, which matches the track and the time of typhoon "Sam" passing over the TMB. **Figure 3.8** shows one-hour strain data on August 22, 1999, which reveals that the typhoon induced strain-time curve has much more cycles of strain range with large amplitudes than that obtained under normal traffic and wind conditions as illustrated in **Figure 3.4**.

3.4 Statistical Analysis of Stress Spectrum

3.4.1 Rainflow Cycle Counting Technique

When the strain time histories recorded by the strain gauge SSTLS13 are available, the stress time histories at the same location are obtained through simply multiplying the measured strain data by the elasticity modulus of steel since the strains are elastic. As illustrated in the above sections, it can be easily observed that the strain time histories are composed of many pulses of strain due to the random and dynamic characteristics of the loadings applied on the bridge, and hence it is difficult to define a stress cycle directly. In order to predict the fatigue life of the structural component monitored by the strain gauge SSTLS13, it is therefore necessary to use a cycle counting method to perform a data reduction process by transferring the complex irregular stress histories into a set of constant stress range frequency data (stress spectrum). A stress spectrum contains two elements which are referred to as the stress range (*S*-value) and the number of cycles corresponding to each specified stress range (*n*-value).

Some cycle counting techniques are available, including peak counting, mean-crossing peak counting, level-crossing counting, simple range counting, range-mean counting, and rainfow cycle counting (Dowling 1972). Among them the rainflow cycle counting method is the most widely used which was first presented by Matsuishi and Endo to the Japan Society of Mechanical Engineers in 1968 (Matsuishi and Endo 1968). Downing and Socie (1982) developed one of the most widely referenced and utilized rainflow counting algorithms in 1982, which was included as one of the cycle counting algorithms in the American Society for Testing

and Materials (ASTM) specification. The rainflow cycle counting method has a fundamental physical characteristic of its compatibility with the corresponding stress-strain relation by simply extracting stress amplitudes and cycles in the stress time history associated with closed hysteresis loops, as shown in **Figure 3.9**.

Figure 3.10 illustrates the schematic of rainflow cycle counting method. The basic procedures of rainflow cycle counting method are as follows: (i) reduce the stress time history to a sequence of tensile peaks and compressive troughs; (ii) imagine that the stress time history with lines joining the peaks and valleys is a template for a rigid sheet (pagoda roof); (iii) turn the sheet clockwise 90^0 (earliest time to the top) and the stress time history is plotted so that the time axis is vertically downwards; (iv) each tensile peak is imagined as a source of virtual rain that "drips" down the pagoda and a complete cycle or a half cycle of stress is defined by the path of the rain flow; (v) count the number of half-cycles by looking for terminations in the flow occurring when either: (1) it reaches the end of the stress time history, (2) it merges with a flow that started at an earlier tensile peak, or (3) it flows opposite a tensile peak of greater magnitude; (vi) repeat step (v) for compressive troughs; (vii) assign a magnitude to each half-cycle equal to the stress difference between its start and termination; and (viii) pair up half-cycles of identical magnitude (but opposite sense) to count the number of complete cycles. Typically, there are some residual half-cycles.

3.4.2 Derivation of Standard Daily Stress Spectrum

In this section, the rainflow counting algorithm is used to obtain the daily stress spectra using the strain time histories from the strain gauge SSTLS13. After specifying a resolution for the stress range interval, a histogram of the stress spectrum is obtained. The resolution for the stress range interval is chosen as 1 MPa and 0.1 MPa herein, and four typical daily stress spectra under normal traffic and wind conditions are illustrated in **Figure 3.11**. The stress cycles with amplitudes less than 2 MPa are discarded because the lower valid limit of the strain gauge is 10 micro-strains. In fact, the resolution for the stress range interval is not sensitive to evaluating the fatigue life because it only affects the shape of the spectrum but does not affect the effective stress range as defined by Schilling *et al*. (1978).

An insight into **Figure 3.11** reveals that the daily stress spectra are similar for different days experiencing normal traffic and wind conditions. It is therefore reasonable to average a number of daily stress spectra resulting from different days to obtain a standard traffic-stress spectrum, as shown in **Figure 3.12**. Also, a standard typhoon-stress spectrum can be derived using the strain measurement data obtained under typhoon conditions, which is shown in **Figure 3.13**. It is observed from **Figure 3.13** that the stress spectrum under typhoon conditions has a pattern of approximate Rayleigh distribution which is different from that under normal traffic and wind conditions, as observed by Li *et al*. (2002).

After obtaining the standard traffic-stress spectrum and the standard typhoon-stress

spectrum, a standard daily stress spectrum can be achieved by proportionally combining the two standard stress spectra accounting for both traffic (highway and railway) and typhoon effects. With such a standard daily stress spectrum, the fatigue life of the structural component monitored by the strain gauge SSTLS13 can be evaluated by regarding that the monitored detail is suffered from a block of daily repeated cycles corresponding to the obtained standard daily stress spectrum. The determination of optimal number of daily strain data for derivation of a standard daily stress spectrum will be described in the following section.

3.5 Monitoring-Based Fatigue Life Assessment

3.5.1 Presentation of Procedure

BS5400 Part 10 (BSI 1980) is a commonly adopted standard for bridge design, which specifies methods for fatigue damage and life assessment. The TMB was designed according to this standard. Therefore, the fatigue life evaluation will also be carried out based on BS5400 Part 10. All methods for fatigue design and assessment described in BS5400 Part 10 are based on the Miner's rule for fatigue damage accumulation, which is expressed by

$$D = \sum_i \frac{n_i}{N_i} \tag{3.1}$$

where D is the fatigue damage accumulation index; n_i is the specified number of

cycles for the ith stress range, S_i; and N_i is the corresponding number of cycles to failure for the ith stress range.

As described in the above sections, the stress ranges and the corresponding number of cycles suffered by the structural components are obtained by rainflow cycle counting of the strain measurement data. It is found from the stress spectra, as illustrated in **Figure 3.11**, that the TMB is subjected to a very large number of relatively small stress ranges. This is a common situation for bridge structures (AASHTO 1990). The method to treat the low stress ranges recommended by BS5400 is to reduce the number of repetitions of each stress range less than the fatigue limit, S_0, by multiplying a reducing factor, λ_i, which is defined as

$$\lambda_i = \begin{cases} (S_i / S_0)^2 & \text{if } S_i < S_0 \\ 1 & \text{if } S_i > S_0 \end{cases} \tag{3.2}$$

In order to calculate the cumulative fatigue damage on the structural component by the Miner's rule, the number of repetitions to failure of the specified stress range is needed and obtained from the *S*-*N* curves or *S*-*N* relationships, which are established from the experimental results for different materials or connection details. In BS5400 the *S*-*N* relationships have been established from statistical analyses of available experimental data (using linear regression analysis of log*S* and log*N*) with minor empirical adjustments to ensure compatibility of results between various categories. The equation is given as

$$N \times S^m = K_0 \times \Delta^d \tag{3.3}$$

where m is the inverse slope of the mean-line log$S$-log$N$ curve; K_0 is a constant relating to the mean-line log$S$-log$N$ curve; Δ is the reciprocal of the anti-log of the standard deviation of log$N$; and d is the number of standard deviations below the mean-line log$S$-log$N$ curve, which is also called the probability factor of which different values correspond to different probabilities of failure.

For the purpose of fatigue assessment, each construction detail subject to fluctuating stress should, where possible, have a particular class designated in BS5400. The detail of the weld joint near to the strain gauge SSTLS13 is shown in **Figure 3.2**. It is categorized as class F_2. The S-N relationships designated in BS5400 for different detail classes are shown in **Figure 3.14**.

By use of the Miner's rule, the total cumulative fatigue damage generally should not be greater than unity; otherwise the structural component will be considered to have fatigue failure. As the standard daily stress spectrum is an average value on daily stress cycles, the Miner's summation will represent the cumulative fatigue damage generated per day on the structural component. The fatigue life is a period for the fatigue damage to reach a critical value, if the critical value of the fatigue damage is equal to 1, the fatigue life, F, in the number of year, will be expressed by

$$F = \frac{1}{365 \times \sum_i \frac{\lambda_i n_i}{N_i}} \tag{3.4}$$

In summary, a flowchart of monitoring-based fatigue life assessment method in accordance with BS5400 is shown in **Figure 3.15**.

3.5.2 Determination of Optimal Number of Daily Strain Data

A major issue in converting the field strain data to construct stress range frequency is the duration of the data acquisition process. In general, a two or three-day period for highway bridges and five to ten-day period for railway bridges is satisfactory since during this period nearly all stress ranges experienced by a critical component in a bridge are captured (Mohammadi *et al*. 1998). For the TMB, which contains not only highway but also railway traffic, the strain data have been recorded continuously by the long-term SHM system. It will provide a good chance for establishing a realistic representation of all stress ranges and their frequencies. However, it is impractical and impossible to take all the daily strain data into account for the fatigue life evaluation. Therefore, it is essential to investigate the influence of number of daily strain data on the predicted fatigue life and seek an optimal number of daily strain data for derivation of a standard daily stress spectrum.

The measurement for 80 typical days under normal traffic and wind conditions obtained from the strain gauge SSTLS13 are selected for fatigue life analysis.

Theoretically, each daily stress spectrum can be used to predict a fatigue life at this detail. **Figure 3.16** shows the predicted fatigue life from the measured daily stress spectra sorted in an ascending order. It is evident that the predicted fatigue life is different from different daily stress spectra, ranging from 620 to 1001 years. The reason which can be easily found is because each day has different daily stress spectrum although it is similar.

Figure 3.17 shows the predicted fatigue lives with different number of daily strain data extracted from the above mentioned 80 typical days. Firstly, 5 daily strain data are used and drawn out randomly from 80 typical daily strain data, and the mentioned dates will be included in the next calculation, the rest may be deduced by analogy. From **Figure 3.17**, it is seen that fatigue lives are little changed for more than 10 daily strain data and almost the same when more than 20 daily strain data are taken into account. Therefore, it is reasonable to assess the fatigue life by using a standard daily stress spectrum obtained from adequate daily strain data. For the TMB as a specific case study, it is appropriate to assess the fatigue life by using 20 daily strain data to obtain a standard daily stress spectrum.

Preferably, it should take the effect of weekend and workday traffic variations as well as seasonal changes in traffic patterns into consideration for the fatigue life evaluation. **Figure 3.18** shows the results of the influence of weekend and workday traffic variations together with seasonal changes in traffic patterns on the predicted

fatigue life when taking different combinations of traffic patterns include (i) 20 daily strain data on weekend, (ii) 20 daily strain data on workday, (iii) 10 daily strain data on weekend and 10 daily strain data on workday, (iv) 20 daily strain data in summer, (v) 20 daily strain data in winter, and (vi) 10 daily strain data in summer and 10 daily strain data in winter. It is seen from **Figure 3.18** that these two factors only have little effect on the results of the predicted fatigue life. The main reason is that the TMB plays a very important role in the transportation between the Hong Kong International Airport and downtown, and the traffic is substantive and little change during one whole year on the bridge excluding some disastrous issues such as typhoon.

3.5.3 Fatigue Life Assessment of TMB

As has been validated in the aforementioned section, the stress spectra under typhoon conditions should be included for fatigue life evaluation when using the standard daily stress spectrum method. It is observed from **Table 3.1** that a total of 22 days out of 365 days were under typhoon conditions in 1999. According to this proportion, the strain data acquired from 20 days including one day under typhoon conditions are chosen to construct a standard daily stress spectrum, as illustrated in **Figure 3.19**. With such an obtained standard daily stress spectrum, the fatigue life of the welded detail monitored by the strain gauge SSTLS13 is evaluated.

Since the weld joint near the strain gauge SSTLS13 is categorized as F_2, the values of parameters K_0, Δ, and m are determined as $K_0 = 1.23\times10^{12}$, $\Delta = 0.592$, and $m = 3.0$. When the probability factor is assumed as $d = 2$ which corresponds to the failure probability of 2.3% and the standard S-N design curve (BSI 1980), the fatigue life of the welded detail monitored by the strain gauge SSTLS13 is calculated as 718 years. It is slightly different from the calculated fatigue life by using the standard traffic-stress spectrum, as illustrated in **Figure 3.17**. This is because the strain data under typhoon conditions account for a small portion in one year in comparison with the strain data under normal traffic and wind conditions. The fatigue damage is mainly caused by the highway and railway traffic for the TMB.

Table 3.2 lists the predicted fatigue lives of the welded detail monitored by the strain gauge SSTLS13 with different probabilities of failure by using the achieved standard daily stress spectrum, which is also illustrated in **Figure 3.20**. It is observed from **Figure 3.20** that the values of the predicted fatigue life are decreased with the decreasing failure probabilities. In addition, the predicted fatigue lives for the welded detail near the strain gauge SSTLS13 are much longer than 120 years, the design life of the TMB. This is because a great attention has been paid on the issue of fatigue due to the railway traffic during the design stage of the bridge. Another important reason is that most of the stress ranges in the standard daily stress spectrum are below the fatigue limit of the joint class F_2, with a value of 35 MPa. As a consequence, it can be concluded that the bridge would not be failed by fatigue

within its design life.

3.6 Summary

SHM has become an increasingly accepted technology for diagnosing and prognosing bridge condition and safety. The continuously measured strain data from a long-term monitoring system can be used to assess the status of fatigue which is among the most critical forms of damage potentially occurring in steel bridges. In this chapter, a standard daily stress spectrum method for fatigue analysis of steel bridges instrumented with SHM system has been developed and successfully applied to conduct fatigue life assessment of the fatigue-prone weld details of the TMB according to the procedure for fatigue life evaluation stipulated in BS5400 specification.

Based on the statistical analysis of the stress spectra and the fatigue life evaluation results using the strain measurement data from the TMB, the following specific conclusions can be obtained:

(i) A standard daily stress spectrum can be achieved for fatigue life evaluation by combining the standard traffic-stress spectrum and standard typhoon-stress spectrum proportionally. The results demonstrate that the predicted fatigue life using the standard daily stress spectrum has not much different in comparison with the calculated fatigue life by using the standard traffic-stress

spectrum under normal traffic and wind conditions. The reason is that strain data under typhoon conditions account for little portion in one year compared with those under normal traffic and wind conditions. Thus, for the TMB, the fatigue damage is mainly attributed to the highway traffic and railway traffic;

(ii) In applying the standard daily stress spectrum method for fatigue life assessment of the TMB, the fatigue lives do not change much when using more than 10 daily strain data and are almost the same when more than 20 daily strain data are taken into account. Therefore, it is reasonable to assess the fatigue life by using a standard daily stress spectrum obtained from adequate daily strain data, and strain data acquired from 20 days including one day under typhoon conditions are adequate for constructing a standard daily stress spectrum. The influence of weekend and workday traffic variations and seasonal changes in traffic patterns has little effect on the results of the predicted fatigue life; and

(iii) Assessment of fatigue life by using field measured data from the SHM system instrumented on the bridge gives a practical and accurate estimation of the fatigue life of bridge components, from which the bridge administrative authority and managers can make an appropriate decision on fatigue-related inspection, maintenance, and management of the bridge.

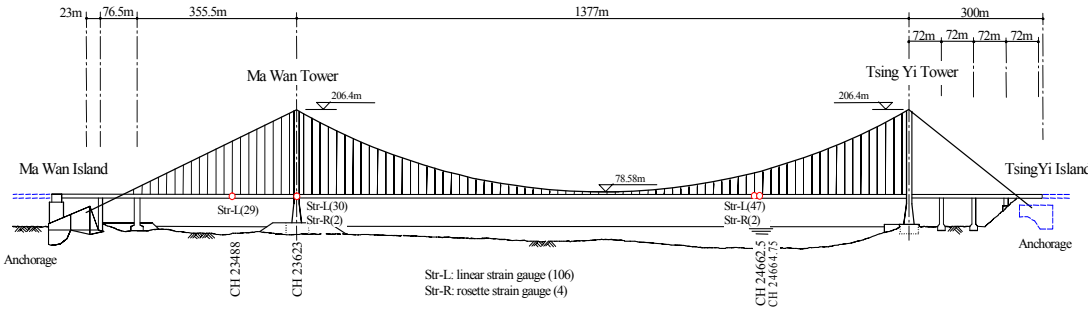

Figure 3.1 Layout of strain gauges on TMB

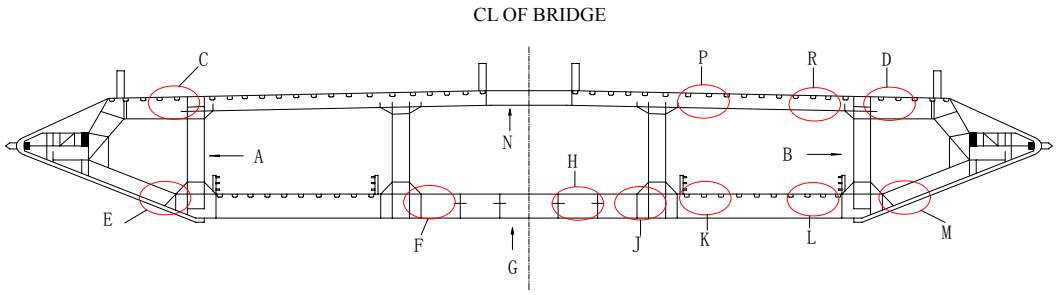

(a)

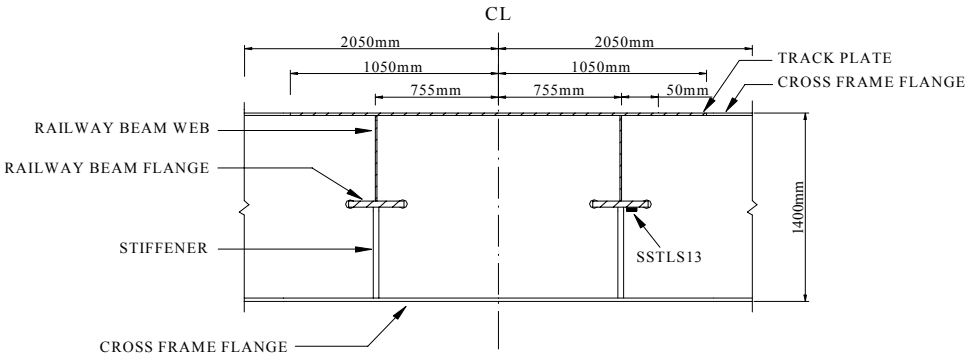

(b)

Figure 3.2 Location of strain gauge SSTLS13 on rail track section at CH24662.5: (a) Deck cross-section at CH24662.5; (b) Sectional view of Detail H

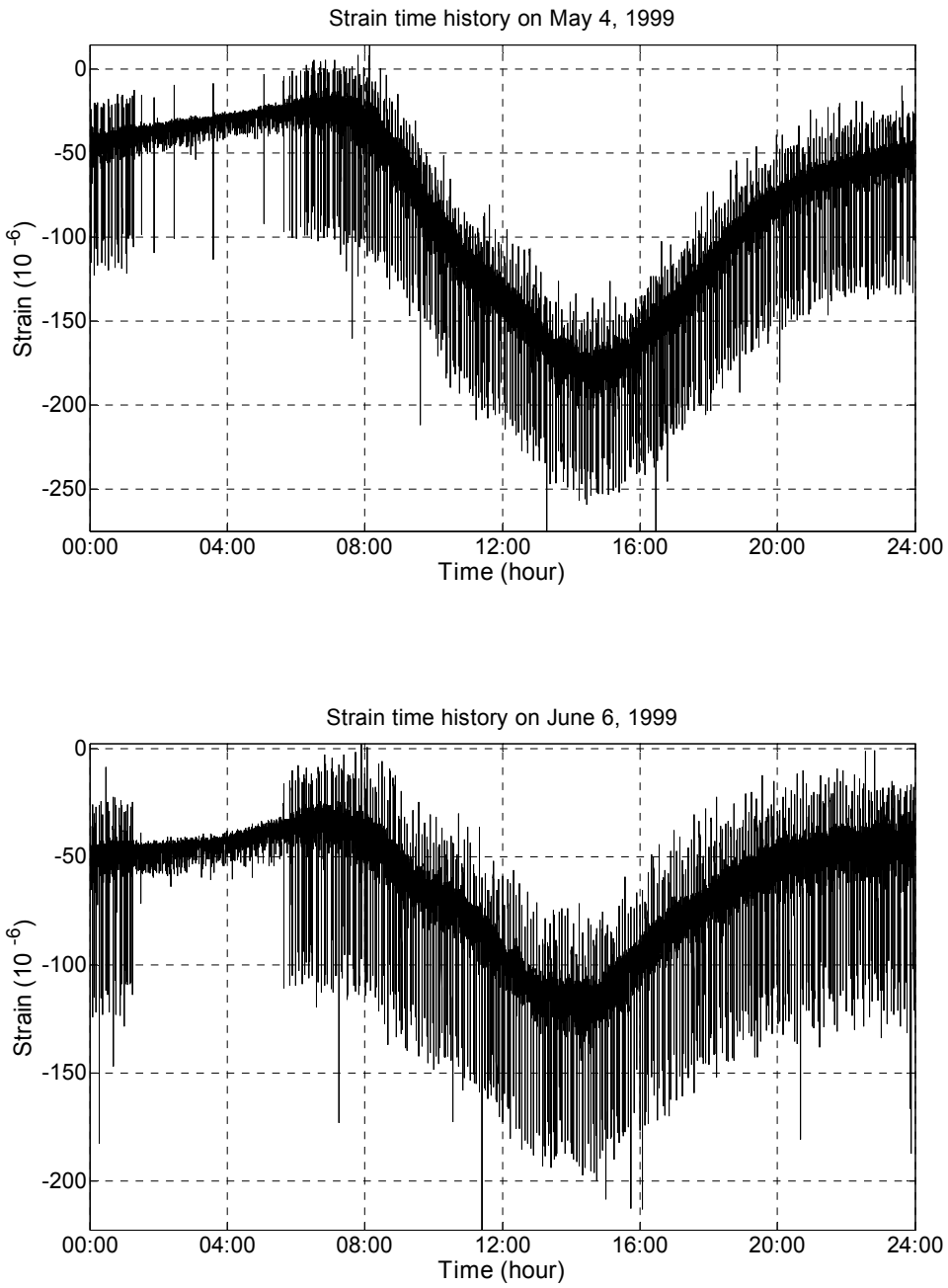

Figure 3.3(a) Measured daily strain time histories under normal traffic and wind conditions by strain gauge SSTLS13

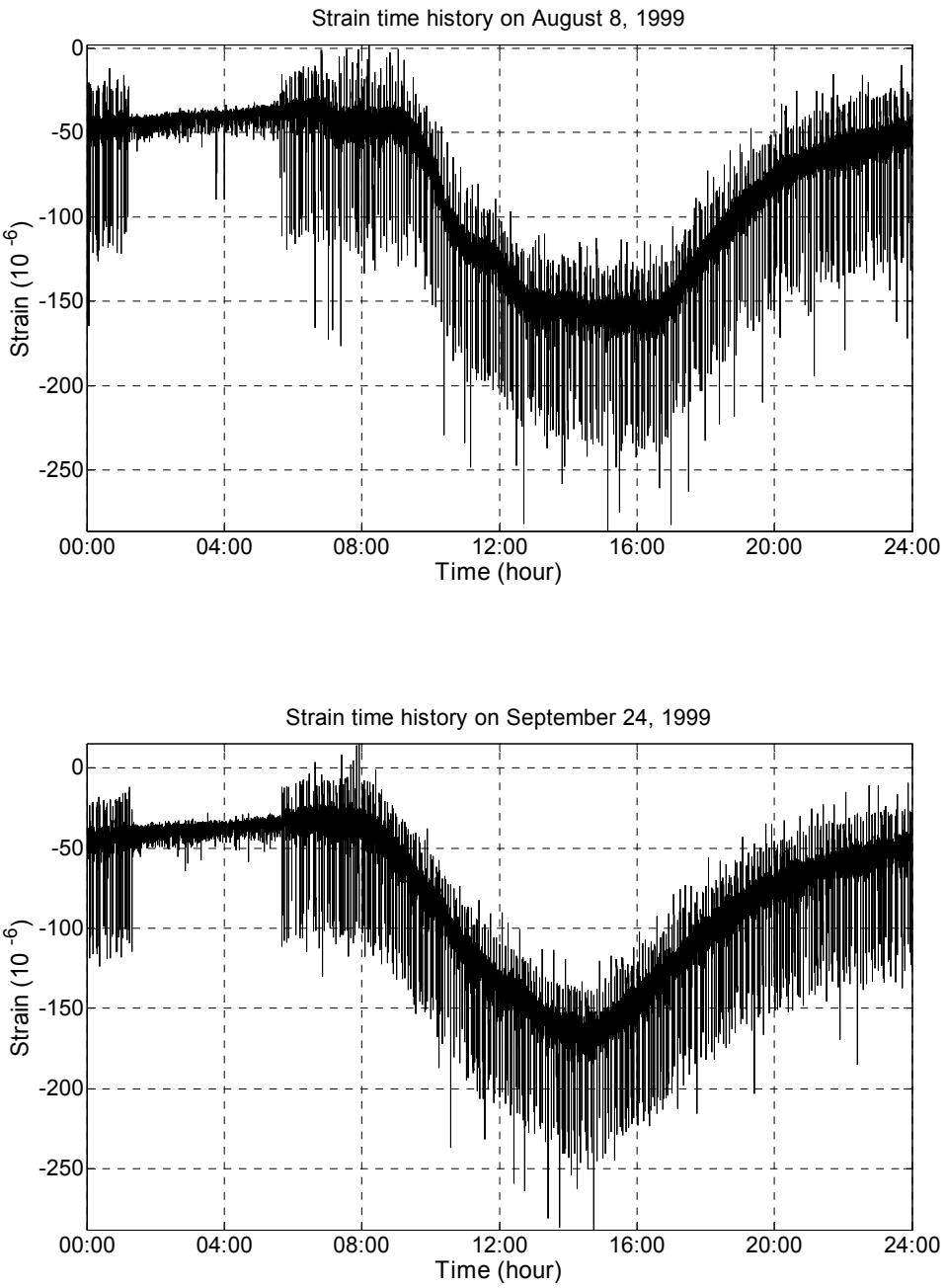

Figure 3.3(b) Measured daily strain time histories under normal traffic and wind conditions by strain gauge SSTLS13

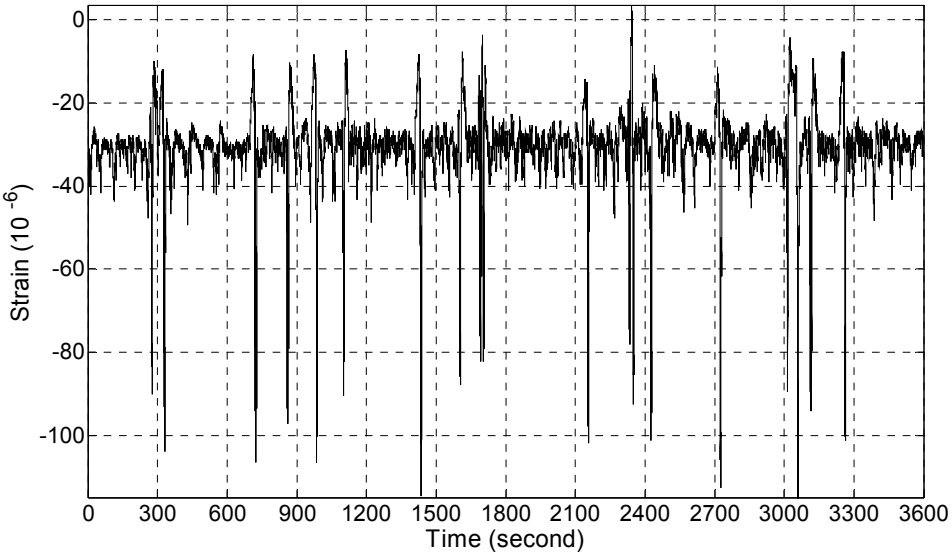

Figure 3.4 One-hour strain data measured by strain gauge SSTLS13 on September 24, 1999

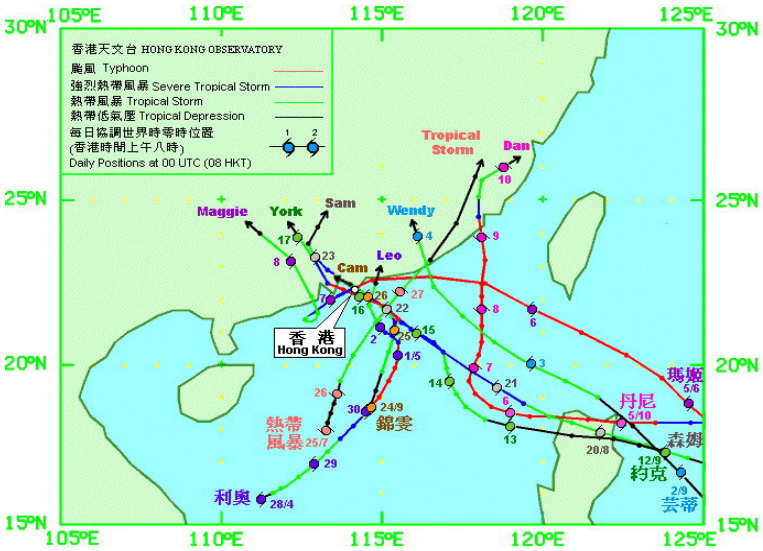

Figure 3.5 Tracks of typhoon affecting Hong Kong in 1999 (Hong Kong Observatory)

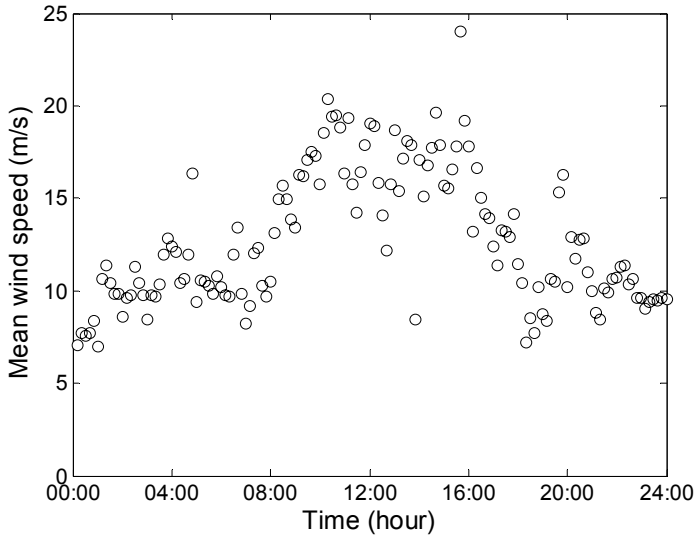

(a)

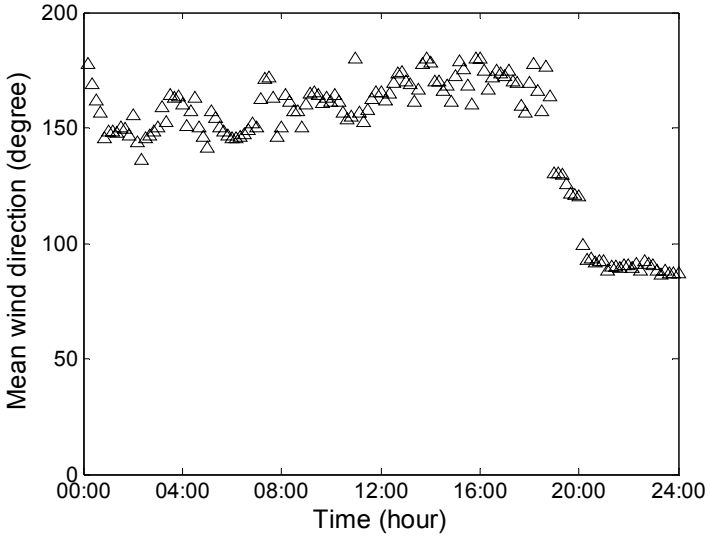

(b)

Figure 3.6 Mean wind speed and direction from anemometer WITJN01: (a) 10-minute mean wind speed; (b) 10-minute mean wind direction

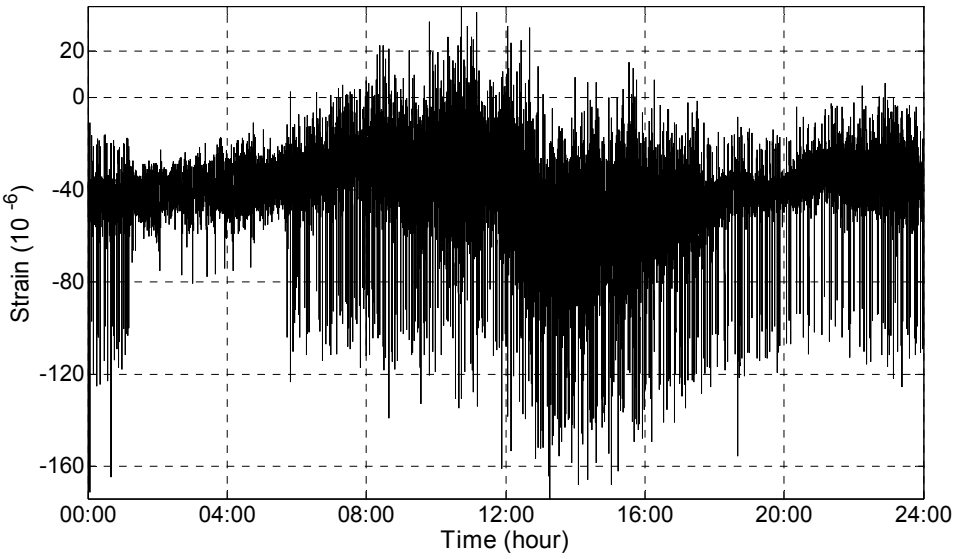

Figure 3.7 Measured daily strain time history by strain gauge SSTLS13 on August 22, 1999 during typhoon "Sam"

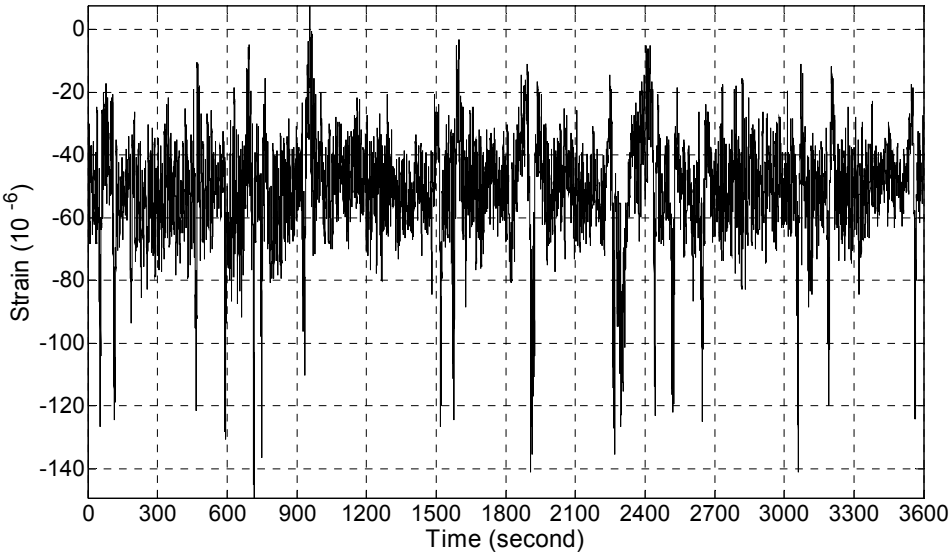

Figure 3.8 One-hour strain data measured by strain gauge SSTLS13 on August 22, 1999 during typhoon "Sam"

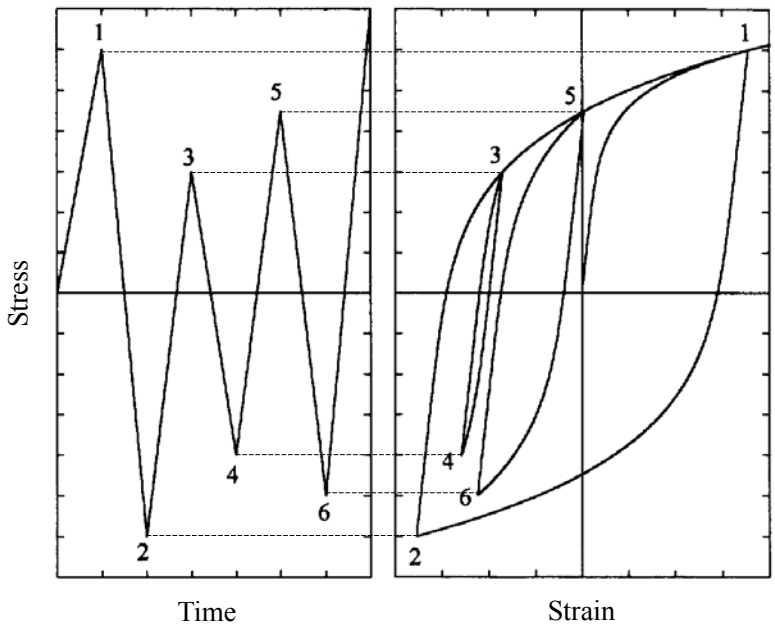

Figure 3.9 Stress time history and stress-strain hysteresis loops

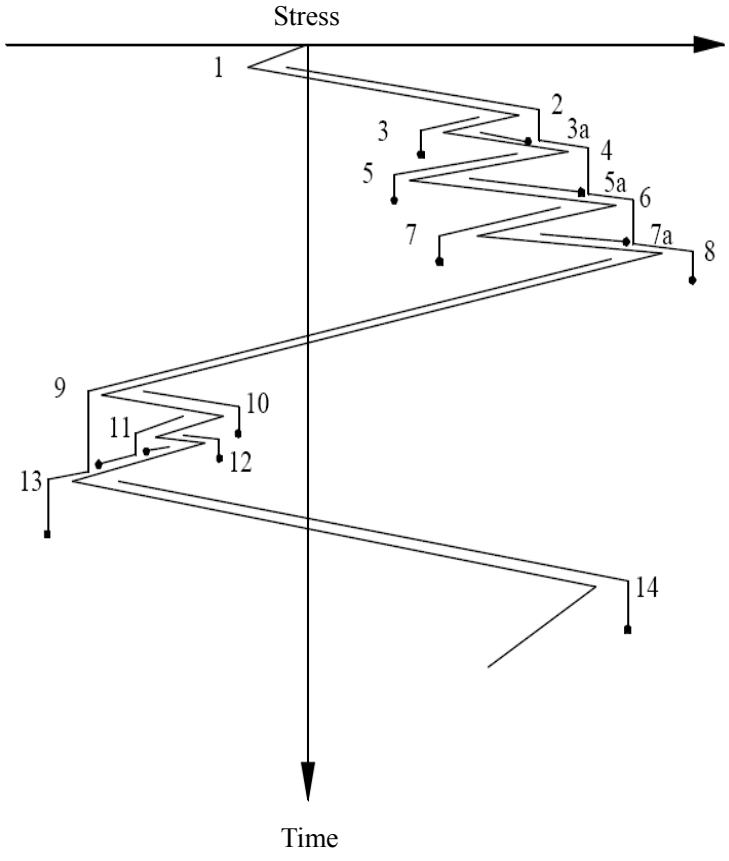

Figure 3.10 Schematic of rainflow cycle counting method

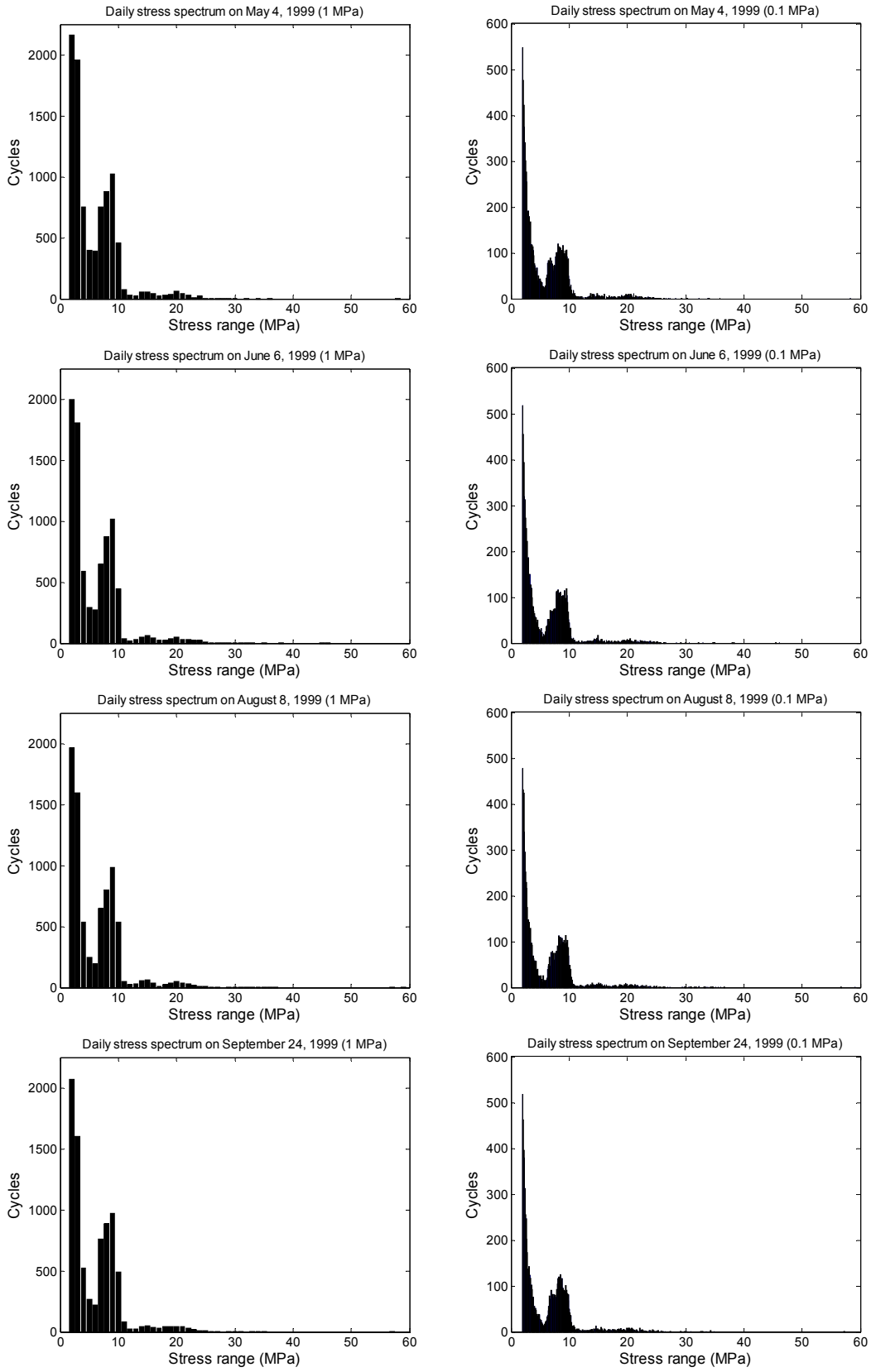

Figure 3.11 Histograms of daily stress spectra under normal traffic and wind conditions with different resolutions

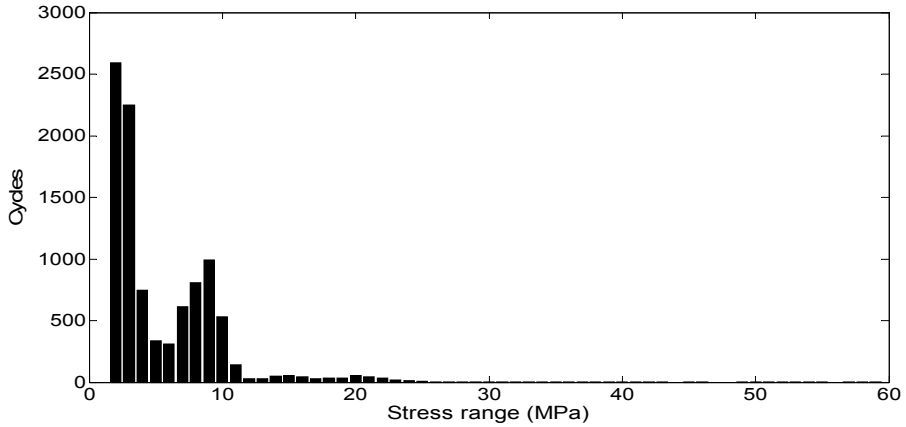

Figure 3.12 Standard traffic-stress spectrum

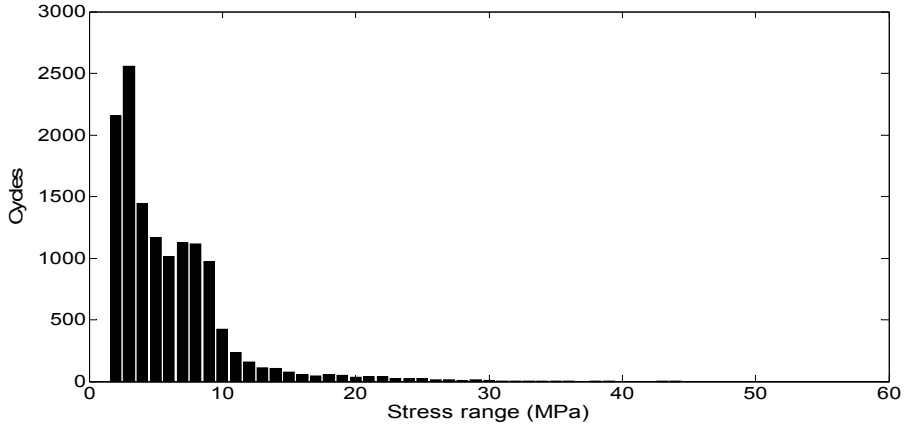

Figure 3.13 Standard typhoon-stress spectrum

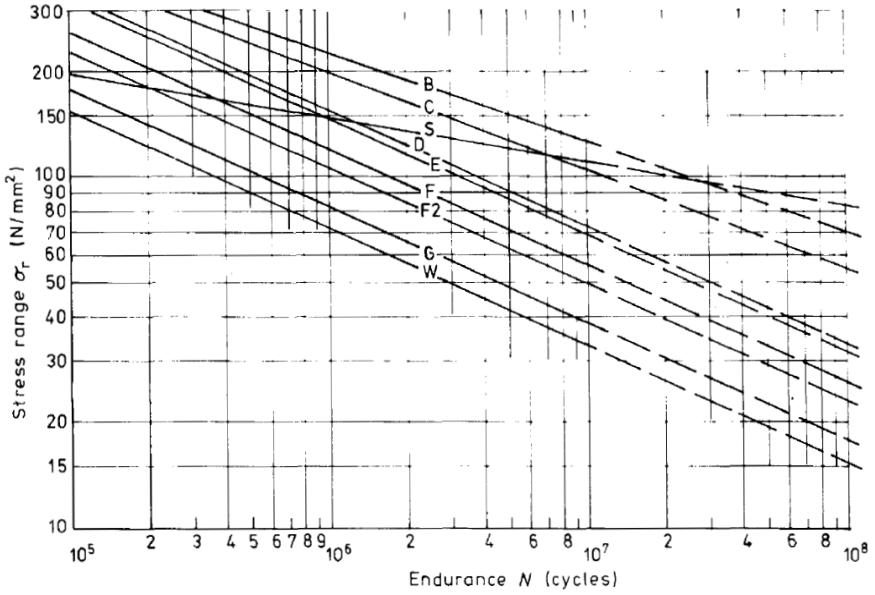

Figure 3.14 *S-N* relationship designated in BS5400

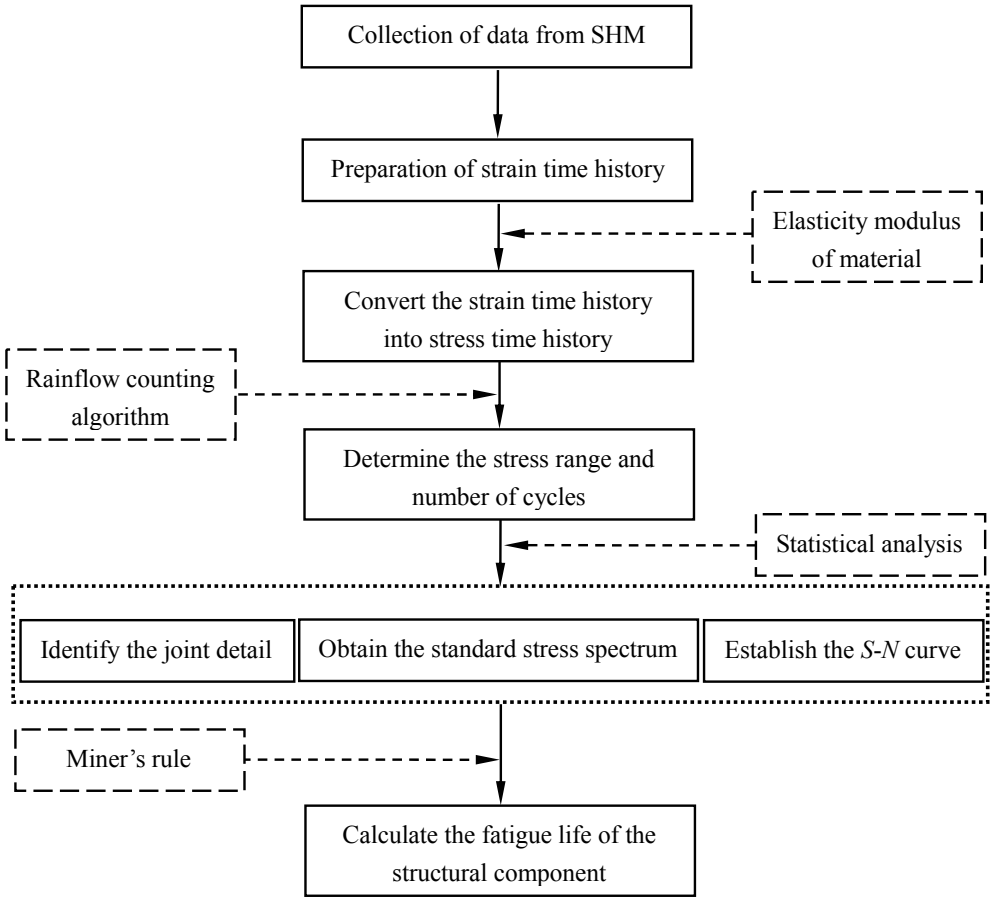

Figure 3.15 Flowchart of monitoring-based fatigue life assessment method

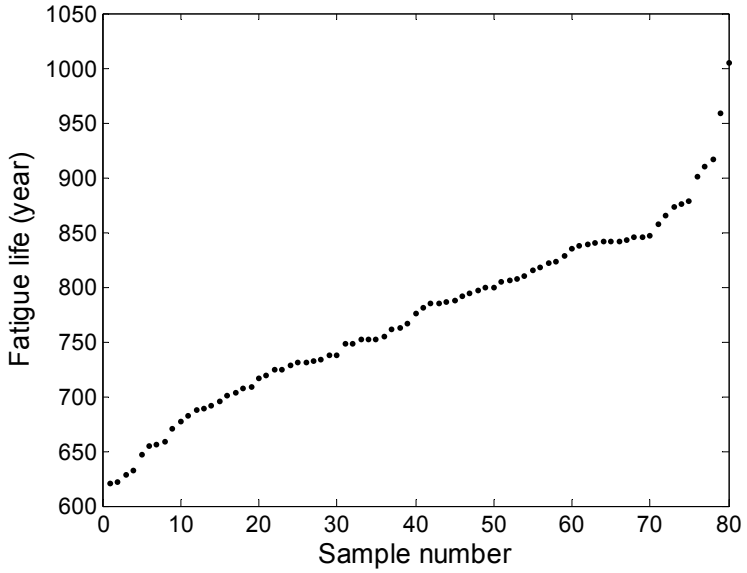

Figure 3.16 Fatigue life predicted from different daily stress spectra

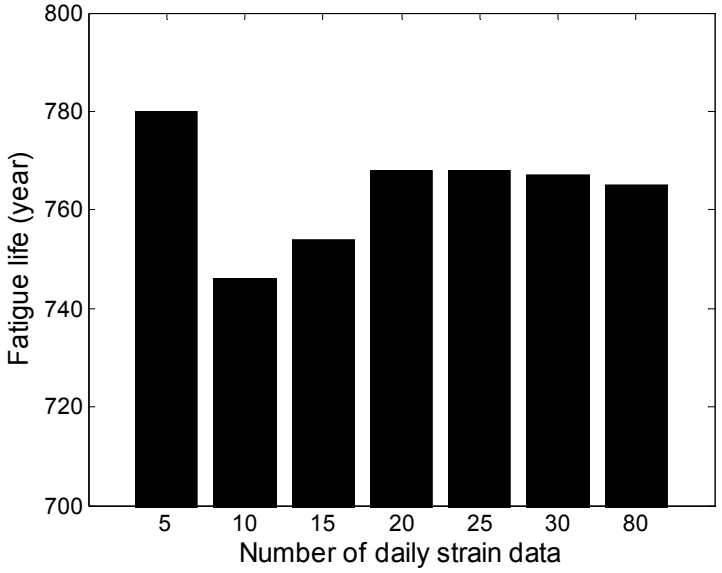

Figure 3.17 Predicted fatigue lives with different number of daily strain data

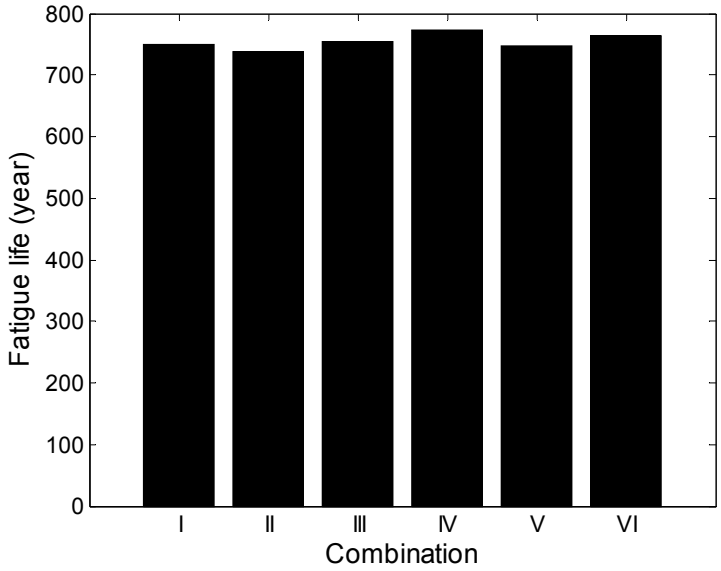

Figure 3.18 Influence of traffic pattern on fatigue life

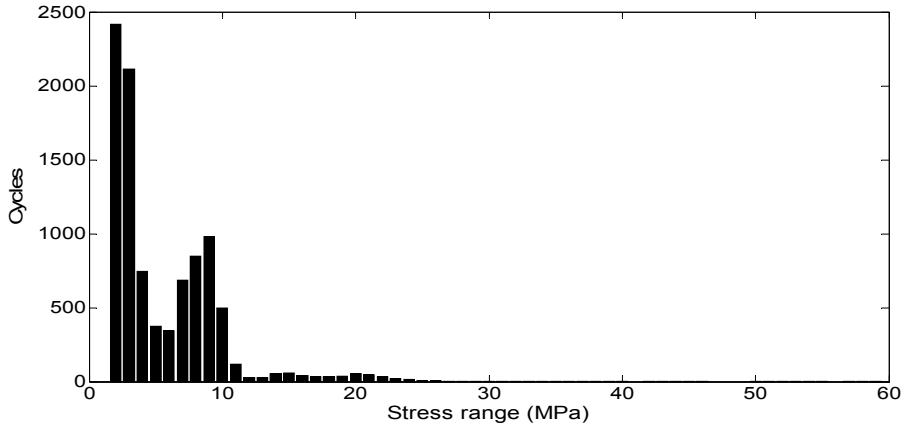

Figure 3.19 Histogram of standard daily stress spectrum

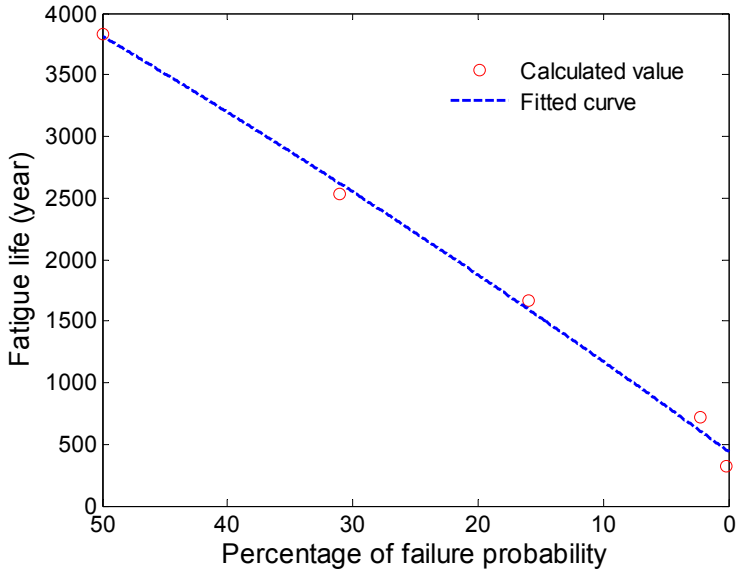

Figure 3.20 Predicted fatigue lives with different probabilities of failure

Table 3.1 Typhoon warning signals in 1999 (Hong Kong Observatory)

Name	Signal	Issuing		Canceling	
		hh mm	dd/mon/yyyy	hh mm	dd/mon/yyyy
Leo	1	09:40	29/Apr/1999	16:15	30/Apr/1999
Leo	3	16:15	30/Apr/1999	13:30	02/May/1999
Leo	8 NE	13:30	02/May/1999	17:30	02/May/1999
Leo	3	17:30	02/May/1999	20:45	02/May/1999
Maggie	1	23:45	05/Jun/1999	14:15	06/Jun/1999
Maggie	3	14:15	06/Jun/1999	00:30	07/Jun/1999
Maggie	8 NW	00:30	07/Jun/1999	02:45	07/Jun/1999
Maggie	9	02:45	07/Jun/1999	05:45	07/Jun/1999
Maggie	8 NE	05:45	07/Jun/1999	10:30	07/Jun/1999
Maggie	3	10:30	07/Jun/1999	14:45	07/Jun/1999
Maggie	1	22:30	07/Jun/1999	00:45	08/Jun/1999
Maggie	3	00:45	08/Jun/1999	13:45	08/Jun/1999
Sam	1	16:15	20/Aug/1999	02:30	22/Aug/1999
Sam	3	02:30	22/Aug/1999	12:30	22/Aug/1999
Sam	8 NW	12:30	22/Aug/1999	20:10	22/Aug/1999
Sam	8 SW	20:10	22/Aug/1999	03:50	23/Aug/1999
Sam	3	03:50	23/Aug/1999	21:00	23/Aug/1999
York	1	10:45	13/Sep/1999	10:15	15/Sep/1999
York	3	10:15	15/Sep/1999	03:15	16/Sep/1999
York	8 NW	03:15	16/Sep/1999	05:20	16/Sep/1999
York	9	05:20	16/Sep/1999	06:45	16/Sep/1999
York	10	06:45	16/Sep/1999	17:45	16/Sep/1999
York	8 SW	17:45	16/Sep/1999	22:10	16/Sep/1999
York	3	22:10	16/Sep/1999	00:45	17/Sep/1999
Dan	1	20:45	05/Oct/1999	05:35	07/Oct/1999
Dan	3	05:35	07/Oct/1999	16:15	07/Oct/1999
Dan	1	16:15	07/Oct/1999	09:25	09/Oct/1999

Table 3.2 Predicted fatigue lives with different probabilities of failure

Probability of failure (%)	Probability factor, *d*	Fatigue life (year)
50	0	3,836
31	0.5	2,528
16	1.0	1,664
2.3	2.0	718
0.14	3.0	323

CHAPTER 4

MULTI-MODAL STRESS SPECTRUM MODELING USING LONG-TERM MONITORING DATA AND FINITE MIXTURE DISTRIBUTIONS

4.1 Introduction

In the stress-life fatigue analysis of stochastically loaded structures, one of the critical issues is to transform the simulated or measured stress time histories into stress spectra. A rainflow counting method is generally used by extracting the stress ranges and the corresponding number of stress cycles from the stress time histories. The parameters of the stress spectra include: the stress range, the mean stress, and the number of stress cycles. Usually, fatigue damage is estimated with the one-parameter rainflow method on the basis of the stress range with the corresponding cycle amounts under the assumption that the influence of the mean stress can be neglected.

However, if the fatigue failure occurs due to a large number of stress cycles with small amplitudes and very different means, the influence of the mean stress should not be underestimated. When the mean stress needs to be considered in the

estimation of fatigue damage, the extraction of the stress cycles from the stress time histories is performed with a two-parameter rainflow method. A stress cycle is then represented with two components: the stress range and the mean stress. The stress spectrum is then defined by the corresponding rainflow stress matrix of relative frequencies in the two-dimensional space. Fatigue damage caused by individual stress cycle then depends on the stress range and mean stress.

A good estimation of fatigue damage of a structure can be obtained using the Miner's linear damage rule and rainflow cycle counting method only if a recorded stress time history is long enough, so that it will contain adequate stress cycles with high amplitudes. In the case of random stress states that are composed of relatively short random stress time histories, it is necessary to conduct statistical modeling of stress spectrum with the measured data and extrapolate the distribution of stress cycles to the region where there are no data recorded.

In this chapter, the research efforts for modeling of the rainflow-counted stress spectra are presented using the method of finite mixture distributions in conjunction with a hybrid mixture parameter estimation algorithm. With the long-term strain monitoring data from the instrumented TMB, a wavelet-based filtering method is used to eliminate the temperature effect from the original measured data. The stress spectra are obtained by extracting the stress range and mean stress data from the stress time histories with the aid of rainflow counting algorithm. The obtained stress

spectra and predicted fatigue life by using the original and filtered strain data are also compared. Based on the features captured from the daily stress spectra under normal traffic and wind conditions, a representative sample of stress spectrum accounting for highway traffic, railway traffic, and typhoon effects is derived. Then, the multi-modal modeling of the stress range is performed by use of finite mixed normal, lognormal, and Weibull distributions. The joint PDF of the stress range and mean stress is also estimated by means of a mixture of multivariate Weibull-normal distributions.

4.2 Finite Mixture Distributions

The finite mixture distributions are commonly employed for modeling complex probability distributions and enable the statistical modeling of random variables with multi-modal behavior where a simple parametric model fails to depict the characteristics of the observations adequately (McLachlan and Peel 2000). It has attracted strong and sustained attention since the late 1950s and been widely used in statistical data processing particularly for capturing specific properties of real data such as multimodality, skewness, kurtosis, and unobserved heterogeneity (Snoussi and Mohammad-Djafari 2007).

4.2.1 Structure of Finite Mixture Distributions

The basic structure of finite mixture distributions for independent scalar or vector observations **y** can be written as (Richardson and Green 1997)

$$f(\mathbf{y} \mid c, \mathbf{w}, \boldsymbol{\theta}) = \sum_{l=1}^{c} w_l f_l(\mathbf{y} \mid \boldsymbol{\theta}_l) \tag{4.1}$$

$$\sum_{l=1}^{c} w_l = 1 \quad \text{and} \quad w_l \geq 0 \tag{4.2}$$

where $f(\mathbf{y} \mid c, \mathbf{w}, \boldsymbol{\theta})$ is a predictive mixture density; $f_l(\mathbf{y} \mid \boldsymbol{\theta}_l)$ is a given parametric family of the lth predictive component densities indexed by the scalar or vector parameters $\boldsymbol{\theta}_l$. The objective of the analysis is inference about the unknowns which include the number of components or groups, c, the component weights, w_l, summing to 1, and the component parameters, $\boldsymbol{\theta}_l$.

Thus, for instance, the finite mixed normal distributions, the finite mixed lognormal distributions, and the finite mixed Weibull distributions can be expressed respectively by

$$f(\mathbf{y} \mid c, \mathbf{w}, \boldsymbol{\theta}) = \sum_{l=1}^{c} w_l \frac{1}{\sqrt{2\pi}} \exp\left\{-\frac{1}{2}\frac{(y-\mu_l)^2}{\sigma_l^2}\right\} \tag{4.3}$$

$$f(\mathbf{y} \mid c, \mathbf{w}, \boldsymbol{\theta}) = \sum_{l=1}^{c} w_l \frac{1}{\sqrt{2\pi}\sigma_l y} \exp\left\{-\frac{1}{2}\frac{(\ln(y)-\mu_l)^2}{\sigma_l^2}\right\} \tag{4.4}$$

$$f(\mathbf{y} \mid c, \mathbf{w}, \boldsymbol{\theta}) = \sum_{l=1}^{c} w_l \frac{\beta_l}{\theta_l}\left(\frac{y}{\theta_l}\right)^{\beta_l - 1} \exp\left\{-\left(\frac{y}{\theta_l}\right)^{\beta_l}\right\} \tag{4.5}$$

Then, the cumulative distribution functions (CDFs) are obtained respectively by

$$F(\mathbf{y} \mid c, \mathbf{w}, \boldsymbol{\theta}) = \sum_{l=1}^{c} w_l \Phi\left(\frac{y - \mu_l}{\sigma_l}\right) \tag{4.6}$$

$$F(\mathbf{y} \mid c, \mathbf{w}, \boldsymbol{\theta}) = \sum_{l=1}^{c} w_l \Phi\left(\frac{\ln y - \mu_l}{\sigma_l}\right) \tag{4.7}$$

$$F(\mathbf{y} \mid c, \mathbf{w}, \boldsymbol{\theta}) = 1 - \sum_{l=1}^{c} w_l \exp\left\{-\left(\frac{y}{\theta_l}\right)^{\beta_l}\right\} \tag{4.8}$$

where μ_l and σ_l are the mean values and standard deviations of normal mixture parameters; β_l and θ_l are the Weibull shape parameters; and $\Phi(\cdot)$ is the standard normal CDF.

4.2.2 Hybrid Mixture Parameter Estimation

From an algorithmic point of view, the mixture problem can be formulated as an incomplete data problem (Steiner and Hudec 2007), and the identification of the mixture parameters as a latent variable problem is generally based on the well known expectation maximization (EM) algorithm albeit other methods are available (Titterington *et al*. 1985). In this study, a hybrid mixture parameter estimation approach (Nagode and Fajdiga 2006) is used for estimation of the parameters of the finite mixture distributions, which is a hybrid between non-parametric and parametric probability density estimation techniques and can be used either

independently or in combination with the renowned EM algorithm.

The specific features of the hybrid parameter estimation approach are: (i) an arbitrary set of observations from an unknown number of classes are treatable, and the initial weights and component parameters are not required; (ii) the preprocessing of observations can be accomplished either by the histogram, Parzen window or *k*-nearest neighbor approach; (iii) the predictive component densities can be alternatively picked out of normal, lognormal, and Weibull parametric families; (iv) the numerical procedure is computationally fast, stable, and insensitive to the number of components and singularities; and (v) the optimal number of components, weights, and component parameters are gained iteratively by using the Akaike's information criterion (AIC) (Akaike 1974) as a measure of the goodness-of-fit of an estimated statistical model (Nagode *et al*. 2006).

4.2.2.1 Overview of hybrid mixture parameter estimation method

The synopsis of the hybrid mixture parameter estimation method is illustrated in **Figure 4.1**. Firstly, the set of independent scalar or vector observations is counted into a finite number of bins and meanwhile empirical densities are calculated. Then component weights and component parameters are estimated. This process consists of rough and enhanced component parameter estimation and the separation of observations, which is repeated till the discrepancy between the densities is beyond

an acceptable limit. Thus the convergence of the predictive component density to the empirical one is the theoretical ground for the validation of the procedure. Subsequently, residual frequencies are distributed between the components by the Bayes decision rule (Duda and Hart 1973). Finally, optimal AIC is searched for iteratively, where the optimal number of components, optimal weights and optimal component parameters always coincide with minimal AIC.

There are three key ideas in the treatment of this hybrid parameter estimation method. Firstly, the most deviating observations are transferred between the component and the residue. In other words, the observations belonging to the predictive component density are kept, whilst the rest of observations belonging to other components join the residue. This enables a successive procedure instead of simultaneous mixture estimation. When the convergence criterion is fulfilled, it is presumed that the separation of observations is completed. Secondly, the number of components equals one and the residue is void initially. Only when the separation phase for the predictive component density is completed, the number of components is increased if the number of observations in the residue is beyond a critical value. The number of components thus determined is influenced by both the convergence criterion and the critical size of the residue. Finally, the critical size of the residue is initiated in order to restrain the appearance of insignificant components in the mixture. When the number of observations in the residue is below the critical value, the remaining observations are assigned to the existing components although they might form new

components with a low probability of occurrence.

4.2.2.2 Procedure of hybrid mixture parameter estimation

❖ *Preprocessing of observations*

Assuming that $f(\mathbf{y} \mid c, \mathbf{w}, \boldsymbol{\theta})$ is continuous and does not vary appreciably over the jth bin region, R_j, of the jth bin volume, V_j (in case of one random variable, V_j stands for the width of the bin of histogram), the probability for a new independent observation, $\mathbf{y}_j$, which falls inside R_j is given by (Bishop 1995)

$$\int_{R_j} f(\mathbf{y} \mid c, \mathbf{w}, \boldsymbol{\theta}) dy \approx f(\mathbf{y}_j \mid c, \mathbf{w}, \boldsymbol{\theta}) V_j = \frac{k_j}{n} \tag{4.9}$$

where n stands for the total number of independent scalar or vector observations; and k_j is the fraction of observations falling into R_j.

The total number of p-dimensional independent scalar or vector observations may be counted into a finite number of non-overlapping, equally sized, and regularly distributed bins initially. Assuming that bin, meaning $\mathbf{y}_j = [y_{1j},\ldots,y_{pj}]^{\mathrm{T}}$, is given by

$$y_{ij} = y_{i0} + \text{'an arbitrary integer'} \times h_{ij} \quad i = 1,\ldots,p \tag{4.10}$$

and the fraction of observations k_j for $j = 1,\ldots, k$ falling in region R_j is counted out. Region R_j is taken to be a hypersquare with the sides of length $\mathbf{h}_j = [h_{1j},\ldots, h_{pj}]^{\mathrm{T}}$

centered on $\mathbf{y}_j$ (in case of one random variable, $V_j = h_j$). Its volume is then

$$V_j = \prod_{i=1}^{p} h_{ij} \tag{4.11}$$

whilst $\mathbf{y}_0$ stands for an arbitrary origin; and k depicts the number of bins.

❖ *Global mode detection*

The global mode coincides with $\mathbf{y}_q$ where empirical density f_{lj} takes on a maximum value

$$q = \max \arg f_{lj} \to \left(\mathbf{y}_q, f_{lq}\right) \tag{4.12}$$

then

$$f_{lj} = \frac{k_{lj}}{n_l} \frac{1}{V_j}, \quad j = 1, \ldots, k \tag{4.13}$$

where k_{lj} is the observation frequencies of component l in the jth bin; while the frequencies for the first component are all set to k_j, and the total number of observations in the lth component, n_l, is

$$n_l = \sum_{j=1}^{k} k_{lj}, \quad l = 1, \ldots, c \tag{4.14}$$

The component weight is

$$w_l = \frac{n_l}{n}, \quad l = 1, \ldots, c \tag{4.15}$$

❖ *Rough component parameter estimation*

To separate the observations corresponding to the *l*th component from the rest of the observations, it is necessary to decide which one to extract. Reasonably, those surrounding the global mode are extracted first, as at least one component is supposed to be in its vicinity. Thus it has to prevent the component to flow away from the mode by introducing restrains. The first restrain is to ensure the equivalence of probability densities at $\mathbf{y}_q$ by

$$f_{lq} = f\left(\mathbf{y} = \mathbf{y}_q \mid \boldsymbol{\theta}_l\right) \tag{4.16}$$

The second is to make the mode of component density coincide with $\mathbf{y}_q$ by

$$\frac{\partial f\left(\mathbf{y} = \mathbf{y}_q \mid \boldsymbol{\theta}_l\right)}{\partial \mathbf{y}} = 0 \tag{4.17}$$

By inserting Equation (4.3) into Equations (4.16) and (4.17), rough normal component parameters are obtained as

$$\mu_l = y_q \tag{4.18}$$

$$\sigma_l = \frac{1}{\sqrt{2\pi} f_{lq}} \tag{4.19}$$

Similarly, rough lognormal component parameters

$$\mu_l = \ln\left(y_q\right) + \sigma_l^2 \tag{4.20}$$

$$f(\sigma_l) = \sqrt{2\pi} f_{lq} y_q - e^{-\frac{\sigma_l^2}{2}} = 0 \tag{4.21}$$

and rough Weibull component parameters

$$\theta_l = y_q \left(\frac{\beta_l - 1}{\beta_l} \right)^{-\frac{1}{\beta_l}}, \quad \beta_l > 1 \tag{4.22}$$

$$f(\beta_l) = f_{lq} y_q - (\beta_l - 1) e^{-\frac{\beta_l - 1}{\beta_l}} = 0 \tag{4.23}$$

can be calculated by, e.g., using the Newton-Raphson method.

❖ *Enhanced component parameter estimation*

As $\mathbf{y}_m$ is affected by the neighboring components, the global mode position does not necessarily coincide with $\mathbf{y}_m$. Therefore, maximum likelihood is applied to get enhanced component parameters. When the histogram is applied, enhanced normal component parameters are given by

$$\mu_l = \frac{1}{n} \sum_{j=1}^{k} k_{lj} y_j \tag{4.24}$$

$$\sigma_l^2 = \frac{1}{n_l} \sum_{j=1}^{k} k_{lj} y_j^2 - \mu_l^2 \tag{4.25}$$

Likewise enhanced lognormal component parameters

$$\mu_l = \frac{1}{n} \sum_{j=1}^{k} k_{lj} \ln(y_j) \tag{4.26}$$

$$\sigma_l^2 = \frac{1}{n_l}\sum_{j=1}^{k} k_{lj} \ln\left(y_j\right)^2 - \mu_l^2 \tag{4.27}$$

and enhanced Weibull component parameters

$$\theta_l^{\beta_l} = \frac{1}{n_l}\sum_{j=1}^{k} k_{lj} y_j^{\beta_l} \tag{4.28}$$

$$f\left(\beta_l\right) = \frac{1}{\beta_l} + \frac{1}{n_l}\sum_{j=1}^{k} k_{lj} \ln\left(y_j\right) - \frac{\sum_{j=1}^{k} k_{lj} y_j^{\beta_l} \ln\left(y_j\right)}{\sum_{j=1}^{k} k_{lj} y_j^{\beta_l}} = 0 \tag{4.29}$$

are estimated.

❖ *Component mean and variance calculation*

Component means and variances of the normal distributions

$$m_l = \mu_l \tag{4.30}$$

$$V_l = \sigma_l^2 + \mu_l^2 \tag{4.31}$$

lognormal distributions

$$m_l = e^{\mu_l + \frac{\sigma_l^2}{2}} \tag{4.32}$$

$$V_l = e^{2\mu_l + 2\sigma_l^2} \tag{4.33}$$

or Weibull distributions

$$m_l = \theta_l \Gamma\left[1 + \frac{1}{\beta_l}\right] \tag{4.34}$$

$$V_l == \theta_l^2 \Gamma\left[1 + \frac{2}{\beta_l}\right] \tag{4.35}$$

are calculated to enable the classification of the remaining observations, in which $\Gamma(\cdot)$ is the Gamma function.

❖ *Bayes classification of the remaining observations*

With an increase in the number of components, the number of the remaining observations decreases. When the component weight is below the critical value, $w_{\min}$,

$$\frac{n_l}{n} \leq w_{\min} \tag{4.36}$$

it is assumed that the remaining observations belong to the existing classes and do not form the new ones.

The correlation between the critical component weight, $w_{\min}$, and the critical absolute relative deviation, $D_{\min}$, exists as (Nagode and Fajdiga 2006)

$$w_{\min} = \frac{l \times D_{\min}}{2} \tag{4.37}$$

To gain an optimal estimate for $D_{\min}$, the AIC is used to obtain the optimal number of components, weights, and component parameters. In the general case, the AIC is defined as

$$\mathrm{AIC} = 2Q - 2\ln\left[L(c, \mathbf{w}, \boldsymbol{\theta})\right] \tag{4.38}$$

where Q is the number of parameters in the statistical model; and $L(\cdot)$ is the maximized value of the likelihood function for the estimated model.

The classification of the remaining observations is accomplished by the Bayes decision rule

$$l = \max \arg w_l f\left(\mathbf{y}_j \mid \boldsymbol{\theta}_l\right) \tag{4.39}$$

$$w_l = w_l + \frac{k_{lj}}{n} \tag{4.40}$$

$$m_l = m_l + \frac{k_{lj}\left(y_j - m_l\right)}{n w_l} \tag{4.41}$$

$$V_l = V_l + \frac{k_{lj}\left(y_j^2 - V_l\right)}{n w_l} \tag{4.42}$$

k_{lj} is added to the lth class and the component weight, the component mean as well as the component variance are recalculated (Bishop 1995). Once all k bin means or all n observations are processed, mixture parameters can be gained by inverting Equations (4.30) to (4.35).

The whole procedure stops when

$$(c+1)D_{\min} < D \tag{4.43}$$

is fulfilled, in which D is the total of absolute relative deviations.

4.3 Preprocessing and Analyzing Measurement Data

4.3.1 Wavelet Processing of Measured Dynamic Strain

For the TMB, the temperature-induced strain contributes little to the stress because the majority of temperature-induced strain is released by the boundary adjustment at the expansion joints and bearings. However, the overall drift of strain time history mainly caused by temperature will make a great influence on the mean stress for each stress cycle, though it has little effect on the calculation of stress range. Therefore, the original measurement data should be preprocessed to eliminate the temperature effect for modeling the stress spectra.

As described in Chapter 3, 20 days' strain time histories measured by the strain gauge SSTLS13 including one day under typhoon conditions have been chosen to construct a representative data sample. The rainflow-counted stress range and mean stress data acquired from this representative data sample are chosen for modeling the PDF of stress spectra as shown later. **Figure 4.2** shows four typical daily strain time histories obtained from the strain gauge SSTLS13 after eliminating the temperature effect from the original measured strain data by making use of a wavelet-based filtering method (Ni *et al*. 2008). **Figure 4.3** illustrates the corresponding

rainflow-counted stress range and mean stress of four typical filtered daily strain data from the strain gauge SSTLS13, in which the stress ranges less than 2 MPa are disregarded; while the obtained rainflow-counted stress range and mean stress of the 20 days' filtered strain data are illustrated in **Figure 4.4**.

4.3.2 Effect of Mean Stress on Predicted Fatigue Life

Figure 4.5 shows a comparison of four typical daily stress spectra using both the original measured strain data and those after eliminating the temperature effects. It is seen from **Figure 4.5** that the results are almost the same since the drift of strain time history caused by temperature only affects the rainflow-counted mean stress, while there is almost no effect on the stress range and cycles, which are the most important parameters affecting the predicted fatigue life. This can also be observed from **Figure 4.6** which shows a comparison of the obtained two standard daily stress spectra by averaging 20 days' original and filtered strain data. **Figure 4.7** illustrates the fatigue lives predicted by using 20 daily original and filtered strain data, respectively, which reveals that the fatigue lives using the filtered strain data are a little bit larger than those predicted by using the original strain data.

4.4 Multi-Modal PDF of Stress Range

4.4.1 Prediction of PDF of Stress Range Using Different Distributions

In this section, the rainflow-counted stress ranges from 2 to 30 MPa, resulting from the 20 days' filtered strain data measured by the strain gauge SSTLS13, are extracted for modeling the PDF of the stress range, as this scope covers all the stress ranges caused by vehicle and train traffic passing through the TMB. The total observation number of the 20 days' stress range data is 190,391, and the number of classes, K, is obtained as 19 by using the Sturges classification rule (Sturges 1926), which is expressed by

$$K = \lceil 1 + \log_2 M \rceil \tag{4.44}$$

where M represents the total number of the data samples; and $\lceil\ \rceil$ is the ceiling operator, i.e., taking the closest integer above the calculated value.

Figures 4.8 and **4.9** show the finite mixed PDFs and CDFs of the 20 days' stress range data acquired by the strain gauge SSTLS13 when using normal, lognormal, and Weibull distributions. The corresponding estimated parameters of the component distributions are given in **Table 4.1**. It can be seen that the scatter of the stress ranges is well modeled by the finite mixture distributions and easily extrapolated to the region beyond the measured stress ranges. The accuracy of the stress range prediction and the extrapolation ability rely on the probability distribution of the stress range. In addition, the scattered level and the record length of the stress range will also affect the accuracy when extrapolating beyond the measured stress ranges (Nagode and Fajdiga 1998). It is observed in **Figure 4.8** that the predicted stress

range distribution is a two-modal PDF separated by 6 MPa. The stress ranges less than 6 MPa are caused by highway traffic, and the stress ranges larger than 6 MPa are mainly attributed to train traffic.

Figure 4.10 shows the variation of the AIC values with the iteration number of the three mixed PDFs (normal, lognormal, and Weibull) of the 20 days' stress range data. The best model of the stress range distribution is determined with the lowest AIC value. It is found that the AIC values for the three PDFs converge rapidly after 5 iterations and the mixed Weibull PDF results in the lowest AIC value. As a result, the Weibull distribution is taken herein as the component distribution for modeling the measured stress ranges. The AIC value helps the selection of both the optimal number of components and the parametric family.

4.4.2 Mixed Weibull PDF of Stress Range

Figure 4.11 illustrates the predicted mixed Weibull PDFs of four daily rainflow-counted stress range data obtained from the strain gauge SSTLS13. The corresponding estimated parameters of the component distributions are given in **Table 4.2**, from which it is observed that the mixed Weibull PDF with six components are enough for modeling the daily rainflow-counted stress range data. A further observation into **Figure 4.11** reveals that the stress range distribution on August 22, 1999 has a pattern different from others, the region between two peaks of

stress range distribution being partly filled. This is mainly due to the fact that typhoon "Sam" buffeted Hong Kong on August 22, 1999, and the typhoon-induced strain time history as well as the stress spectrum has a different mode in comparison with those obtained under normal traffic and wind conditions.

4.5 Modeling of Stress Matrix

4.5.1 Multivariate Mixture Models

In general, an arbitrary rainflow stress matrix contains two random variables, i.e., stress range and mean stress. From the standpoint of finite mixture distributions, the joint PDF of rainflow stress matrix, $f(\mathbf{s})$, can be defined as a weighted sum of joint component distributions. That is

$$f(\mathbf{s}) = \sum_{l=1}^{c} w_l f_l(\mathbf{s}) \tag{4.45}$$

where $\mathbf{s} = [s_r, s_m]^{\mathrm{T}}$, in which s_r and s_m stand for stress range and mean stress, respectively; and $f_l(\mathbf{s})$ represents the lth joint component PDF of the two random variables.

As described in the aforementioned section, it has been demonstrated that stress range can be modeled reliably by a mixture of two-parameter Weibull distributions, and mean stress should be described by a mixture of normal distributions, as not all

the mean stress data are positive. The joint component PDF of stress range and mean stress can thus be expressed by a mixture of Weibull-normal distributions on the assumption that the two random variables corresponding to the *l*th joint component distribution are independent (Bishop 1995), which can be expressed as

$$f_l(\mathbf{s}) = f_l(s_r) f_l(s_m) = \frac{\beta_l}{\sqrt{2\pi}\sigma_l s_r} \left(\frac{s_r}{\theta_l}\right)^{\beta_l} \exp\left\{-\left(\frac{s_r}{\theta_l}\right)^{\beta_l} - \frac{(s_m - \mu_l)^2}{2{\sigma_l}^2}\right\} \quad (4.46)$$

Then, the joint component CDF of stress range and mean stress is therefore obtained by

$$F_l(\mathbf{s}) = F_l(s_r) F_l(s_m) = \left(1 - \exp\left\{-\left(\frac{s_r}{\theta_l}\right)^{\beta_l}\right\}\right) \Phi\left(\frac{s_m - \mu_l}{\sigma_l}\right) \quad (4.47)$$

where $f_l(s_r)$ and $f_l(s_m)$ are the PDF of stress range and the PDF of mean stress corresponding to the *l*th joint component distribution, respectively; and $F_l(s_r)$ and $F_l(s_m)$ are the CDF of stress range and the CDF of mean stress corresponding to the *l*th joint component distribution, respectively.

For the parameter estimation of multivariable mixture distributions, the EM algorithm has been proved to be the most appropriate method to estimate the unknown parameters for a mixture of multivariate normal distributions (Titterington *et al*. 1985). However, it turned out to be unsuitable for distributions like Weibull-normal mixtures because the estimated parameters depend decisively on the

initial conditions of iteration and the algorithm does not necessarily converge and/or becomes slow and unreliable, especially if the number of components is high. In this study, the algorithm developed by Nagode and Fajdiga (2001) for parameter estimation of multivariate mixture distributions is used to model, extrapolate, and predict the scatter of rainflow-counted stress range and mean stress data.

For a joint Weibull-normal distribution, the corresponding parameters can be estimated by using a numerical method such as the Newton-Raphson procedure to solve the following equations

$$\mu_l = \frac{1}{N}\sum_{i=1}^{N} s_{mi} \tag{4.48}$$

$$\sigma_l{}^2 = \frac{1}{N}\sum_{i=1}^{N}\left(s_{mi} - \mu_l\right)^2 \tag{4.49}$$

$$\theta_l = \left(\frac{1}{N}\sum_{i=1}^{N} s_{ri}^{\beta_l}\right)^{1/\beta_l} \tag{4.50}$$

$$\frac{1}{\beta_l} + \frac{1}{N}\sum_{i=1}^{N}\ln\left(s_{ri}\right) - \frac{\sum_{i=1}^{N} s_{ri}^{\beta_l}\ln\left(s_{ri}\right)}{\sum_{i=1}^{N} s_{ri}^{\beta_l}} = 0 \tag{4.51}$$

4.5.2 Joint PDF of Stress Matrix

Figures 4.12 and **4.13** illustrate the joint PDF and CDF of the 20 days' stress range

and mean stress data obtained from the strain gauge SSTLS13 by using the Weibull-normal mixture distributions. It is seen that the scatter of the stress range and mean stress data is well modeled by the mixed Weibull-normal distributions. The corresponding estimated parameters of the component distributions are given in **Table 4.3**, from which it is seen that a joint PDF of Weibull-normal mixtures with twelve components is appropriate for modeling the stress range and mean stress data. Also, the predicted joint PDFs of four daily stress range and mean stress data are shown in **Figure 4.14**, which reveals that the joint PDF of stress range and mean stress on August 22, 1999 has a slightly different pattern from the others due to the typhoon effect.

4.6 Summary

In this chapter, the modeling of bivariable stress spectrum has been accomplished by use of the method of finite mixture distributions in combination with a hybrid parameter estimation algorithm. The addressed procedure was illustrated using the long-term monitoring data of dynamic strain from the instrumented suspension TMB. A wavelet-based filtering method was used to eliminate the temperature effect from the original measured data, and the rainflow counting algorithm was employed for extracting the stress range and mean stress data from the stress time histories. In consideration of highway and railway traffic and typhoon effects, a monitoring-based representative sample of stress spectrum was achieved by carefully examining

one-year strain measurement data.

Based on the modeling analysis results of the derived stress range and mean stress data, the following conclusions can be drawn: (i) a fairly good conformity is observed between the obtained distribution functions and the measurement data, it therefore can be concluded that the method of finite mixture distributions is effective for modeling of stress spectrum; (ii) the multi-modal PDF of the stress range can be generated by use of the finite mixed Weibull distributions, while the joint PDF of the stress range and the mean stress is achieved by means of a mixture of multivariate Weibull-normal distributions; and (iii) the achieved results from this study will serve as a useful tool to facilitate the fatigue reliability assessment of steel bridges instrumented with SHM system.

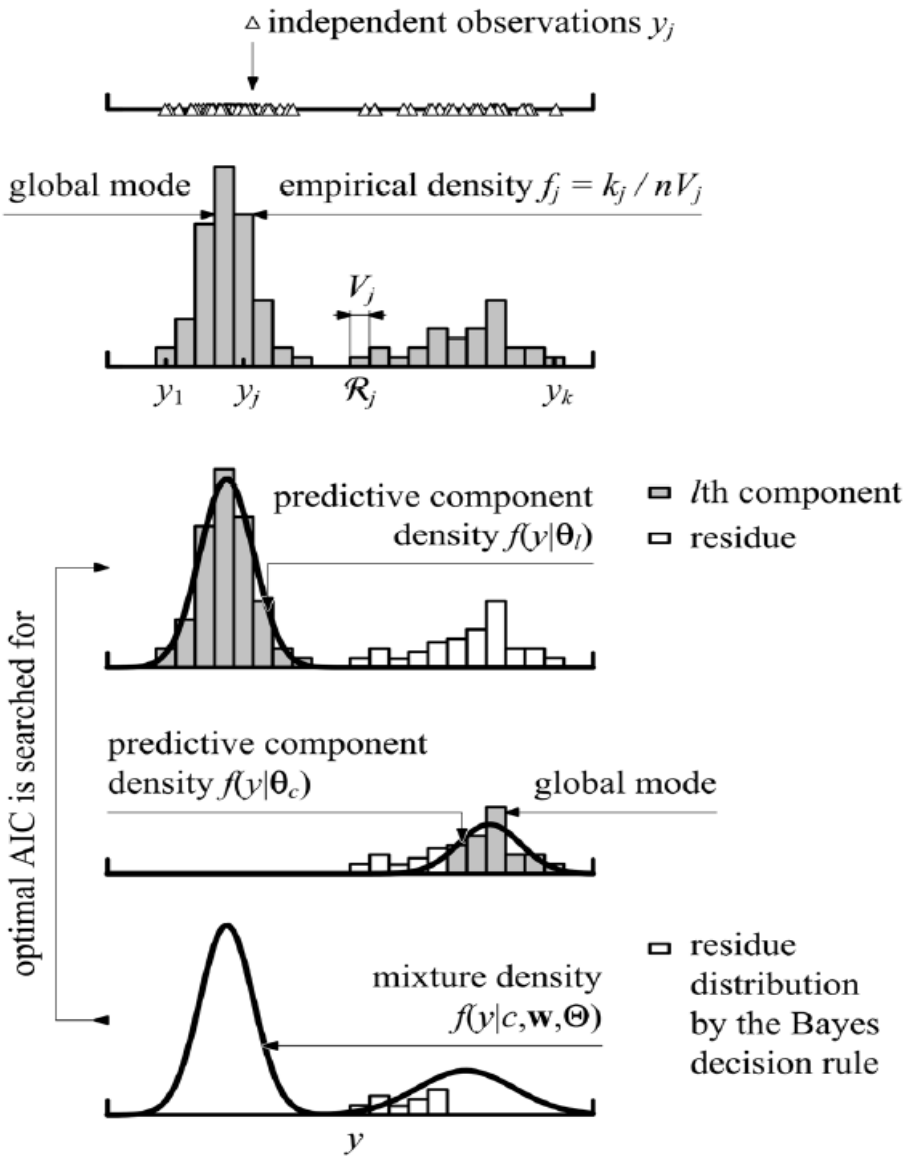

Figure 4.1 Procedural diagram of hybrid mixture parameter estimation

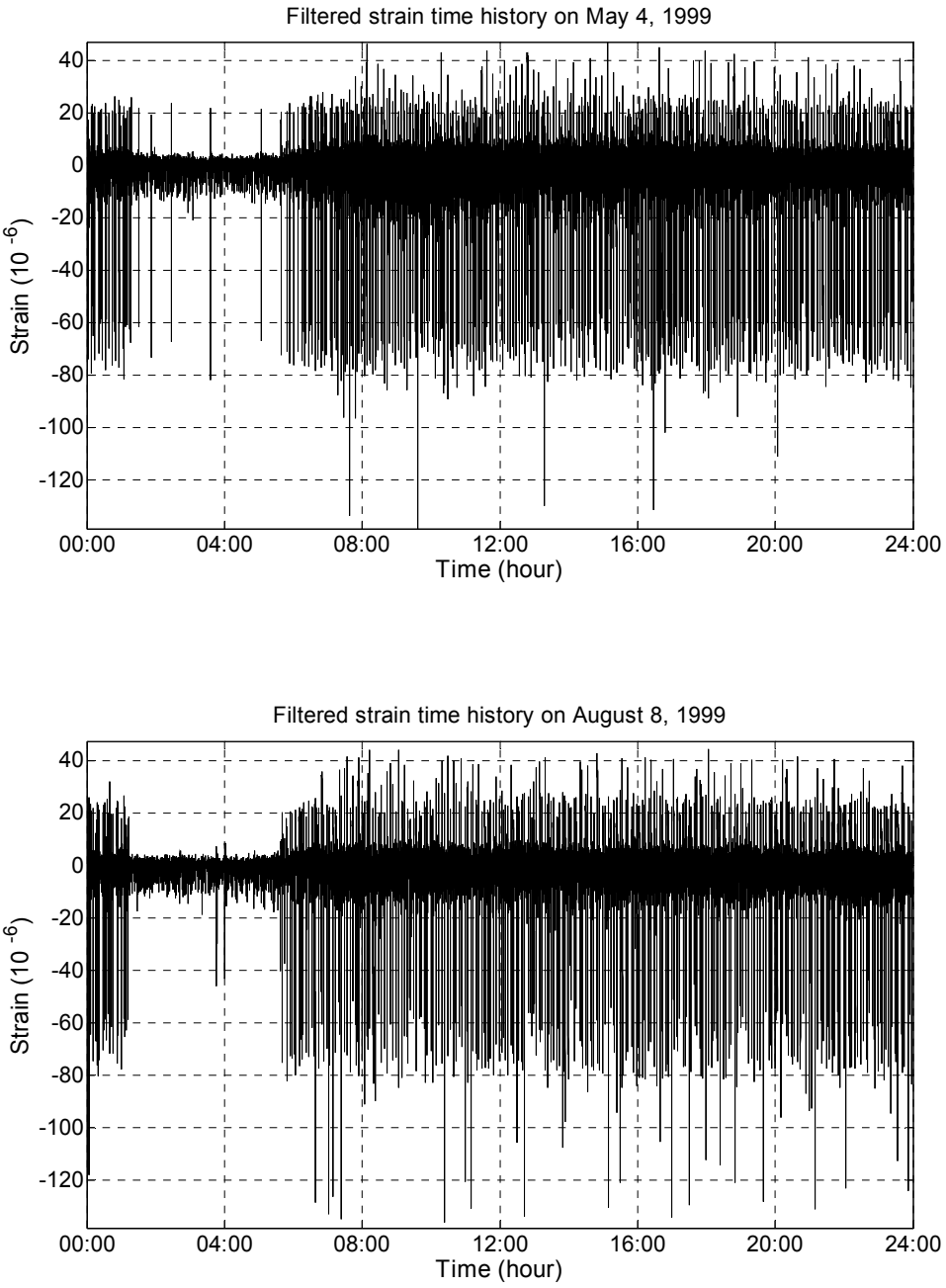

Figure 4.2(a) Strain time histories after eliminating temperature effect

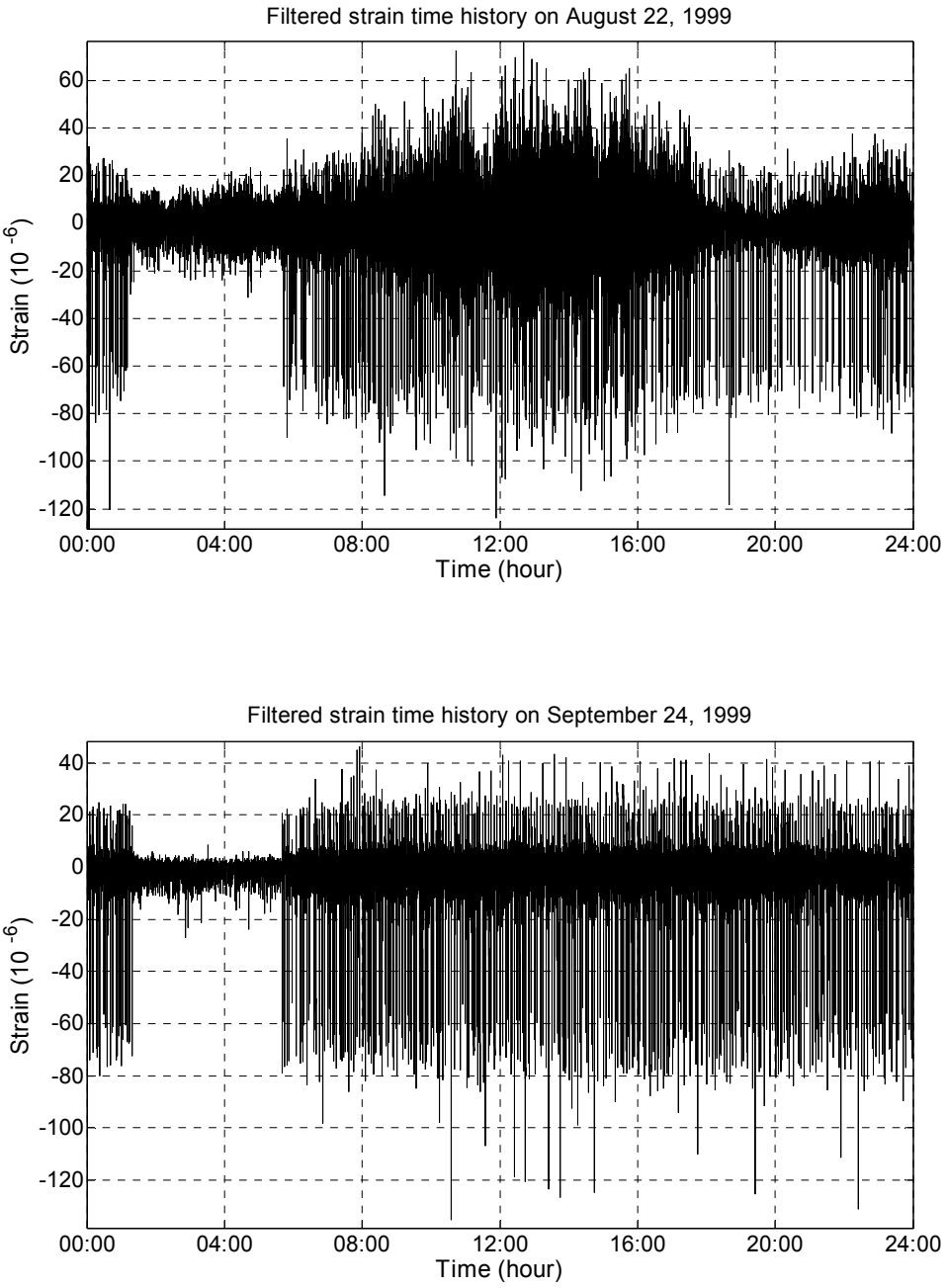

Figure 4.2(b) Strain time histories after eliminating temperature effect

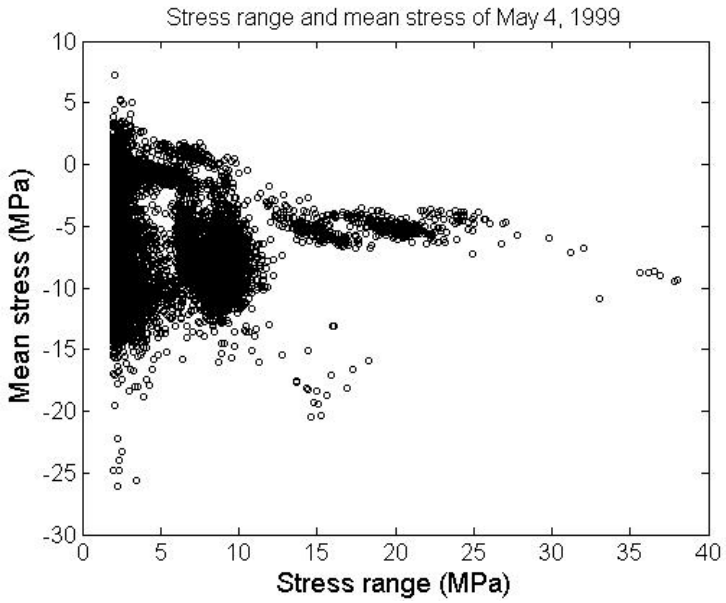

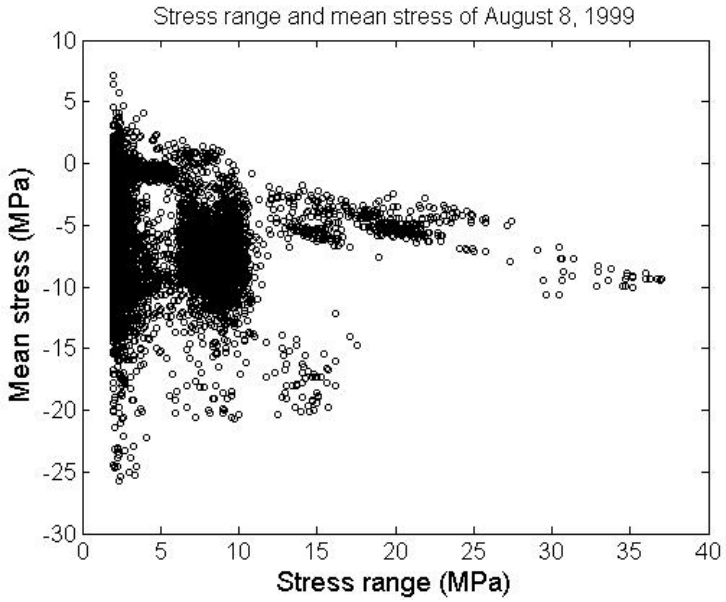

Figure 4.3(a) Stress range and mean stress of filtered daily strain data

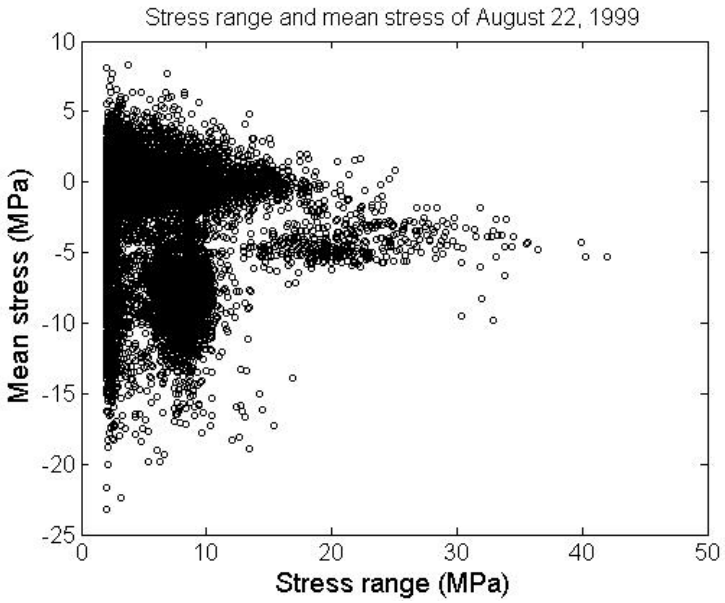

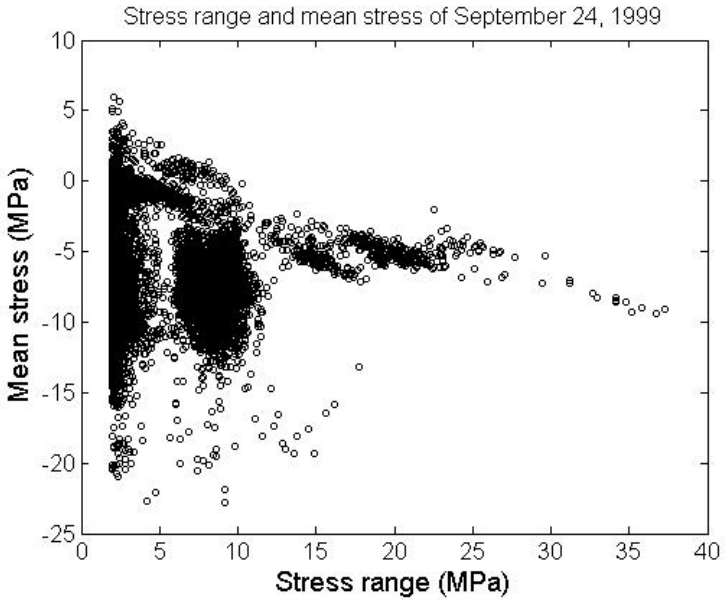

Figure 4.3(b) Stress range and mean stress of filtered daily strain data

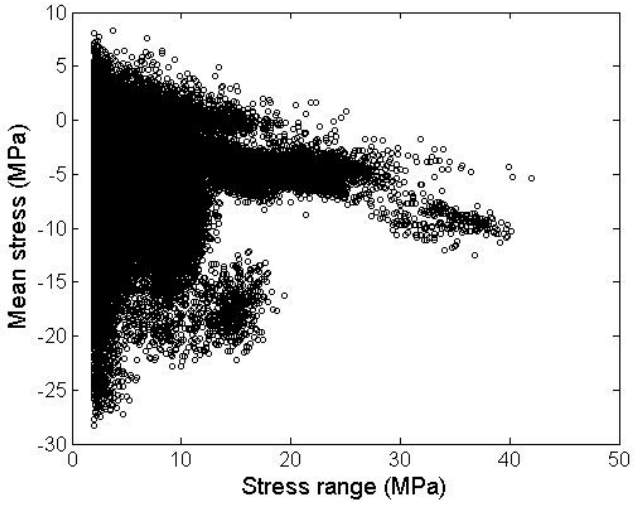

Figure 4.4 Stress range and mean stress of 20 days' filtered strain data

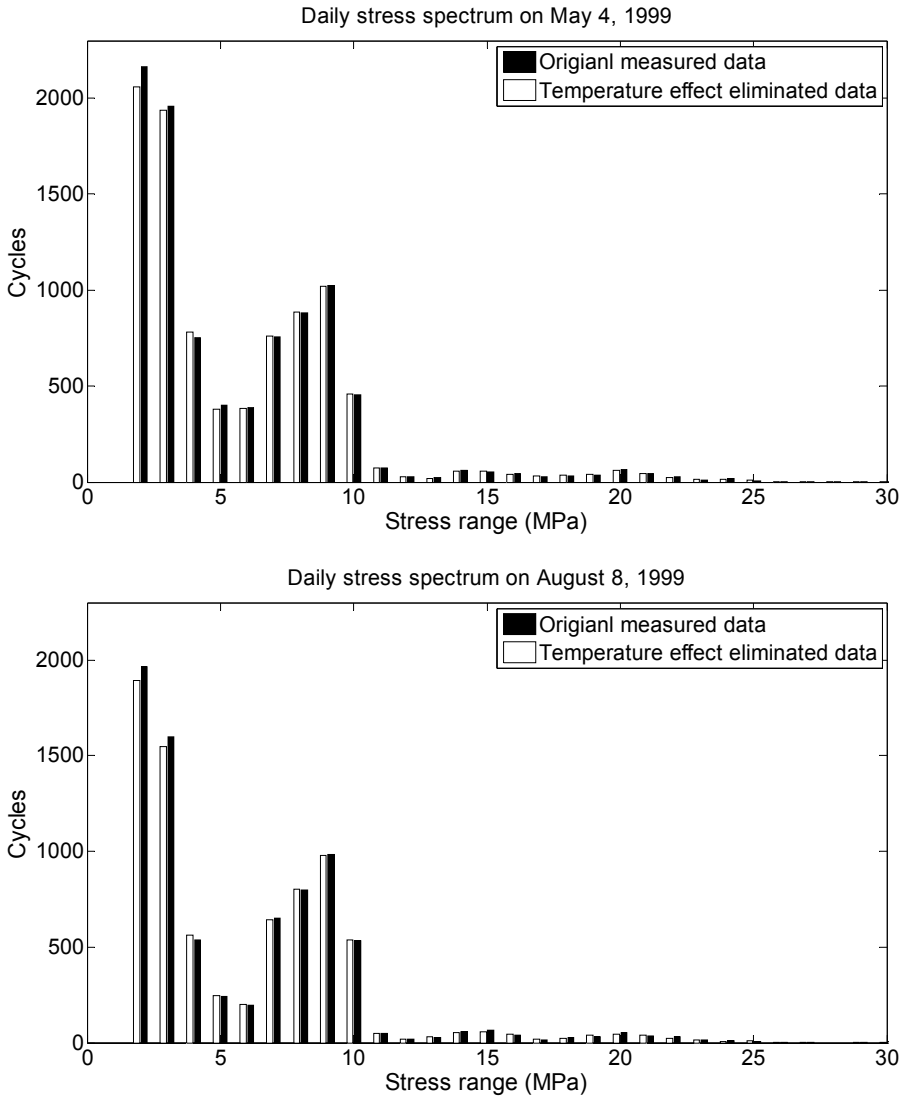

Figure 4.5(a) Comparison of daily stress spectra

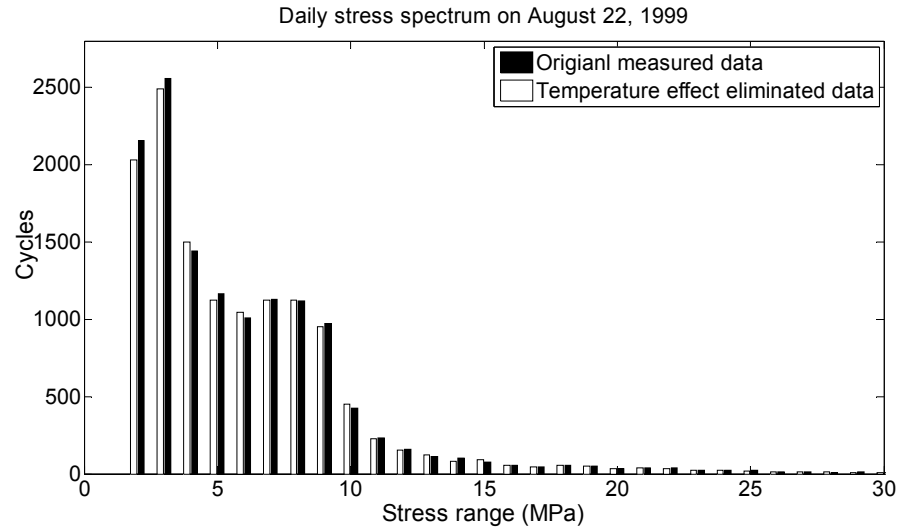

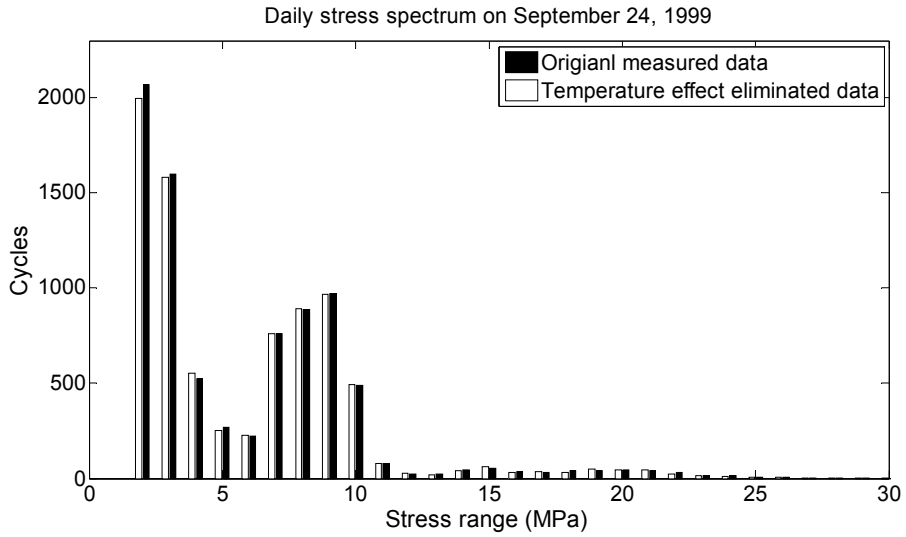

Figure 4.5(b) Comparison of daily stress spectra

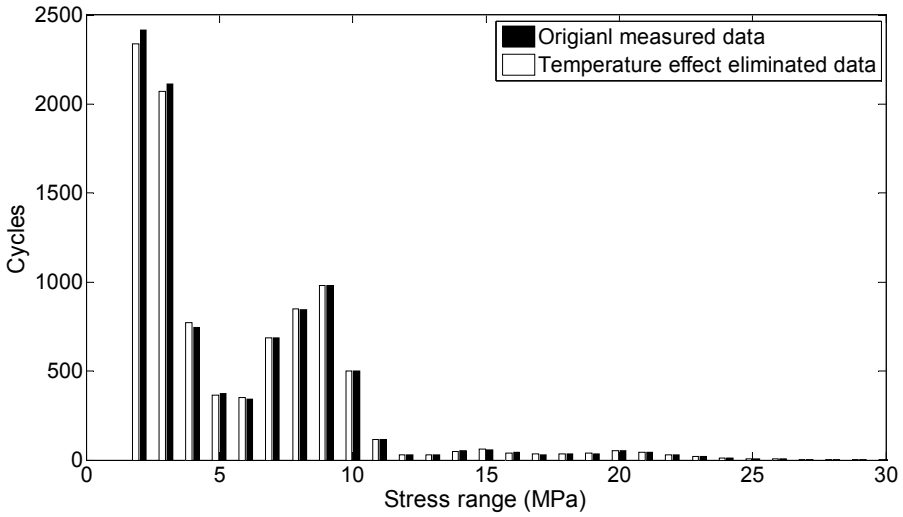

Figure 4.6 Comparison of standard daily stress spectra

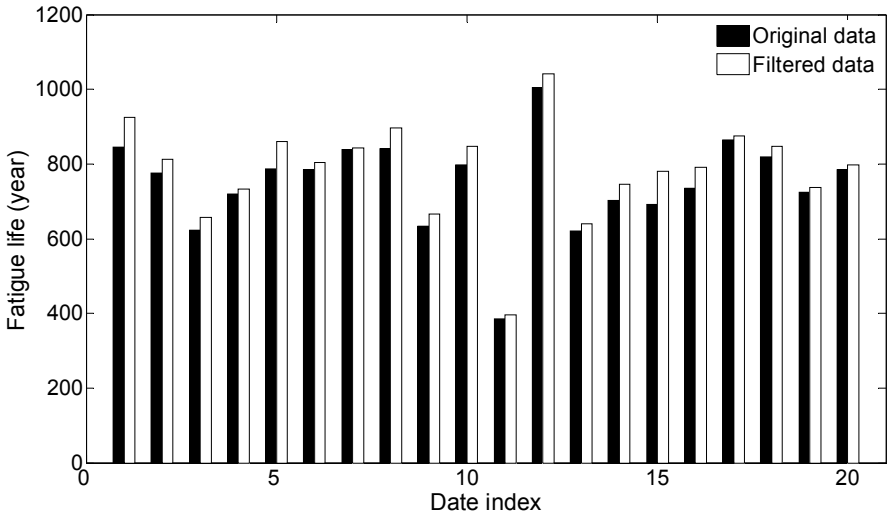

Figure 4.7 Comparison of predicted fatigue life of daily strain data

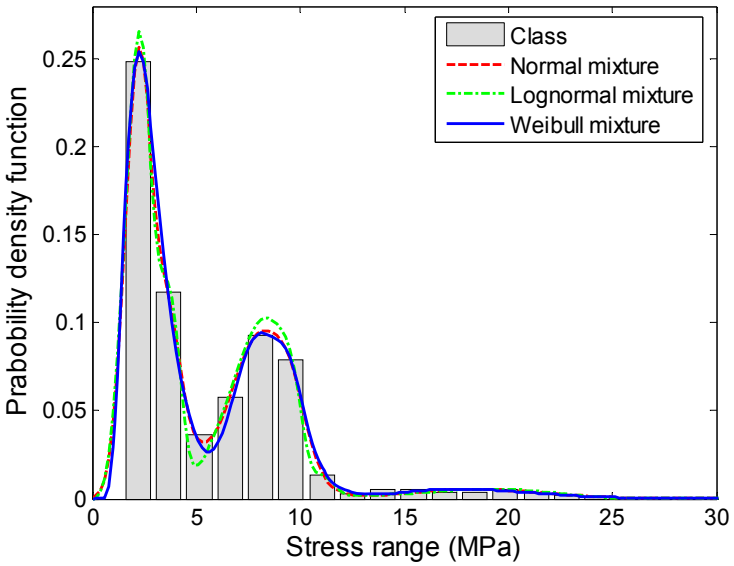

Figure 4.8 Mixed PDFs of 20 days' stress range data

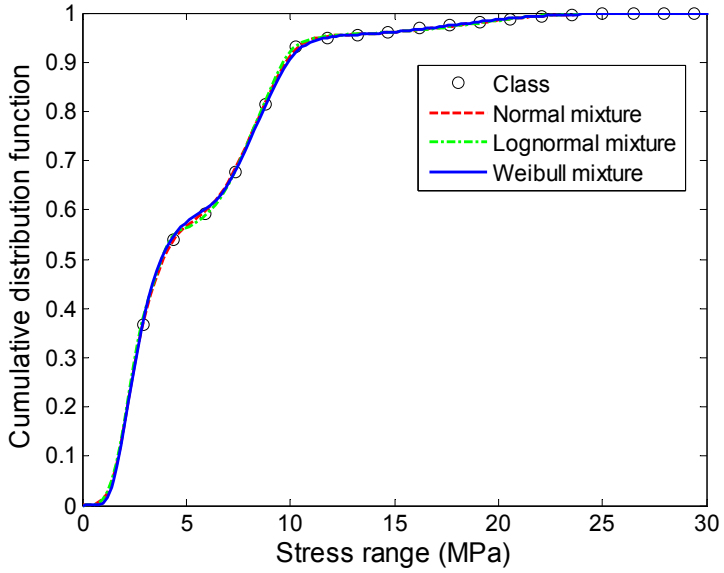

Figure 4.9 Mixed CDFs of 20 days' stress range data

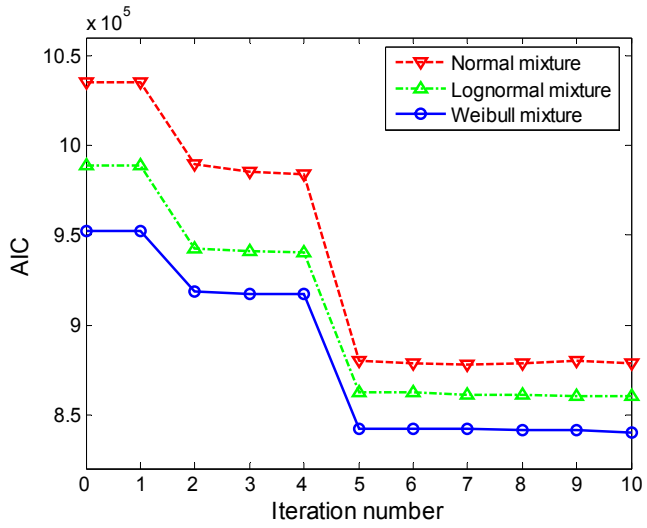

Figure 4.10 AIC values of mixed PDFs of 20 days' stress range data

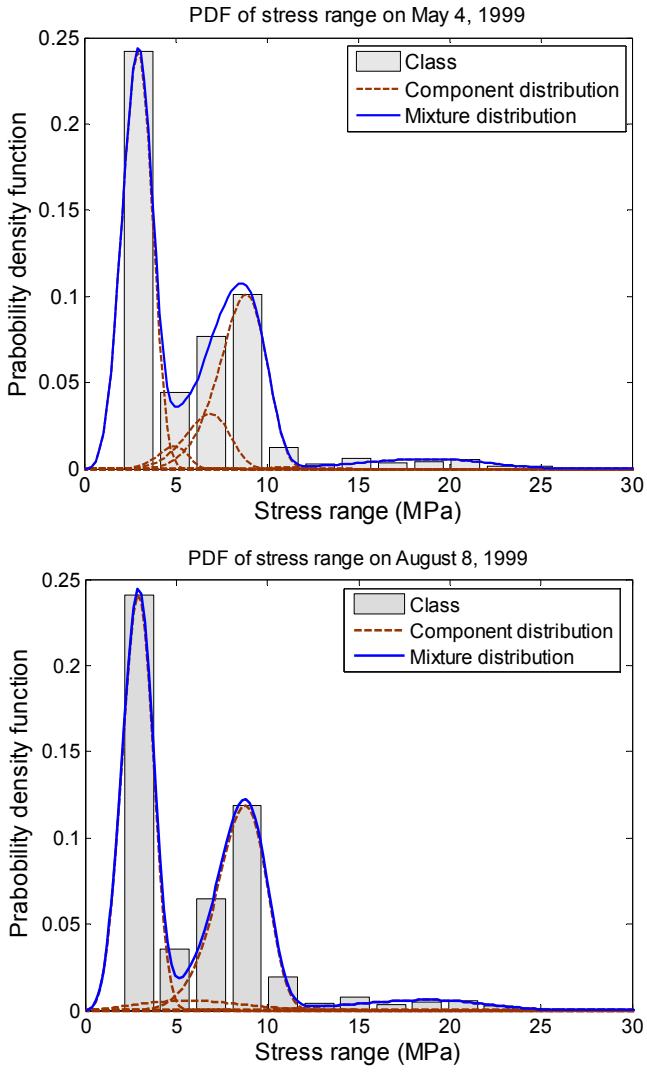

Figure 4.11(a) Mixed Weibull PDFs of four daily stress range data

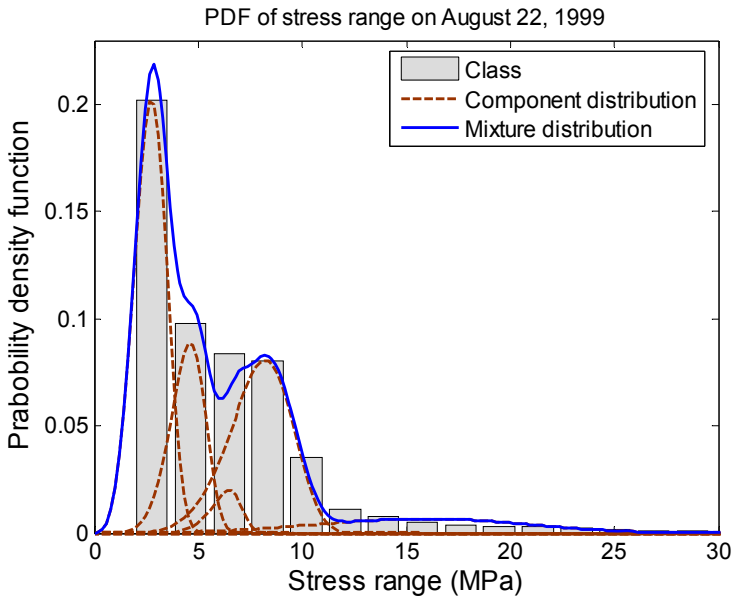

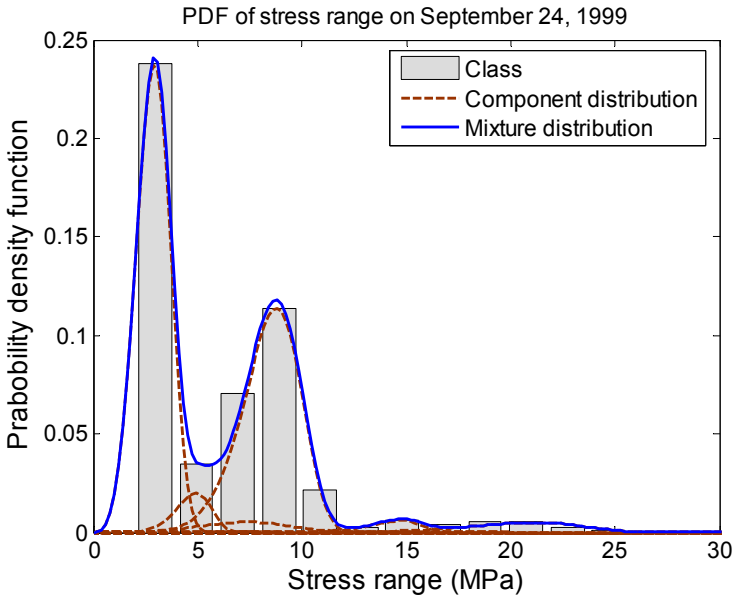

Figure 4.11(b) Mixed Weibull PDFs of four daily stress range data

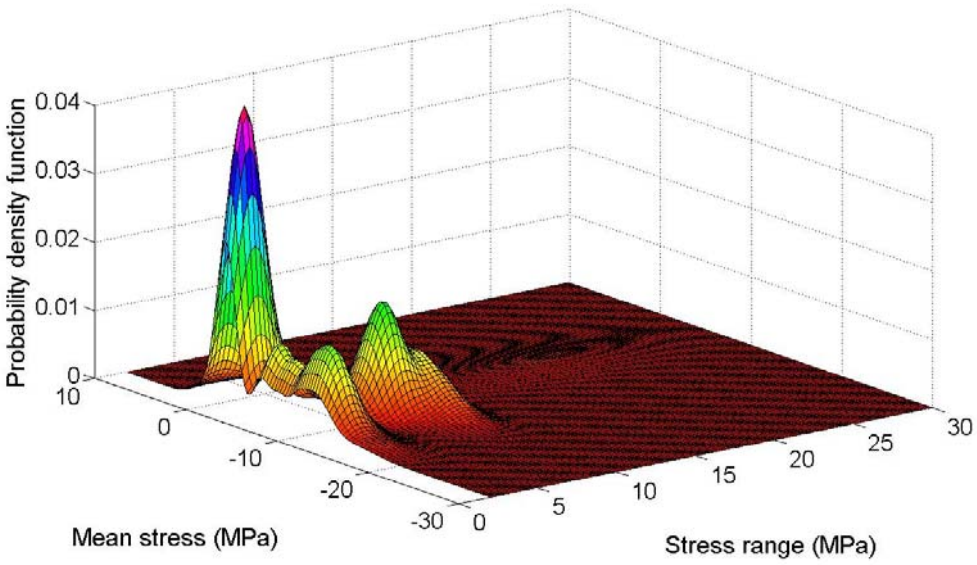

Figure 4.12 Joint PDF of 20 days' stress range and mean stress data

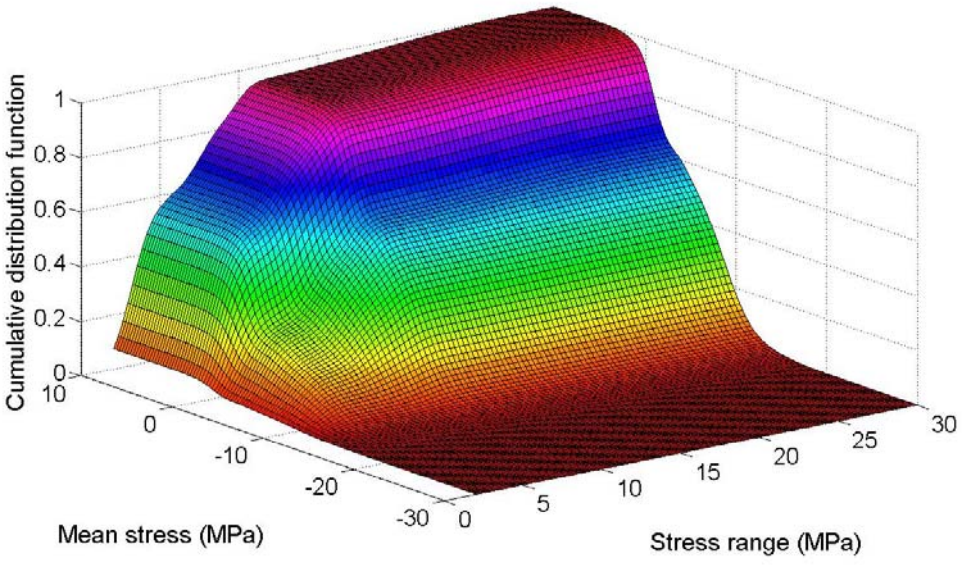

Figure 4.13 Joint CDF of 20 days' stress range and mean stress data

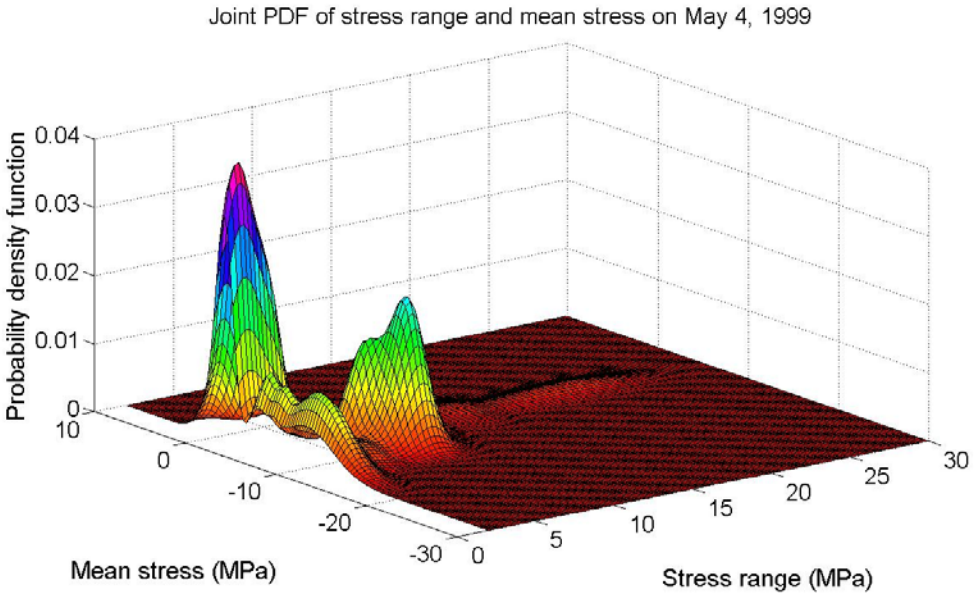

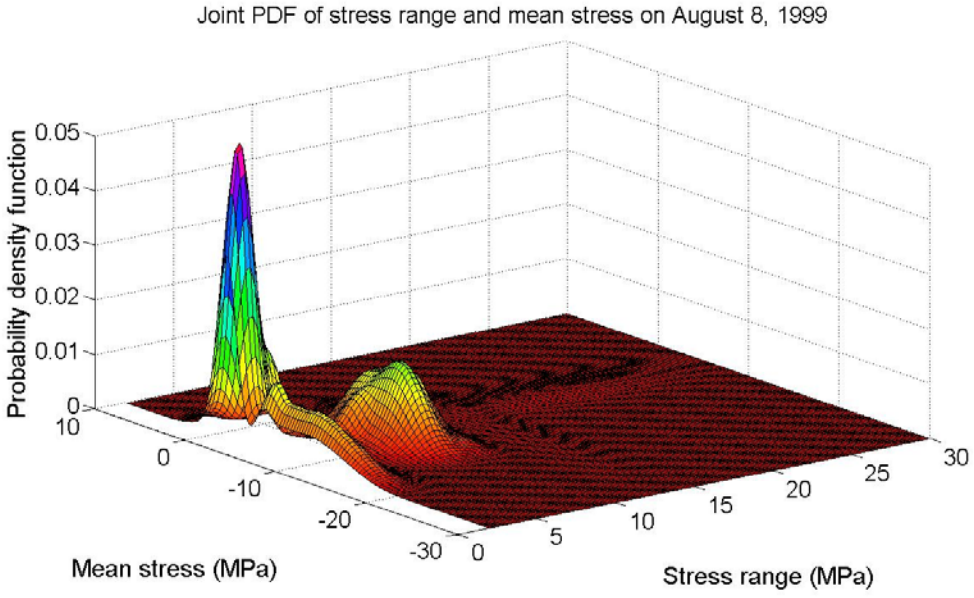

Figure 4.14(a) Joint PDFs of four daily stress range and mean stress data

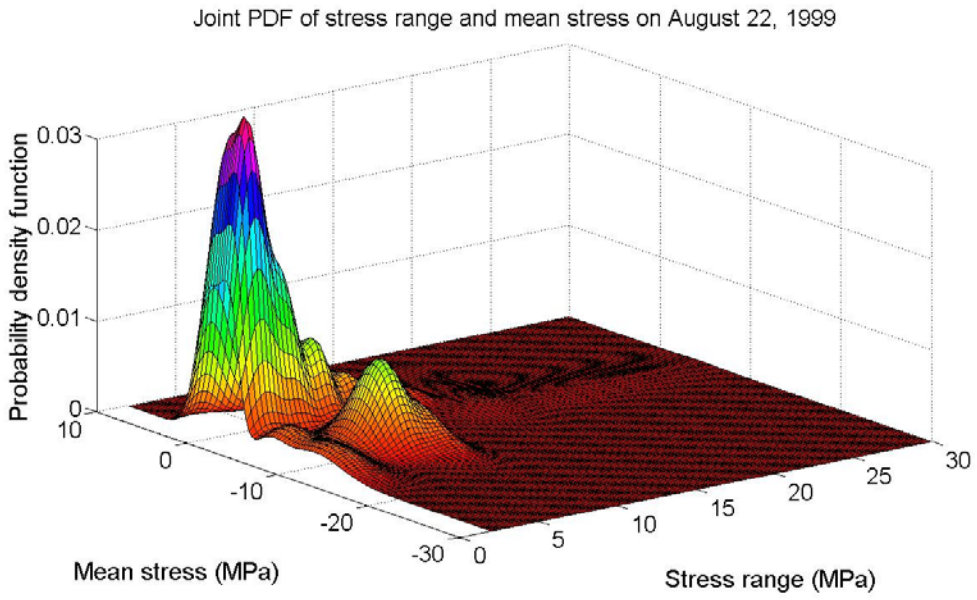

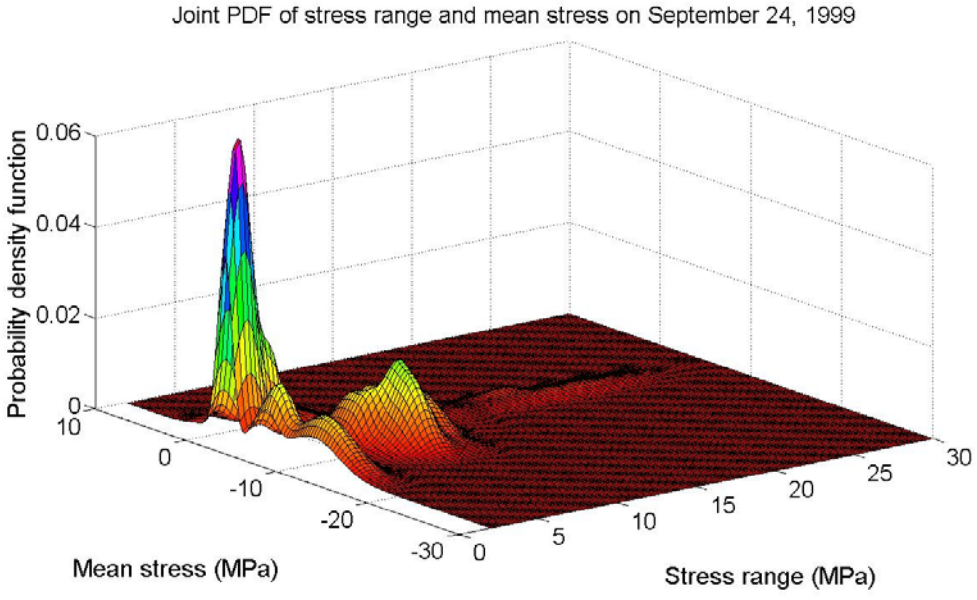

Figure 4.14(b) Joint PDFs of four daily stress range and mean stress data

Table 4.1 Estimated parameters of component distributions from 20 days' stress range data

Parametric family	Weight (w_l)	Mean value (μ_l)	Standard deviation (σ_l)
Normal	0.397	2.207	0.637
	0.158	3.679	0.651
	0.349	8.094	1.487
	0.032	9.563	0.636
	0.018	5.149	0.587
	0.046	18.473	3.393
Lognormal	0.555	0.933	0.376
	0.312	2.118	0.165
	0.036	2.262	0.063
	0.052	1.409	0.327
	0.045	2.906	0.178
Weibull		Shape parameter (θ_l)	Shape parameter (β_l)
	0.375	2.348	4.101
	0.166	3.752	6.795
	0.306	8.211	6.701
	0.062	9.580	17.173
	0.024	6.287	1.831
	0.021	11.052	16.181
	0.046	19.739	6.429

Table 4.2 Estimated parameters of component distributions from four daily stress range data

Date	Weight (w_l)	Shape parameter (θ_l)	Shape parameter (β_l)
May 4, 1999	0.496	3.169	4.063
	0.328	9.042	7.502
	0.098	7.092	6.241
	0.027	5.063	6.803
	0.051	19.515	5.845
August 8, 1999	0.503	3.154	3.969
	0.405	8.981	7.090
	0.039	6.911	2.476
	0.053	19.354	5.831
August 22, 1999	0.391	2.961	4.025
	0.184	4.744	6.155
	0.305	8.494	6.016
	0.037	6.544	9.525
	0.083	17.414	3.648
September 24, 1999	0.483	3.147	4.082
	0.395	9.001	6.969
	0.041	5.041	6.479
	0.028	7.964	3.896
	0.019	14.818	12.805
	0.034	21.451	8.452

Table 4.3 Estimated mixture parameters from 20 days' stress range and mean stress data

Component index	Weight (w_l)	Shape parameter (θ_l)	Shape parameter (β_l)	Mean value (μ_l)	Standard deviation (σ_l)
1	0.279	3.470	3.530	-0.964	1.030
2	0.139	7.480	8.000	-8.680	1.550
3	0.120	3.420	3.770	-10.600	1.660
4	0.183	9.760	9.850	-8.280	3.360
5	0.054	3.480	3.470	-4.820	0.855
6	0.036	3.440	3.660	-6.750	0.842
7	0.024	5.380	6.760	-0.964	0.932
8	0.020	3.490	3.430	-8.680	0.799
9	0.040	4.550	2.210	1.310	1.240
10	0.032	7.470	10.500	-4.010	2.040
11	0.054	20.000	4.460	-5.220	2.400
12	0.019	3.520	3.210	-15.100	2.160

CHAPTER 5

EXPERIMENTAL STUDY ON DETERMINATION OF SCF AND ITS STOCHASTIC CHARACTERISTICS

5.1 Introduction

Due to the limitation of sensor implementation techniques and specific in-situ conditions, the sensors for strain monitoring are usually not deployed at the most critical locations where fatigue cracks are expected to occur and thus only the nominal strain/stress is obtained. The nominal stress approach has been widely used for fatigue evaluation because most design specifications (BSI 1980; AASHTO 1990) for steel structures contain a standard fatigue analysis procedure based on this approach. However, the nominal stress approach cannot be used to find out the most critical stress at the fatigue damage location. An alternative method for fatigue analysis of complicated welded steel joints is the hot spot stress approach which is more accurate and reliable than the nominal stress approach.

When using the hot spot stress method for fatigue design and life prediction of welded structures, a critical issue is focusing on how to determine the SCF for the

welded details. In general, the determination of SCF can be achieved by means of finite element analyses, laboratory experiments, or field tests. Research efforts have been devoted to investigating the SCF determination (Puthli 1988; Karamanos *et al*. 2000; Fung *et al*. 2002; Gho *et al*. 2003; Chan *et al*. 2005; Gao *et al*. 2007), and most of them are related on the welded tubular joints and seldom are devoted to investigating the properties of the SCF for the welded plate joints of large-scale civil engineering structures, especially for the cable-supported steel bridges. Furthermore, because of the considerable effects and sources of uncertainties during the determination of SCF either by finite element analyses or by experimental measurements, an investigation into the stochastic properties of SCF is of vital necessity.

In this chapter, the SCF and its stochastic characteristics for a typical welded steel bridge T-joint composed of two perpendicular steel plates is perceived by conducting full-scale model experiments of a railway beam section of the suspension TMB. The central section of the test model is selected for instrumentation of the traditional electrical strain gauges. The strain data of the pre-allocated measuring points are acquired and the hot spot strain at the weld toe is determined by a linear regression method. The SCF is then calculated as the ratio between the hot spot strain and the nominal strain which is derived from the measured data. To take full account of the effect of predominant factors on the scatter of SCF, experiments are carried out under moving load conditions with a combination of three load weight grades, two

velocities of moving load, and two axle-distances of the test bogie. The statistical properties and probability distribution of the SCF are achieved for the typical welded steel bridge T-joint.

5.2 Experimental Setup

5.2.1 Design and Fabrication of Test Model

Figures 5.1 and **5.2** show the schematic and a photo of the experimental setup for full-scale model experiments of the railway beam section of the TMB. The test model comprising two steel beams with a length of 4.5 m is fixed on both sides by two heavily vertical steel plates. Each steel beam is composed of three welded plates, namely top flange, web plate, and bottom flange, and the main efforts of this experimental study are focused upon the accomplishment of the SCF and its statistical properties and probability distribution for the T-joint which is composed of the web plate and bottom flange, as shown in **Figure 5.3**. Two platforms with runways are designed and extended from the test model to enable tentative parking of the test bogie while moving away from the test model during the experiments.

The structural grade of the steel material for the test model is Q345A as stipulated in Chinese code GB/T1591-94; the material properties are almost identical to those of Grade Fe 510C as specified in BS EN 10 025 (1990) which is utilized for fabrication

of steel components of the TMB. The elastic modulus of Q345A and Grade Fe 510C are 206 GPa and 205 GPa respectively, and the Poisson's ratios are 0.3 for both. The chemical compositions and mechanical properties of the two types of steel materials are listed in **Table 5.1**.

5.2.2 Instrumentation

The main equipment for strain measurement includes the traditional electrical strain gauge (TML PFL-10-11) and a data acquisition system (NI SCXI-1000). The strain data were recorded continuously by the data interrogator at a sampling rate of 10 Hz, and the gauge length of the strain gauge is 10 mm. The total number of the channels in the data acquisition system is 32, of which 13 channels are used for strain measurement of the central section located at one steel beam of the test model. **Figure 5.4** shows the schematic diagram of the measurement setup. All the equipment including the electrical source and automatic voltage regulator was connected with the ground wire in order to eliminate the effect of electromagnetism interference. The initial calibration for data normality checking was carried out before the experiments to ensure the reliability and stability of the strain readings.

Figure 5.5 shows a photo of the welded T-joint between the web plate and bottom flange of the test model, which complies with the specifications in BS5135: 1984@Table 15 according to the drawings for the welded connections of the TMB.

The weld thickness and weld angle are 6 mm and 45^0, respectively. **Figure 5.6** shows the details of the strain gauges deployed on the central section of the test model. It should be noted that the strain gauges from c-8 to c-13 are mainly used for the subsequent damage detection purpose, and the present study focuses on the strain measurement data from the strain gauges c-1 to c-7. A photo of the strain gauges deployed on the central section of the test model is shown in **Figure 5.7**.

5.2.3 Description of Test Load

Two types of load cases in static and moving load conditions with three load weight grades are operated in this experimental study. The moving load is exerted through automatically controlling a specially designed test bogie with a self-weight of 1.12 t, as shown in **Figure 5.8**. This test bogie is self-driven and controlled by an electro-circuit system assembled in a control box, as shown in **Figure 5.9**. A braking device is installed on the test bogie, which is devised for bringing the test bogie to stop by forming a short-circuit in the electro-circuit system at a suitable time when the test bogie is moving near to the end of the runway. The distance between the front and behind axles of the test bogie is adjustable in a dual-choice of 1.025 m and 1.545 m and the velocities of moving load are changeable in 0.15 m/s and 0.45 m/s, respectively. As illustrated in **Figure 5.10**, three load-weight grades in a total weight of 5.982 t (grade I), 9.724 t (grade II), and 14.586 t (grade III) respectively, are used in the experiments.

5.3 Experimental Results and Analysis

5.3.1 Experimental SCF Determination Method

In general SCF can be calculated by dividing the hot spot strain, ε_{hot}, by the nominal strain, ε_{nom}, according to

$$\text{SCF} = \frac{\varepsilon_{hot}}{\varepsilon_{nom}} \tag{5.1}$$

The actual value for the hot spot strain at the weld toe is difficult to be determined due to the complex structural configuration and stress condition, and it can be estimated through the strains at adjacent points away from the weld toe. In the present study, the hot spot strain at the weld toe of the bottom flange is determined using the strain data obtained from the strain gauges c-1 to c-6 by linear regression method, which is considered as the hot spot strain of the weld joint near the strain gauge c-7. Then, the SCF at the location of the strain gauge c-7 where most of the strain gauges are field-installed on the TMB is obtained using Equation (5.1) by regarding the measured strain data from the strain gauge c-7 as the nominal strain. The derived SCF is a deterministic value for each static load case, while a set of random SCF data are generated under different moving load conditions.

5.3.2 Results from Static Load

5.3.2.1 Preliminary analysis of strain data

In the static-load cases, the static load is applied sequentially on seven sections of the test model from the positions P1 to P7, as illustrated in **Figure 5.11**, in which the arrowheads stand for the locations of the two axles of the test bogie. Positions P1 to P4 are allocated at 1/8, 1/4, 3/8, and 1/2 length of the test model, and positions P1 to P3 and P5 to P7 are distributed symmetrically along the steel beam.

With the purpose of eliminating the effect of the inherent uncertainties due to randomness in the measurement data, the recorded strain data with a loading time of 5 seconds are averaged. In this way, the strain value for each load position can be obtained in all the static-load cases with different combinations of load weight grade and axle-distance of the test bogie. **Figure 5.12** shows the strain influence line for the central section of the test model under the condition of load weight grade III and short axle-distance of the test bogie, which reveals that the critical strain values occur when the static load is applied on position P4.

Figure 5.13 shows the strain distributions for the central section of the test model when static load is applied at position P4 under the condition of load weight grade III and short axle-distance of the test bogie. It indicates that the recorded strain data from the strain gauges c-1 to c-6 on the bottom flange of the test model are tension strains, while those from the strain gauges c-10 to c-13 on the top flange of the test

model are compression strains. Regarding the strain gauges installed on the web plate of the test model, the recorded strain data from the strain gauges c-7 and c-9 are tension strains and compression strains, respectively. The recorded strain data from the strain gauge c-8 are near to zero since the sensor is installed close to the neutral axis of the steel beam.

5.3.2.2 Linear regression analysis

An observation into **Figure 5.13** indicates that the strain values along the bottom flange of the steel beam decrease slightly away from the weld toe, thus a regression analysis of the strain measurement data from the strain gauges c-1 to c-6 can be carried out with the intention of determining the hot spot strain at the weld toe of the bottom flange. The regression model is assumed by the following linear relationship

$$\varepsilon = \alpha_0 + \alpha_1 \delta \tag{5.2}$$

where ε is the strain value along the bottom flange of the steel beam; δ is the distance from the weld toe at the bottom flange of the steel beam; and α_0 and α_1 are the regression coefficients which can be obtained by the least-squares approach as

$$\alpha_1 = \frac{S_{\varepsilon\delta}}{S_{\delta\delta}} \tag{5.3}$$

$$\alpha_0 = \bar{\varepsilon} - \alpha_1 \bar{\delta} \tag{5.4}$$

where $S_{\delta\delta}$ is the variance of δ; $S_{\varepsilon\delta}$ is the covariance between ε and δ; and $\bar{\varepsilon}$ and $\bar{\delta}$ are the means of ε and δ, respectively.

The coefficient of determination, R^2 is obtained by

$$R^2 = 1 - \frac{\sum_i (\varepsilon_i - \hat{\varepsilon}_i)^2}{\sum_i (\varepsilon_i - \bar{\varepsilon})^2} \tag{5.5}$$

where ε_i is the observed data of ε; $\hat{\varepsilon}_i$ is the estimator of ε_i; and $\bar{\varepsilon}$ is the mean value of ε_i.

Table 5.2 provides the obtained statistical parameters in regression analysis by Equations (5.3) to (5.5), while **Figure 5.14** shows the measured strain data with a best-fit curve from the strain gauges c-1 to c-6 when static load is applied at position P4 in the case of load weight grade III and short axle-distance of the test bogie. It is seen from **Figure 5.14** that the measured strain data are involved in the upper and lower bounds of the fitted curve at 5% level of significance. Likewise, it is found from **Table 5.2** that the values of R^2 are greater than 0.940, indicating that the strain value along the bottom flange of the steel beam is almost linearly with the distance from the weld toe. As a result, the hot spot strain at the weld toe of the bottom flange can be estimated by Equation (5.2) when δ is equal to zero.

By regarding the hot spot strain at the weld toe of the bottom flange as the hot spot

strain of the weld joint near the strain gauge c-7, the SCF at the location of the strain gauge c-7 can then be obtained by using Equation (5.1). **Figure 5.15** illustrates the calculated SCFs at the location of the strain gauge c-7 under different load positions in the case of load weight grade III and short axle-distance of the test bogie, from which it is observed that the SCF at the location of the strain gauge c-7 reaches the largest value when static load is applied at position P4.

5.3.3 Stochastic Characterization of SCF

5.3.3.1 Results from moving load

In the moving load cases, the measured strain data when the entire test bogie is moving along the test model are recorded. To take full account of the effect of critical factors on the scatter of SCF, the experiments are carried out with a combination of three load weight grades, two velocities of moving load, and two axle-distances of the test bogie. In the present study, the recorded strain data under the moving load in a velocity of 0.15 m/s in the case of load weight grade III and short axle-distance of the test bogie are examined and reported.

Figure 5.16 shows the measured strain data from the strain gauge c-1 and the corresponding filtered data after eliminating the transient components by using a wavelet-based filtering method (Ni *et al*. 2008). With the filtered strain data from the

strain gauges c-1 to c-6, the hot spot strains at the weld toe of the bottom flange are calculated by linear regression method. According to the SCF determination method described in the previous section, the derived SCFs at the location of the strain gauge c-7 is then obtained and illustrated in **Figure 5.17**. It is observed that the SCF values at the location of the strain gauge c-7 are highly scattered, and therefore probability and statistical analyses should be conducted to achieve the stochastic characteristics of the SCF.

5.3.3.2 Probability distribution of SCF

With the purpose of recognizing the stochastic characteristics of SCFs for a typical welded T-joint under moving load conditions, the statistical properties and probability distribution of SCFs at the location of the strain gauge c-7 are obtained by analyzing the combined SCF data set from all groups of experiments under different moving load scenarios. **Figure 5.18** shows the data set of SCFs at the location of the strain gauge c-7 presented in an ascending order with 760 samples. **Table 5.3** lists the corresponding statistical properties of SCFs at the location of the strain gauge c-7.

Figures 5.19 and **5.20** illustrate the observed PDF and cumulative distribution function (CDF) of the SCF at the location of the strain gauge c-7 and the corresponding theoretical curves produced by the best-fitted normal distribution.

When plotting the SCF data at the location of the strain gauge c-7 by a histogram, the number of equally spaced classes is known as 11 according to the Sturges classification rule (Sturges 1926).

5.3.3.3 Statistical hypothesis test

The Kolmogorov-Smirnov goodness-of-fit test is widely applied as a nonparametric test, which performs a hypothesis test to examine whether or not the observations follow a specified probability distribution (Kottegoda and Rosso 1997). Let $F_0(x)$ denote a completely specified theoretical continuous CDF, the null hypothesis H_0 is that the true CDF of a continuous variate X, $F_n(x)$ is the same as $F_0(x)$. The test criterion is the maximum absolute difference between $F_n(x)$ and $F_0(x)$, formally defined as

$$D_n = \sup_x \left| F_n(x) - F_0(x) \right| \tag{5.6}$$

where sup denotes supremum. If D_n is less than the critical value, the null hypothesis is not rejected, and vice versa.

The Kolmogorov-Smirnov goodness-of-fit test is used to conduct normality test for the SCF at the location of the strain gauge c-7. The null hypothesis H_0 is that the SCF at the location of the strain gauge c-7 conforms to a normal distribution. The alternative hypothesis H_1 is that the SCF at the location of the strain gauge c-7 has a

different distribution. For a significance level of 0.05, the value of D_n defined in Equation (5.6) is calculated as 0.038, which is less than the critical value of 0.049. It is therefore concluded that the null hypothesis is not rejected, and the SCF of the typical welded bridge T-joint complies statistically with a normal distribution.

5.4 Summary

In this chapter, the determination method and stochastic characteristics of SCF for a typical welded steel bridge T-joint is recognized by conducting full-scale model experiments on a railway beam section of the TMB. Experiments have been conducted under moving load conditions by considering various combinations of key influencing factors including load weight grade, velocity of moving load, and axle-distance of the test bogie. The hot spot strain/stress at the weld toe is calculated by a linear regression method using the strain data recorded from pre-allocated strain gauges, and the nominal strain/stress is attained from the measured data at the location of desired strain gauge. The SCFs at the location of desired strain gauge are derived with a feature of high randomness. The statistical properties and probability distribution of SCF for a typical welded steel bridge T-joint are obtained, which reveals that SCFs for the joint in concern conform to a normal distribution. The results achieved from this study provide an effective experimental validation of the probability distribution of SCF for real applications in fatigue reliability assessment of steel bridges.

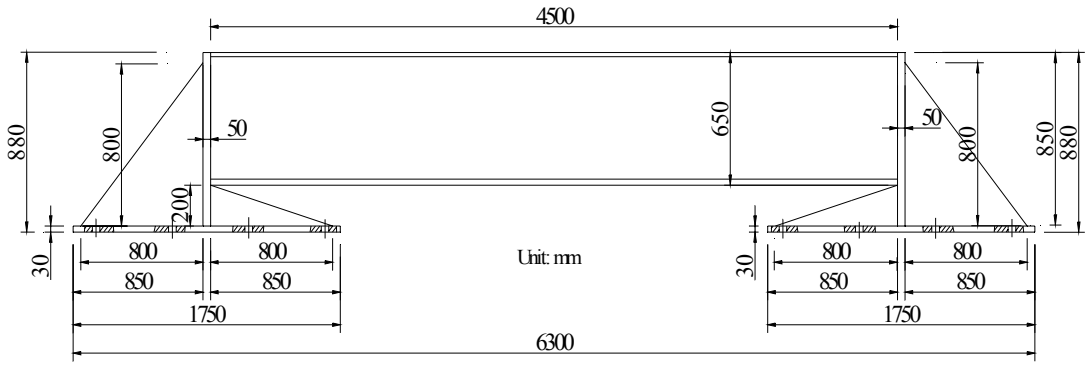

Figure 5.1 Schematic of experimental setup

Figure 5.2 Photo of experimental setup

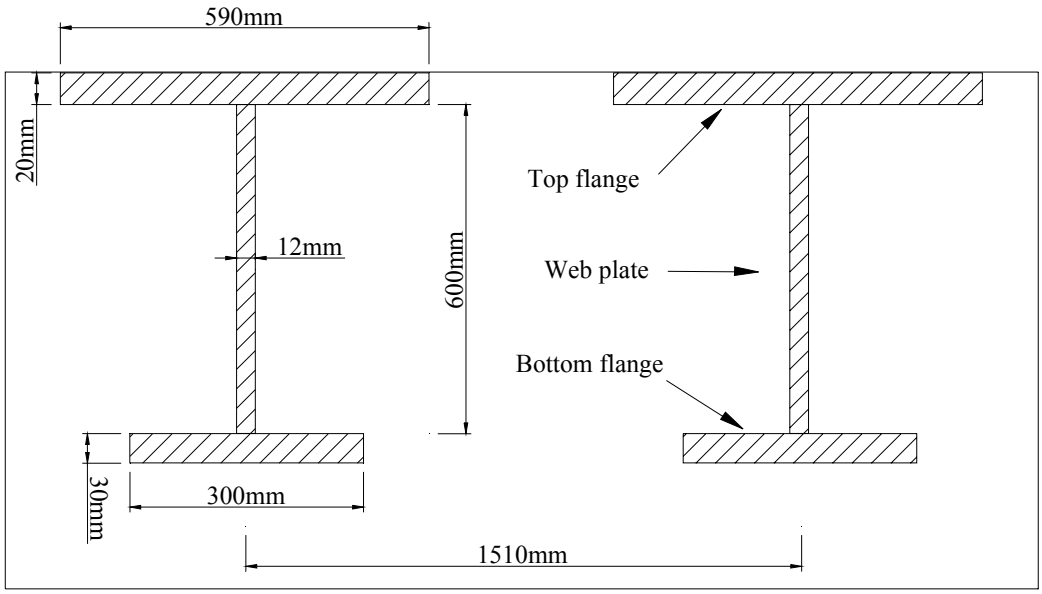

Figure 5.3 Cross-section of tested beams

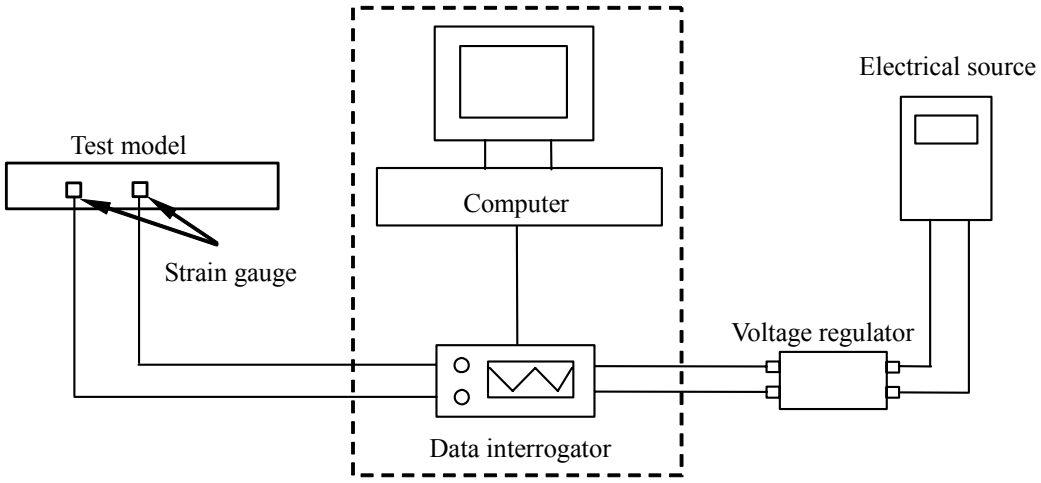

Figure 5.4 Schematic diagram of measurement setup

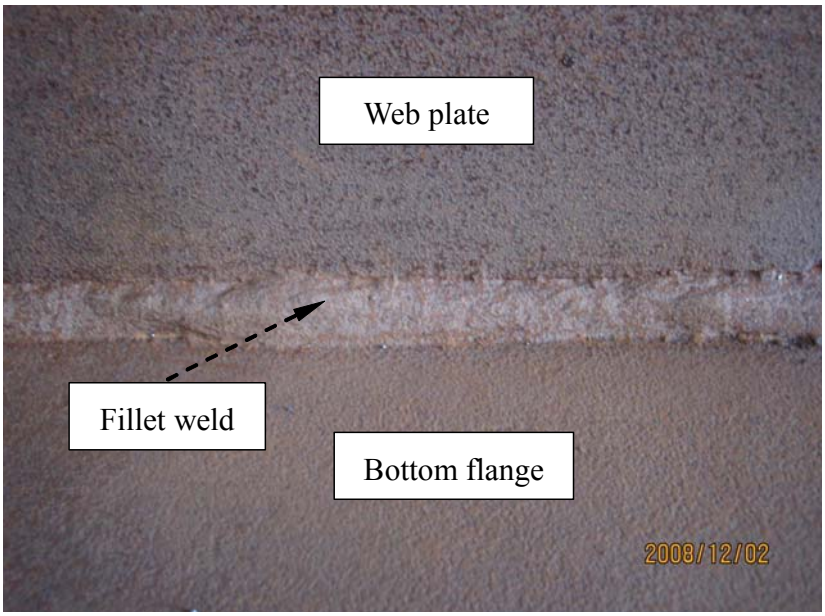

Figure 5.5 Welded T-joint between web plate and bottom flange

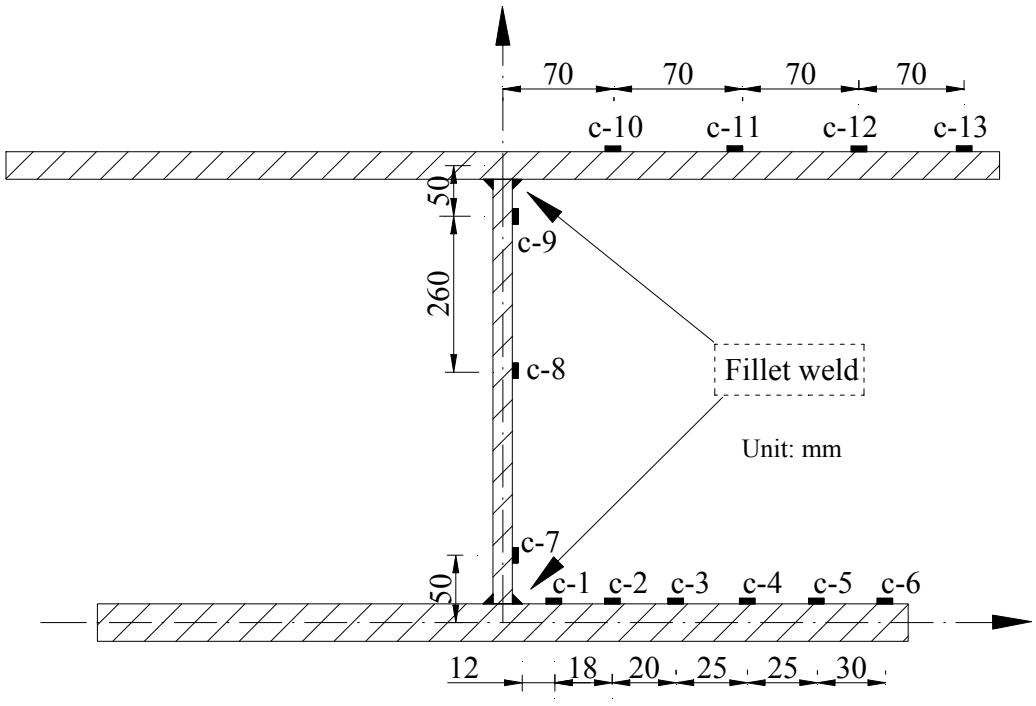

Figure 5.6 Details of strain gauge deployment

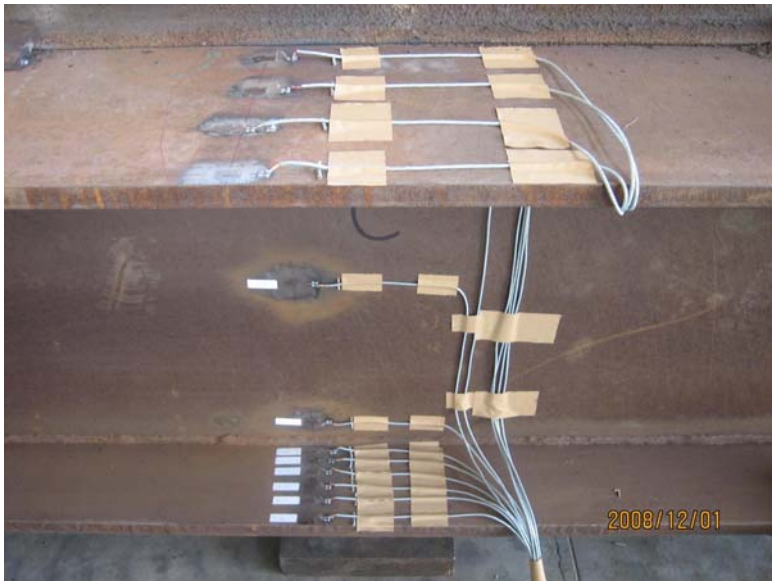

Figure 5.7 Photo of deployed strain gauges

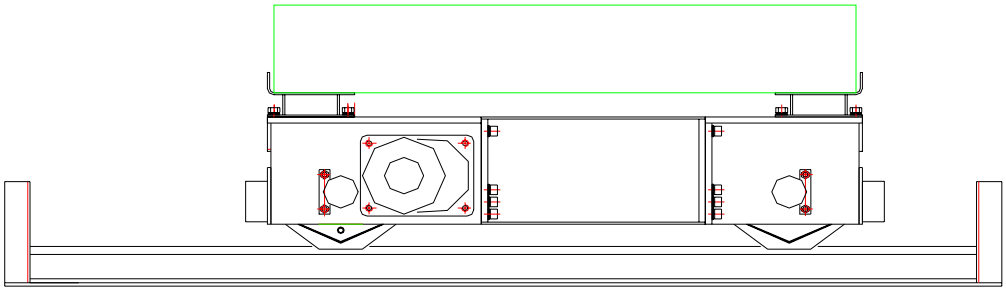

(a)

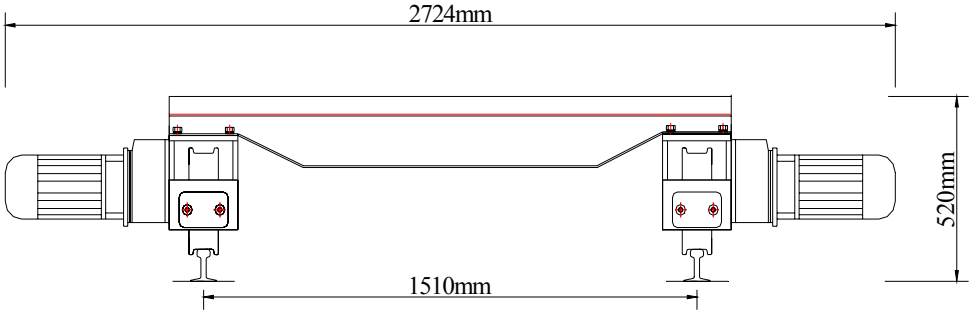

(b)

Figure 5.8 Schematic of test bogie: (a) Front view; (b) Side view

(a)

(b)

(c)

Figure 5.9 Photos of test bogie with electro-circuit system and braking device: (a) Test bogie; (b) Electro-circuit system; (c) Braking device

(a)

(b)

(c)

Figure 5.10 Photos of load weights: (a) Grade I: 5.982 t; (b) Grade II: 9.724 t; (c) Grade III: 14.586 t

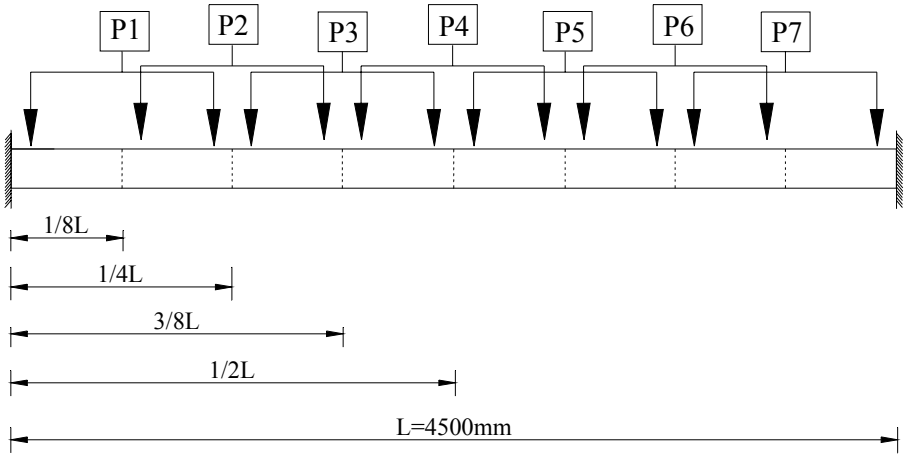

Figure 5.11 Schematic diagram of application of static loads

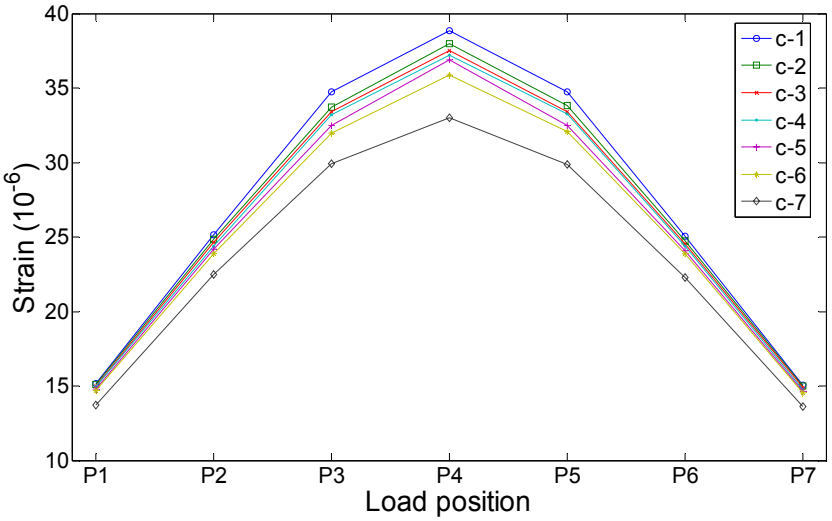

Figure 5.12 Strain influence line of central cross-section under static load

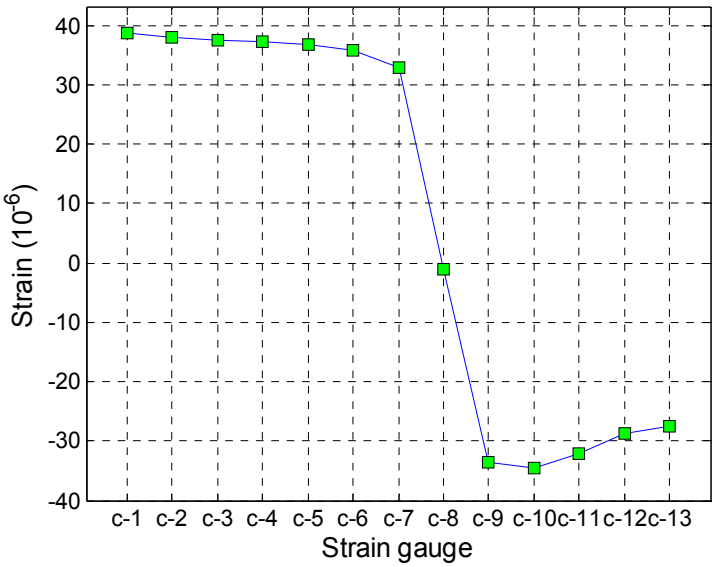

Figure 5.13 Strain distribution on central cross-section under static load applied at position P4

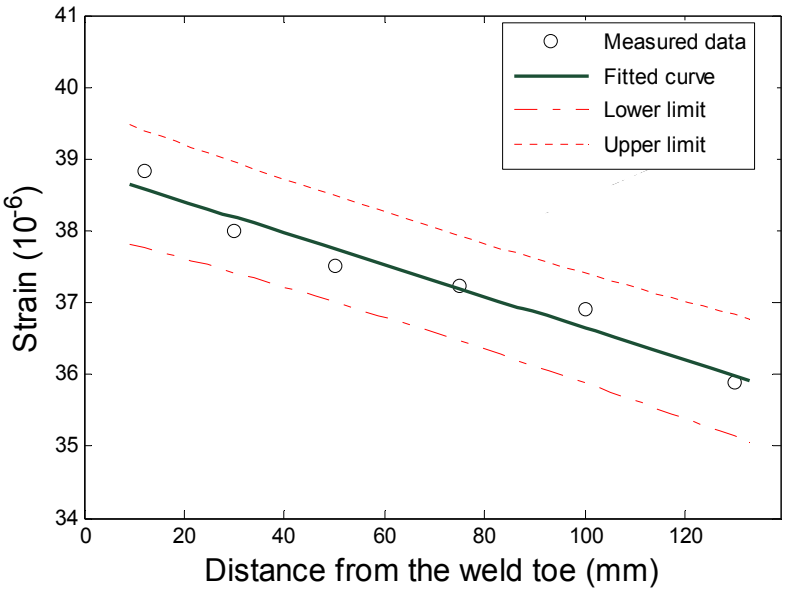

Figure 5.14 Linear regression analysis of strain data at locations of strain gauges c-1 to c-6

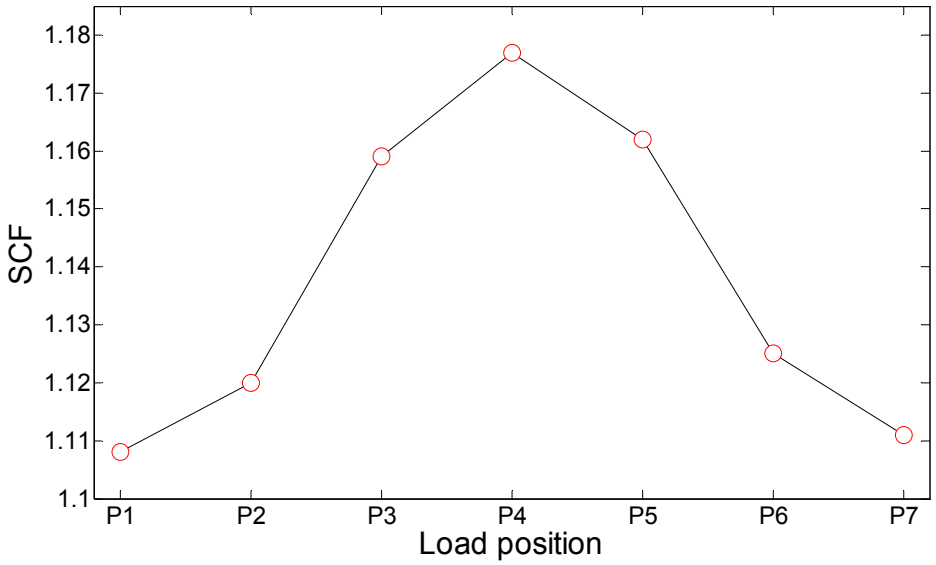

Figure 5.15 Calculated SCFs in case of different load positions

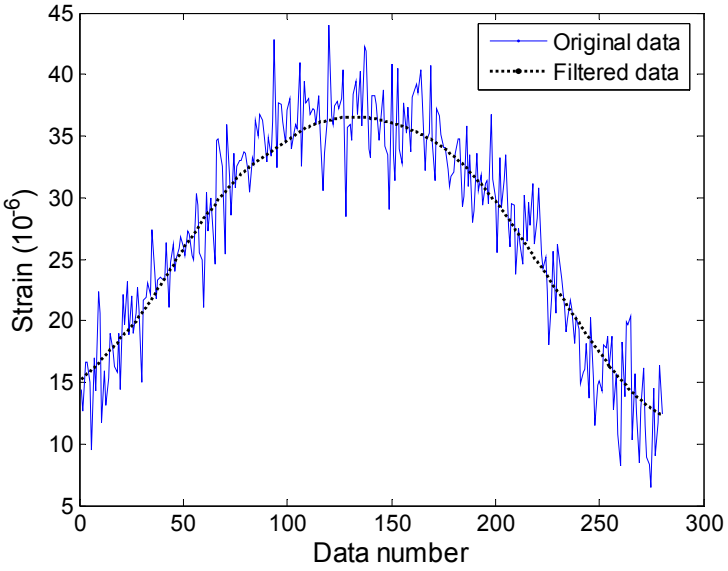

Figure 5.16 Original and filtered strain data from strain gauge c-1

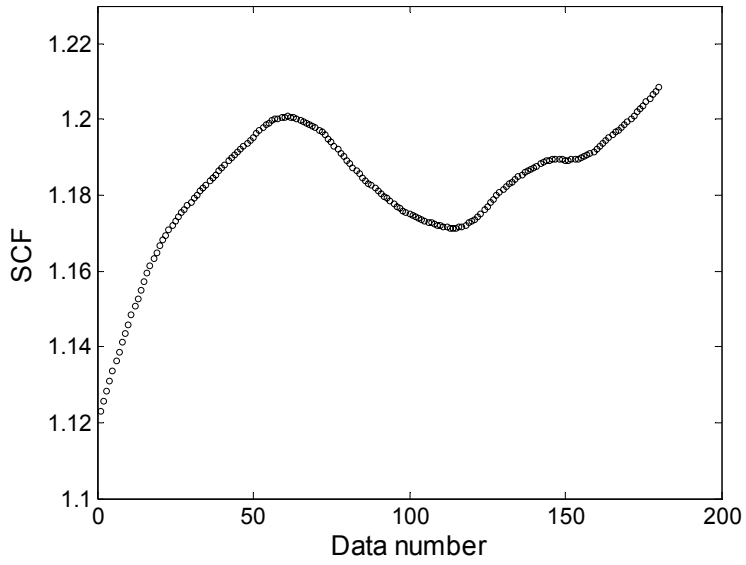

Figure 5.17 Derived SCFs at location of strain gauge c-7

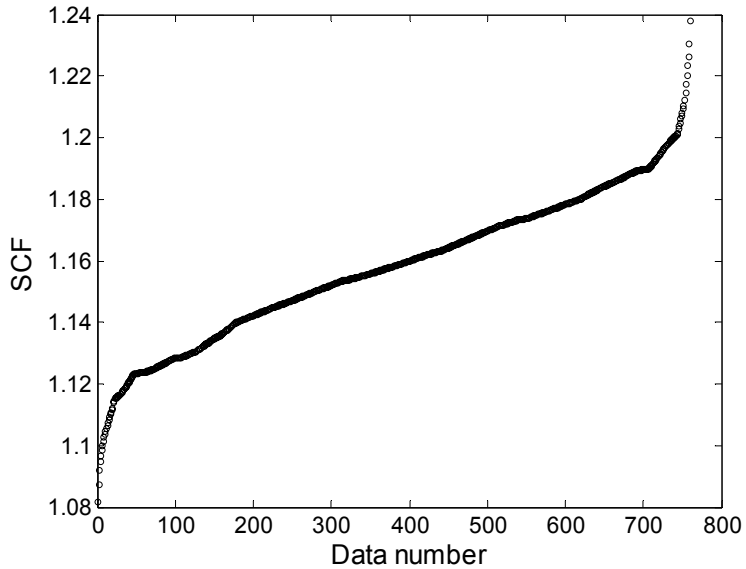

Figure 5.18 Data set of SCFs at location of strain gauge c-7

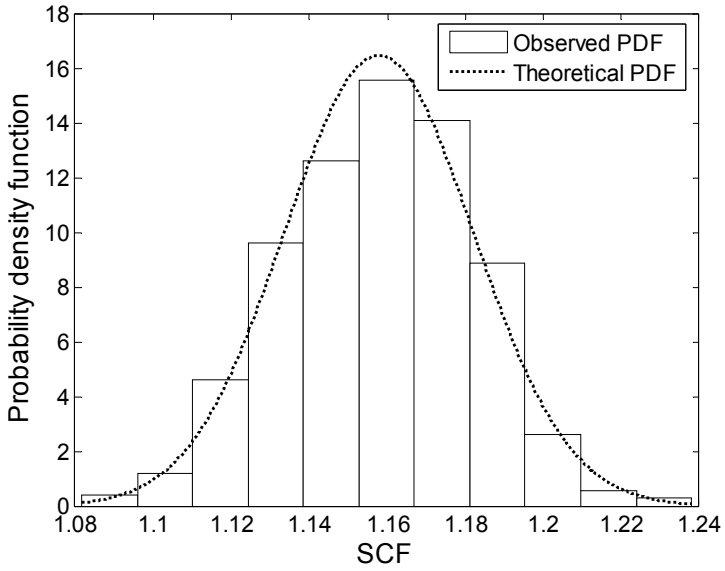

Figure 5.19 PDF of SCF at location of strain gauge c-7

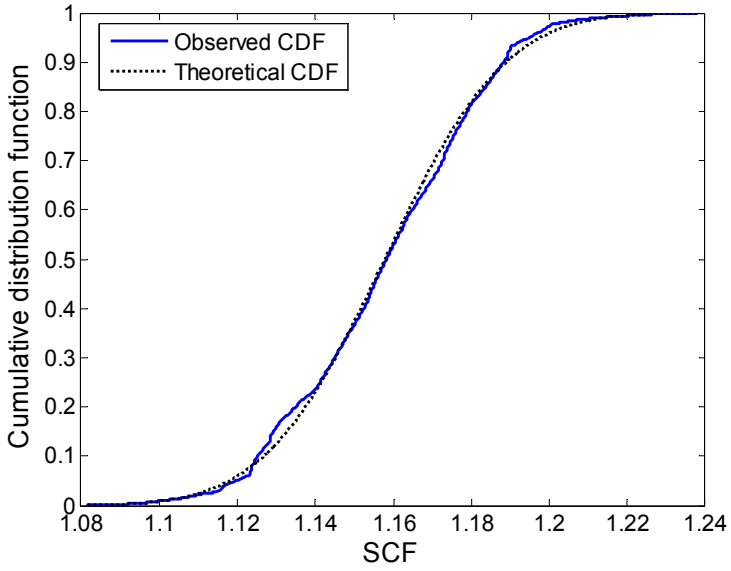

Figure 5.20 CDF of SCF at location of strain gauge c-7

Table 5.1 Chemical and mechanical properties of two types of steel materials

Structural grade	Chemical compositions in % (max.)					Mechanical properties (min.)		
	C	Mn	P	S	Si	Yield strength (MPa)	Tensile strength (MPa)	Elongation (%)
BS EN 10 025 (1990)-Grade Fe 510C	0.23	1.70	0.05	0.05	0.60	355 (≤16mm) 345 (>16mm ≤40mm)	490~630 (>3mm ≤100mm)	22 (>3mm ≤40mm)
Q345A	0.20	1.00 ~ 1.60	0.045	0.045	0.55	345 (≤16mm) 325 (>16mm ≤35mm)	470~630	21

Table 5.2 Statistical parameters in regression analysis of measured strain data under static load

Load position	α_0	α_1	R^2
P1	15.215	-0.003	0.994
P2	25.200	-0.010	0.985
P3	34.666	-0.021	0.943
P4	38.851	-0.022	0.953
P5	34.687	-0.020	0.947
P6	25.090	-0.009	0.978
P7	15.113	-0.004	0.995

Table 5.3 Statistical properties of SCF at location of strain gauge c-7

Maximum SCF	Minimum SCF	Mean value	Standard deviation	Coefficient of variation (COV)
1.238	1.082	1.158	0.024	0.021

CHAPTER 6

DEVELOPMENT OF FATIGUE RELIABILITY MODEL FOR PROBABILISTIC FATIGUE LIFE ASSESSMENT USING STRUCTURAL HEALTH MONITORING DATA

6.1 Introduction

Fatigue condition assessment of welded steel structures is an extraordinarily complicated process involving a great variety of effects. Considerable sources of uncertainties for fatigue damage and life evaluation using the *S*-*N* approach can be mainly categorized into the following aspects: (i) the number of fatigue test data for derivation of the *S*-*N* curves of specific structural joints is limited, and the data are subjected to pronounced statistical scatter; (ii) there are significant disparities when using the stress-life experimental results of a specimen for component-level fatigue life assessment of real structures due to the difference of fatigue features between the test specimen and real structural components; and (iii) the material characteristics as well as the stress history and environment exhibit uncertainty not only in the experimental process of fatigue test, but also during the service life of the real structure.

The methods of structural reliability evaluate the probability that a structure does not perform as intended by taking into account the uncertainties in both the structure and its external loadings, and then a rational analysis and design will be achieved by reducing the computed failure probability to an acceptable level. In the general theory and method of structural reliability, the uncertainties in a structure and its external loadings are characterized by continuous random variables with known distributions. Many approximation methods, such as the Monte Carlo simulation (MCS), FORM, and the second-order reliability method (SORM), can be used to compute the probability that the random variables fall into a predefined failure domain.

Due to the rational basis and mathematical background, methods of structural reliability have gained an increasing acceptance in academic circles and are beginning to be acknowledged and used by engineering practitioners (Estes and Frangopol 2005). In the past few decades, the theory and methods of structural reliability have been comprehensively applied in design and analysis against fatigue of many welded joints of steel structures, such as in bridges (Ang and Munse 1975; Raju *et al*. 1990; Zhao *et al*. 1994a, b; Cho *et al*. 2001; Kim *et al*. 2001; Pourzeynali and Datta 2005), aircraft (Mohammadi 2001; Zhang and Mahadevan 2001), mechanical structures (Tang and Zhao 1995; Tovo 2001; Lee *et al*. 2008), and offshore structures (Engesvik and Moan 1983; Madsen 1984; Wirsching 1984; Jiao and Moan 1992; Amanullah *et al*. 2002; Nazir *et al*. 2008).

In this chapter, a method for probabilistic assessment of fatigue life by using long-term strain measurement data is proposed regarding the daily number of cycles for each stress range as a random variable. The statistics of the number of stress cycles is combined with the *S*-*N* curve to make a probabilistic assessment of fatigue life with the use of the Miner's rule. Furthermore, a fatigue reliability model which integrates the probability distribution of hot spot stress range with a continuous probabilistic formulation of the Miner's damage cumulative rule is developed to facilitate the fatigue life and reliability evaluation of steel bridges using long-term monitoring data. By considering both the nominal stress obtained by measurement and the SCF as random variables, a probabilistic model of the hot spot stress is formulated for evaluating the fatigue life and the probability of failure. The proposed procedure is illustrated using the long-term monitoring data of dynamic strain from the instrumented TMB.

6.2 Probabilistic Fatigue Modeling Methods

To evaluate the fatigue reliability condition of existing steel bridges, it is necessary to develop a robust probabilistic model incorporating primary uncertainties associated with the nature of fatigue damage. Based on the information already available in the literature, the most convenient ways of relating variable-amplitude stochastic stress spectrum to constant-amplitude fatigue data for bridge applications are the effective stress range concept and the Miner's rule for fatigue damage accumulation.

According to Byers *et al*. (1997b), a probabilistic method for fatigue evaluation of highway and railway bridges generally consists of (i) the development of a stress distribution model from field monitoring data or by simulation; (ii) the use of the Miner's rule for fatigue damage analysis in conjunction with an appropriate *S*-*N* relationship; and (iii) the use of a probability function to describe the fatigue reliability of critical structural components. A general outline of these probabilistic fatigue modeling methods is presented in the following section.

6.2.1 Mean Stress Range Method

Combining the *S*-*N* curve expression defined by the Basquin's model (Basquin 1910) in Equation (2.1) with the Miner's damage rule as described in Equation (3.1), the fatigue damage accumulation index can be expressed as

$$D = \sum_i \frac{n_i}{\frac{A}{S_i^m}} \tag{6.1}$$

Assuming $f_S(s)$ is the PDF of the stress range S, in each narrow stress block of width, ΔS, the fractional number of cycles is $f_S(s)\Delta S$. If N_T denotes the total number of stress cycles of a structural component under variable-amplitude stress range in time T, then the number of cycles in the stress block is given by

$$n_i = N_T f_S(s)\Delta S \tag{6.2}$$

Substituting Equation (6.2) into Equation (6.1), gives

$$D = \sum_i \frac{N_T f_S(s)\Delta S}{\frac{A}{S_i^m}} \tag{6.3}$$

As ΔS goes zero, Equation (6.3) can be put in an integral form as

$$D = \frac{N_T}{A}\int_0^\infty S^m f_S(s)dS \tag{6.4}$$

The integral expression of Equation (6.4) is the mean or the expected value of the random variable S^m which can be expressed by $E(S^m)$, also called the mth statistical moment of random variable S. Consequently, the fatigue damage index can be taken as the following form (Zhao *et al*. 1994a; Ayyub *et al*. 2002)

$$D = \frac{N_T}{A} E\left(S^m\right) \tag{6.5}$$

where

$$E\left(S^m\right) = \int_0^\infty S^m f_S(s)dS \tag{6.6}$$

For a given value of m and assumed statistical distribution of stress range, the expected value of S^m can be easily calculated.

According to the Miner's rule, failure due to fatigue occurs when $D \geq 1$. Typical values of D at failure are in the range from 0.5 to 2 (Sobczyk and Spencer 1992). To account for this high level of uncertainty, Wirsching (1984) extended the definition

of fatigue failure as

$$D \geq \Delta \tag{6.7}$$

Wirsching and Chen (1988) studied the test data reported by Miner (1945) and found that Δ, which represents uncertainty associated with the use of the Miner's rule, may be modeled by a lognormal distribution with a mean value of 1 and a COV of 0.3.

Combining Equations (6.5) and (6.7), the limit-state function, *g*, for the mean stress range method can be expressed as

$$g = \frac{N_T}{A} E\left(S^m\right) - \Delta = 0 \tag{6.8}$$

Then, the mathematical expression for probability of fatigue failure, p_f, can be given as

$$p_f = P\left[g = \frac{N_T}{A} E\left(S^m\right) - \Delta \geq 0 \right] \tag{6.9}$$

It is important to quantify the uncertainties in each of the random variables in Equation (6.8) for fatigue reliability assessment. Usually *m* is a constant slope parameter of value 3. *A* is considered to be a random variable with lognormal distribution and the COV of *A* is the same for all the fatigue categories and can be considered to be 0.45 (Wirsching and Chen 1988). The statistical properties of other random variables have been presented in Chapter 2.4.3.

6.2.2 Integration Method

Byers *et al*. (1997a) presented a practical probabilistic formulation based on *S*-*N* curve expression and the Miner's rule. They concluded theoretically that stresses of all ranges can occur in the Miner's damage rule, and the random stress range *S* can be described by the PDF. If N_T cycles occur in time *T*, the fraction of those cycles having stress range *S* is $N_T f_S(s)ds$ and the increment of fatigue damage, D_T, is

$$d(D_T) = \frac{N_T f_S(s)}{N(s)} ds \tag{6.10}$$

Then, in the limit the total damage expressed in Equation (3.1) can be converted into an integral

$$D_T = \int_0^\infty \frac{N_T f_S(s)}{N(s)} ds \tag{6.11}$$

Further evaluation of the integral in Equation (6.11) is possible upon selection of a specific stress distribution. Combining Equations (6.11) and (6.7), the limit-state function for the integration method can be defined as

$$g = \int_0^\infty \frac{N_T f_S(s)}{N(s)} ds - \Delta = 0 \tag{6.12}$$

6.2.3 Effective Stress Range Method

Variable-amplitude random-sequence stress spectrum, such as that which occurs in actual bridges, can be conveniently represented by a single constant-amplitude effective stress range, S_{re}, that would result in the same fatigue life as the variable-amplitude stress spectrum (Schilling *et al*. 1978). The effective stress range is defined by

$$S_{re} = \left[\sum \alpha_i S_{ri}^B\right]^{1/B} \tag{6.13}$$

in which S_{ri} is the midwidth of the ith stress interval in a histogram, defining the variable-amplitude stress spectrum; α_i is the fraction of stress range cycles within that interval; and B is a constant parameter. If B is taken as 2, S_{re} from this equation is equal to the root-mean-square (RMS) stress range; if B is taken as the reciprocal of the slope of the constant-amplitude S-N curve for the particular detail under consideration, which is 3 for most structural details, the equation is equivalent to the Miner's rule. The RMS and Miner values of S_{re} are only slightly different, and both satisfactorily represent the variable-amplitude stress spectrum.

Moses *et al*. (1987) proposed a fatigue reliability model to predict the probability that the fatigue life of steel bridge components will be less than the expected or desired design life, Y_e. Instead of formulating damage in terms of the stress range probability distribution, damage is described in terms of several random variables such as truck weight, average daily truck traffic (ADTT), bending moment. In the evaluation procedure, the effective stress range is computed as

$$S_{re} = \left[\sum \alpha_i S_{ri}^3\right]^{1/3} \tag{6.14}$$

The remaining safe fatigue life in years, Y_f, is then estimated from

$$Y_f = \left[\frac{fK10^6}{T_a C(R_s S_{re})^3}\right] - Y_a \tag{6.15}$$

in which T_a is the estimated lifetime average daily truck volume; C is the number of cycles per truck passage; Y_a is the age of the bridge in years; K is a constant depending on the structural detail; and f is a factor to account for the difference between the mean and allowable S-N curve. The factor $f = 1$ when computing the remaining safe life, and $f = 2$ when computing the remaining mean life. The product $R_s S_{re}$ is the factored stress range. Different values for reliability factor R_s are suggested, depending on whether the structure is considered to be redundant or nonredundant. In any case, $R_s = 1$ if the computation is for the remaining mean life.

The reliability is then formulated as a function of the safety margin which is the difference between the actual fatigue life (or stress cycles to failure) and desired fatigue life (or applied stress cycles), and is the probability that this margin is greater than zero. The limit state function can be defined by the following equation

$$g = Y_f - Y_e = 0 \tag{6.16}$$

6.3 Probabilistic Fatigue Assessment with Random Stress Cycles

Fatigue in metal is a complex failure mechanism which is characterized by gradual reduction in the capacity of structural elements to withstand cyclic loading. The most important parameters in the fatigue damage of welded structures are the stress cycles experienced and their stress range which are random in nature. According to the Miner's rule, the cumulative fatigue damage in a structural component that can be expressed by a summation, as expressed in Equation (3.1). In the present study, n_i will be obtained by rainflow cycle counting of the strain measurement data, while N_i will be determined according to the *S*-*N* relationship which is expressed as Equation (3.3). Failure is assumed to occur when the fatigue damage measured $D = 1$.

6.3.1 Proposed Method

From the strain measurement data for a full day, the daily stress time history can be obtained by simply multiplying the strain data with elasticity modulus. Then the rainflow counting algorithm is applied to obtain one day's stress spectrum, from which the number of cycles for different stress ranges, n_i's, is determined. Because the number of cycles for a specific stress range obtained from different days is different, n_i is regarded as a random variable. The mean value and standard deviation of the random variable n_i are determined by statistical analysis of the long-term measurement data covering a long period.

Since n_i's are random variables, the fatigue life predicted by Equation (3.4) is also a

random variable. The mean value μ_F and variance D_F of the fatigue life are calculated by

$$\mu_F = \frac{1}{365 \times \sum_{i=1}^{n} \frac{\lambda_i \mu_{n_i}}{N_i}} \tag{6.17}$$

$$D_F = \left[\frac{\partial F}{\partial n_i}\right] Diag\left[D_{n_i}\right] \left[\frac{\partial F}{\partial n_i}\right]^T \Bigg|_{n_i = \mu_{n_i}} \tag{6.18}$$

where μ_{ni} and D_{ni} are the mean and the variance of the random variable n_i, which are obtained from the long-term monitoring data. With Equations (6.17) and (6.18), the reliability index for an expected fatigue life, F_e (year), is obtained by

$$\beta = \frac{\mu_F}{\sqrt{D_F}} - \frac{F_e}{\sqrt{D_F}} \tag{6.19}$$

and the probability of failure is obtained by

$$p_f \approx \Phi(-\beta) \tag{6.20}$$

where $\Phi(\cdot)$ is the standard normal CDF.

6.3.2 Application to TMB

In the proposed method, the number of cycles for each stress range, n_i, is regarded as a random variable. A value of n_i for the ith stress range can be obtained from each

daily stress spectrum, and its statistics is then obtained from the measurement data for 80 typical days from the strain gauge SSTLS13. **Figure 6.1** shows the distribution of number of cycles for two stress ranges obtained from the 80-day measurement data.

After obtaining this distribution, the mean value, standard deviation and probability density function of n_i for each of the concerned stress ranges can be estimated. Then the mean value and the variance of the fatigue life are calculated by Equations (6.17) and (6.18). For the structural detail H, the mean value and the COV of the fatigue life are obtained as 765 years and 0.046, respectively. The corresponding reliability index and failure probability for different expected fatigue life (from 650 to 900 years) are estimated by Equations (6.19) and (6.20) and listed in **Table 6.1**.

For comparison, a statistical analysis of the deterministically predicted fatigue lives shown in **Figure 3.17** which are assessed from the measured daily stress spectra for the 80 days is also conducted. **Figure 6.2** illustrates the PDF and the CDF, from which the ensemble mean value and the COV are obtained as 773 years and 0.103. The ensemble mean value is close to the mean fatigue life predicted by the proposed method, but the COV is much larger than that obtained by the proposed method.

6.4 SCF-Integrated Fatigue Reliability Assessment

6.4.1 Development of Analytical Model

The nominal stress range S is represented by an algebraic difference between the maximum stress, $\sigma_{\max}$, and the minimum stress, $\sigma_{\min}$, measured in one stress cycle; and the hot spot stress range, S_h, is evaluated by multiplying the nominal stress range by an SCF. That is,

$$S = \sigma_{\max} - \sigma_{\min} \tag{6.21}$$

$$S_h = S \times \mathrm{SCF} = (\sigma_{\max} - \sigma_{\min}) \times \mathrm{SCF} \tag{6.22}$$

In the present fatigue reliability model, the hot spot stress range is regarded as a function of two random variables: S and SCF. Upon the assumption that the two random variables are independent, the joint PDF of the hot spot stress range, $f(h)$, can be obtained as

$$f(h) = f(s) \times f(t) \tag{6.23}$$

where $f(s)$ and $f(t)$ are the PDFs of the stress range and the SCF, respectively.

When the joint PDF of the hot spot stress range is a continuous function, the Miner's rule given in Equation (3.1) can be re-written as the following expression to evaluate the fatigue damage characterized by a total of n_{tot} stress cycles:

$$D = \iint_H \frac{n_{tot} f(h)}{N_f} dh = \int\int_{ST} \frac{n_{tot} f(s) f(t)}{N_f} ds dt \tag{6.24}$$

where N_f is the stress cycles at failure.

Thus, the expression of fatigue life can be obtained by

$$F = \frac{D_f}{D} = \frac{D_f}{\int\int_{S\,T} \frac{n_{tot} f(s) f(t)}{N_f} dsdt} \tag{6.25}$$

in which,

$$n_{tot} = \sum_{i=1}^{n} \lambda_i n_i \tag{6.26}$$

where D_f is the fatigue damage at failure; λ_i is the reducing factor; and S_0 is the constant amplitude non-propagating stress range.

Then the limit-state function for fatigue damage can be expressed as

$$g(s,t) = D_f - \int\int_{S\,T} \frac{n_{tot} f(s) f(t)}{N_f} dsdt \tag{6.27}$$

The probability of failure and reliability index are further obtained by structural reliability theory as follows

$$p_f = P\{g(s,t) \le 0\} = P\left\{ D_f - \int\int_{S\,T} \frac{n_{tot} f(s) f(t)}{N_f} dsdt \le 0 \right\} \tag{6.28}$$

$$\beta = -\Phi^{-1}(p_f) \tag{6.29}$$

Obviously, one of the key issues involved in the above fatigue reliability model is the exploration of probability distributions for both the stress range and SCF. A flowchart on the implementation of the above fatigue reliability model for probabilistic fatigue life assessment is shown in **Figure 6.3**.

6.4.2 Illustration Using Field Monitoring Data

6.4.2.1 Multi-modal PDF of stress range

In the present study, the monitoring data from the strain gauge SPTLS16 located at Detail H of the deck cross-section CH24662.5 are acquired for fatigue reliability assessment. The strain gauge SPTLS16 was installed under the track plate of the railway beam composed of two inverted T-beams welded to the top flange plate, as illustrated in **Figures 6.4(a)** and **6.4(b)**. The strain data were recorded continuously at a sample frequency of 51.2 Hz. **Figure 6.5** illustrates two typical daily strain time histories obtained from the strain gauge SPTLS16. The stress time history is obtained through simply multiplying the measured strain data by the elasticity modulus of steel. Daily stress spectrum is procured with the aid of the rainflow counting algorithm. **Figure 6.6** shows the histograms of two typical daily stress spectra by specifying a resolution of 1 MPa for the stress range interval, the stress cycles with amplitudes less than 2 MPa being discarded. **Figure 6.7** illustrates the obtained standard daily stress spectrum using the 20 days' daily stress spectra including one

daily strain data under typhoon conditions.

After obtaining the representative data sample, the rainflow-counted stress ranges from 2 to 30 MPa are extracted for modeling the PDF of the stress range measured by the strain gauge SPTLS16. The total observation number of the 20 days' stress range data is 30,986 and the number of classes is obtained as 16 according to the Sturges classification rule. **Figures 6.8** and **6.9** show the finite mixed PDFs and CDFs of the 20 days' stress range data acquired by the strain gauge SPTLS16 when using normal, lognormal, and Weibull distributions, respectively. The corresponding estimated parameters of the component distributions are given in **Table 6.2**. **Figure 6.10** shows the variation of the AIC values with the iteration number of the three mixed PDFs (normal, lognormal, and Weibull) of the 20 days' stress range data. It is found that the AIC values for the three PDFs converge rapidly and the mixed Weibull PDF results in the lowest AIC value. As a consequence, the Weibull distribution is taken as the component distribution for modeling the measured stress ranges.

6.4.2.2 Numerical analysis of SCF

A three-dimensional global FEM of the TMB is established by using the general-purpose commercial software ABAQUS as illustrated in **Figure 6.11**. The beam and shell elements in the ABAQUS element library are chosen to model the structural components of the bridge. There are 7,375 nodes and 17,677 elements in

the global FEM. After verifying the predicted responses (dynamic modal properties and displacement/strain influence lines) of the global FEM by field measurement data (Wang *et al*. 2000; Wong 2005), a three-dimensional local FEM of typical welded connections extracted from the section CH24662.5 where the strain gauge SPTLS16 is attached under the track plate of the railway beam, is formulated as shown in **Figure 6.12**. There are 502,879 nodes and 406,448 elements in this local FEM, and the displacement responses at the deck cross-sections obtained from the global FEM are adopted as boundary conditions of the local FEM.

The dimension of the typical welded joint in the local FEM is identical to the drawing details of the TMB. The weld is simply modeled as a triangle and the weld thickness and weld angle are 6 mm and 45^{o}, respectively. A relatively fine grid mesh is used for the weld seam where stress concentration with a high stress gradient is expected, and a coarse grid mesh is used for the zone where stresses are relatively uniform. As a compromise between the mesh size and the number of degrees of freedom, the 8-node reduced integration continuum element is adopted in modeling the plate and weld.

Figure 6.13 illustrates the weld stress analysis of the welded joint at the strain gauge SPTLS16. It reveals that the hot spot near the strain gauge SPTLS16 is located at the end of the longitudinal weld which is serving as the linkage between the railway beam web and the track plate. A uniformly-distributed load of 1 MPa is applied on

the rail-track areas of the track plate in the local FEM, and then the nominal stress at the location of the strain gauge SPTLS16 and the structural stress at the hot spot are obtained. Finally, the SCF for the welded joint monitored by the strain gauge SPTLS16 is determined as 1.379 according to

$$\text{SCF} = \frac{\sigma_{hot}}{\sigma_{nom}} \tag{6.30}$$

where σ_{hot} is the hot spot stress; and σ_{nom} is the nominal stress.

6.4.2.3 Probabilistic assessment of fatigue life

The joint PDF of hot spot stress range can be obtained by Equation (6.23) when the PDFs of stress range and SCF have been determined as detailed in the abovementioned sections. According to the research findings in Chapter 5, for the welded detail in concern, the SCF is found by full-scale model experiments to conform to the normal distribution with a COV of 0.021. As a result, the PDF of the SCF is formulated by a normal distribution with a mean value of 1.379 and a COV of 0.021 as shown in **Figure 6.14**. The joint PDF of hot spot stress range is subsequently obtained from the multi-modal PDF of stress range and the PDF of SCF, as illustrated in **Figure 6.15**.

In general, fatigue failure of a structural component is assumed to happen when the final summation of the elementary damage reaches a predetermined value known as

fatigue damage index. The fatigue life of the welded detail monitored by the strain gauge SPTLS16 is predicted to be 716 years when the damage index equals to unity as a deterministic value. While the predicted fatigue life is 927 years when using the method illustrated in Byers *et al*. (1997a), in which only the probability distribution of the nominal stress range is accounted for in the fatigue reliability model. It indicates that the predicted fatigue life is reduced by 23% when taking the stress concentration phenomenon into consideration. In fact, the fatigue damage at failure is a random variable which may be modeled by a lognormal distribution with a mean value of 1 and a COV of 0.3 (Wirsching and Chen 1988). The PDF of the fatigue damage at failure is shown in **Figure 6.16**.

By applying the method developed in this section, the failure probability and reliability index versus fatigue life are obtained as shown in **Figures 6.17** and **6.18**, where the range of the counted stress is between 2 and 30 MPa and the coverage of SCF is from 1 to 2. It is seen that fatigue life can be calculated for a given target reliability index or failure probability. In the present study, the predicted fatigue life is related to the structural component failure rather than to the entire bridge failure in a system level. This leads to the predicted fatigue life relatively high and the probability of failure relatively low. Another reason for this concern is because most of the measured stress ranges are lower than the fatigue limit which is 35 MPa for the detail category in this study (BSI 1980).

A target reliability index is defined as the value of reliability index that is acceptable for design or evaluation, and its selection should be based on economic considerations as well, involving cost of construction, inspection, repair, rehabilitation, and replacement. The reliability index in the range between 2 and 4 has been used in establishing code safety margins (AISC 1986) and the value of target reliability index recommended for offshore structural components is 3 (Wirsching and Chen 1987). From **Figure 6.18**, the reliability index is estimated to be approximately 4.5 in accordance with the design fatigue life of 500 years for this bridge and the predicted fatigue life is 796 years if the value of target reliability index is taken as 3. **Figures 6.17** and **6.18** also indicate that the service fatigue life directly affects the probability of failure or reliability index of the structural component. When the service life requirement is increased, the corresponding reliability index decreases sharply.

6.5 Summary

A method for probabilistic assessment of fatigue life by using long-term strain/stress measurement data has been proposed and applied for fatigue reliability analysis of the suspension TMB instrumented with a sophisticated SHM system. In this method, the daily number of cycles for each stress range is considered to be a random variable, and its probability distribution is obtained by statistical analysis of long-term stress measurement data. The statistics of the number of stress cycles is then combined

with the *S*-*N* curve to make a probabilistic assessment of fatigue life with the use of the Miner's rule. With the 80-day strain measurement data from a welded detail on the TMB deck section, the proposed method has been applied to predict the mean value and the COV of the fatigue life, and to evaluate the reliability index and failure probability for an expected fatigue life.

Furthermore, a fatigue reliability model has been proposed by uniquely integrating the probability distribution of hot spot stress range with a continuous probabilistic formulation of the Miner's rule, and has been applied for probabilistic fatigue life assessment of the TMB by use of the strain monitoring data from the long-term SHM system. A monitoring-based representative data sample of stress spectrum was constructed considering highway and railway traffic and typhoon effects. The method of finite mixture distributions was applied to generate the PDF of stress range, while SCFs at fatigue-critical locations were calculated by finite element analysis method. The joint PDF of hot spot stress range and subsequently the failure probability and reliability index versus fatigue life were obtained by structural reliability theory. The results show that (i) the measured stress distribution with multi-modal properties can be accurately represented in an explicit expression by the method of finite mixture distributions in conjunction with a hybrid parameter estimation approach; (ii) the service fatigue life significantly affects the probability of failure or reliability index of the welded detail in study, and the reliability index decreases sharply when the service life requirement is increased; and (iii) the proposed approach provides a

viable approach to conducting monitoring-based fatigue reliability assessment of steel bridges taking account for uncertainty and randomness inherent in the fatigue phenomenon and measurement data.

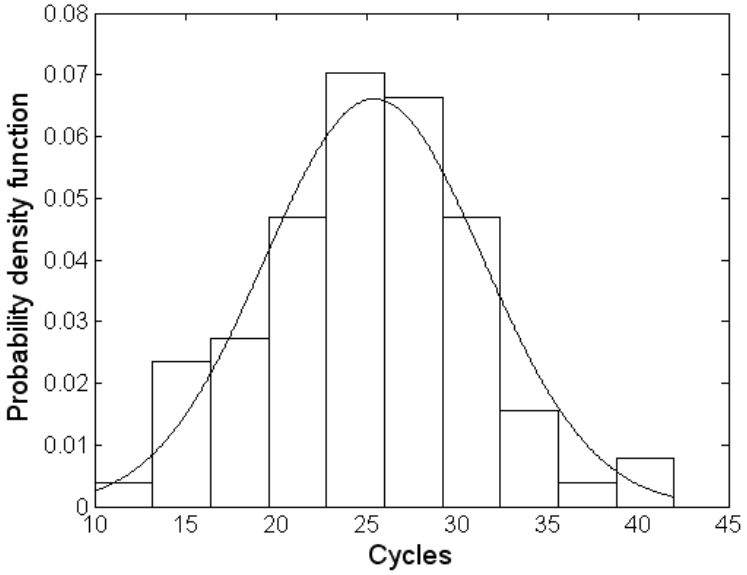

(a)

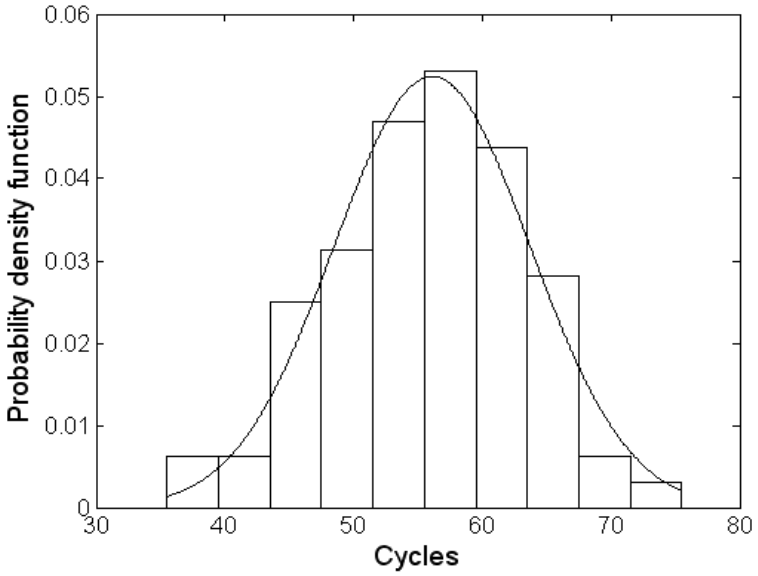

(b)

Figure 6.1 Distribution of number of cycles for two stress ranges: (a) *S* = 13MPa; (b) *S* = 20MPa

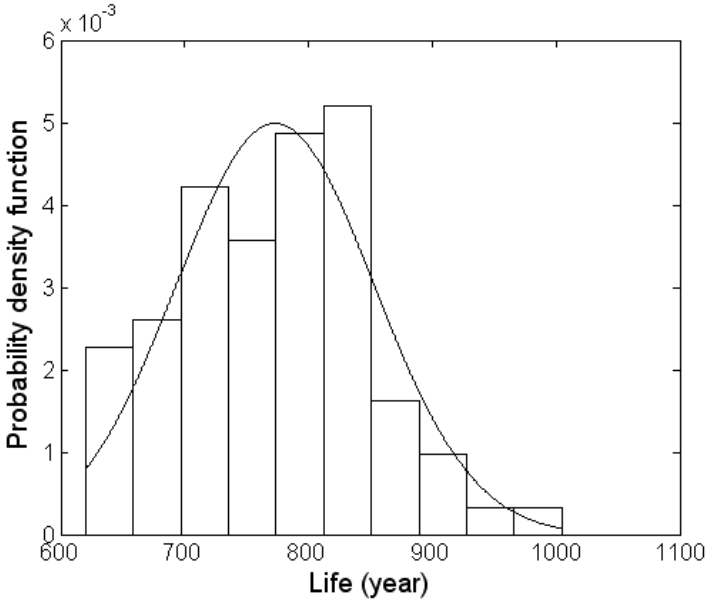

(a)

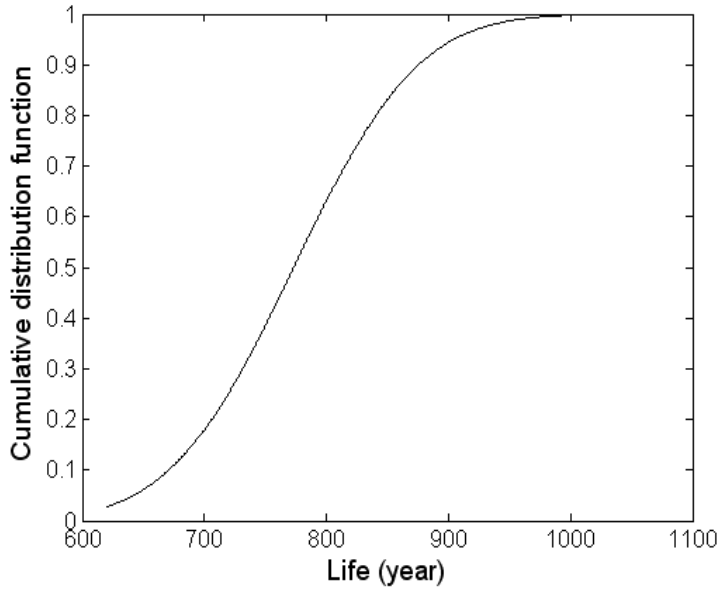

(b)

Figure 6.2 Statistical analysis of fatigue life: (a) PDF; (b) CDF

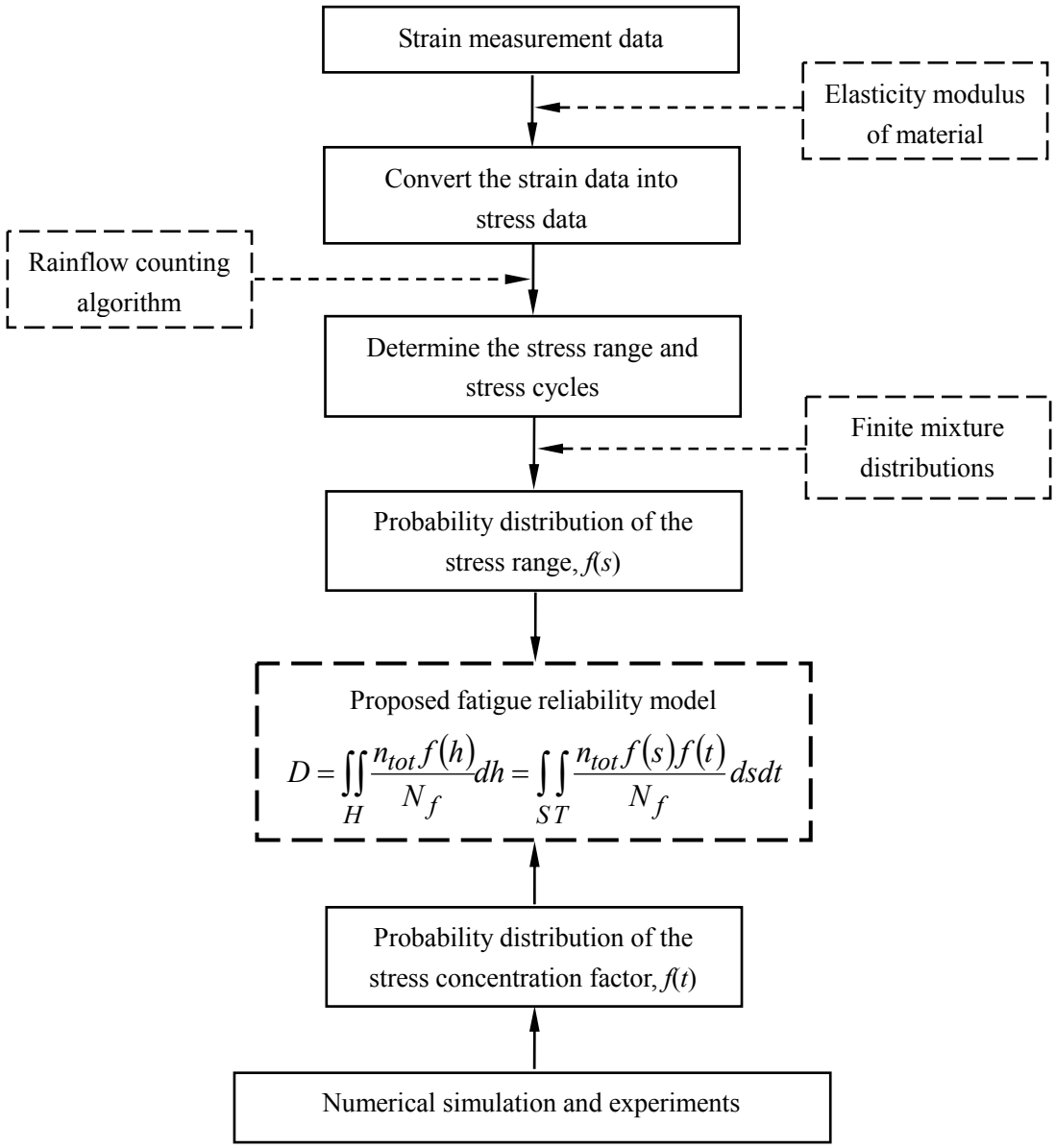

Figure 6.3 Flowchart on implementation of proposed fatigue reliability model

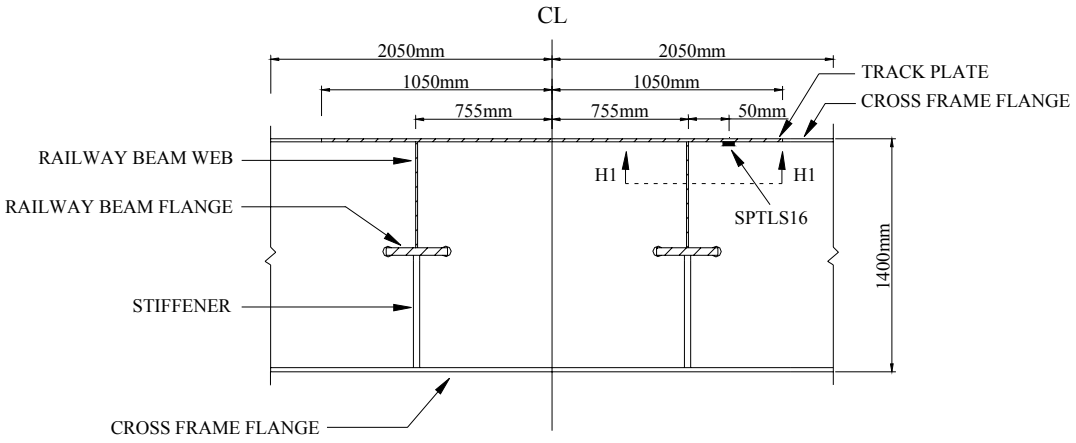

(a)

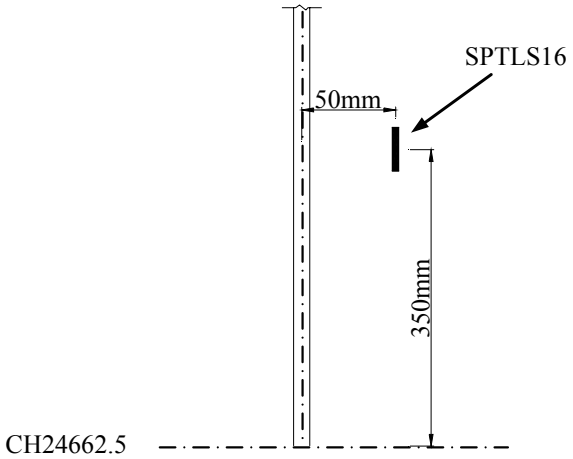

(b)

Figure 6.4 Location of strain gauge SPTLS16 on deck cross-section CH24662.5: (a) Sectional view of Detail H; (b) Sectional view of H1-H1

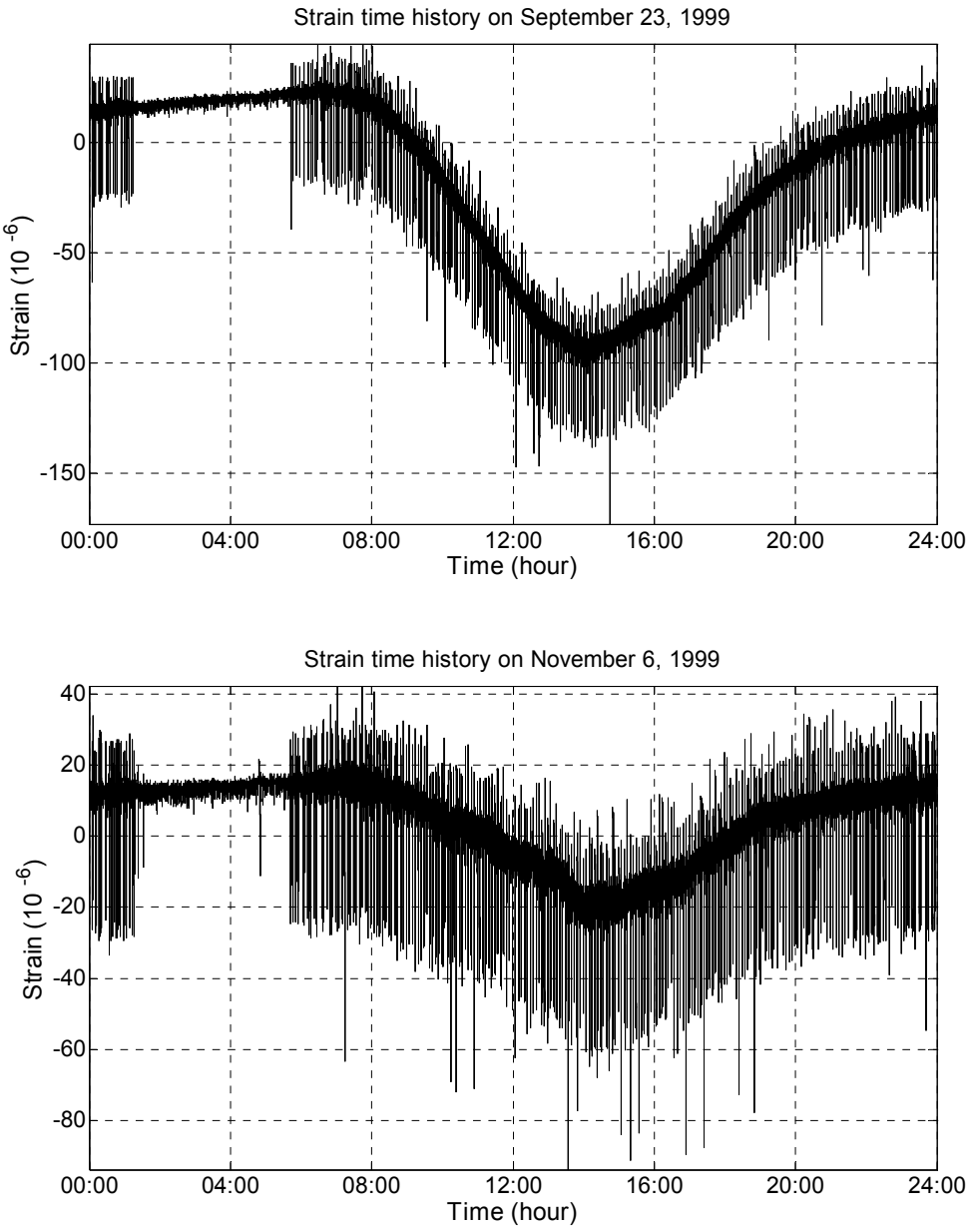

Figure 6.5 Measured daily strain time histories

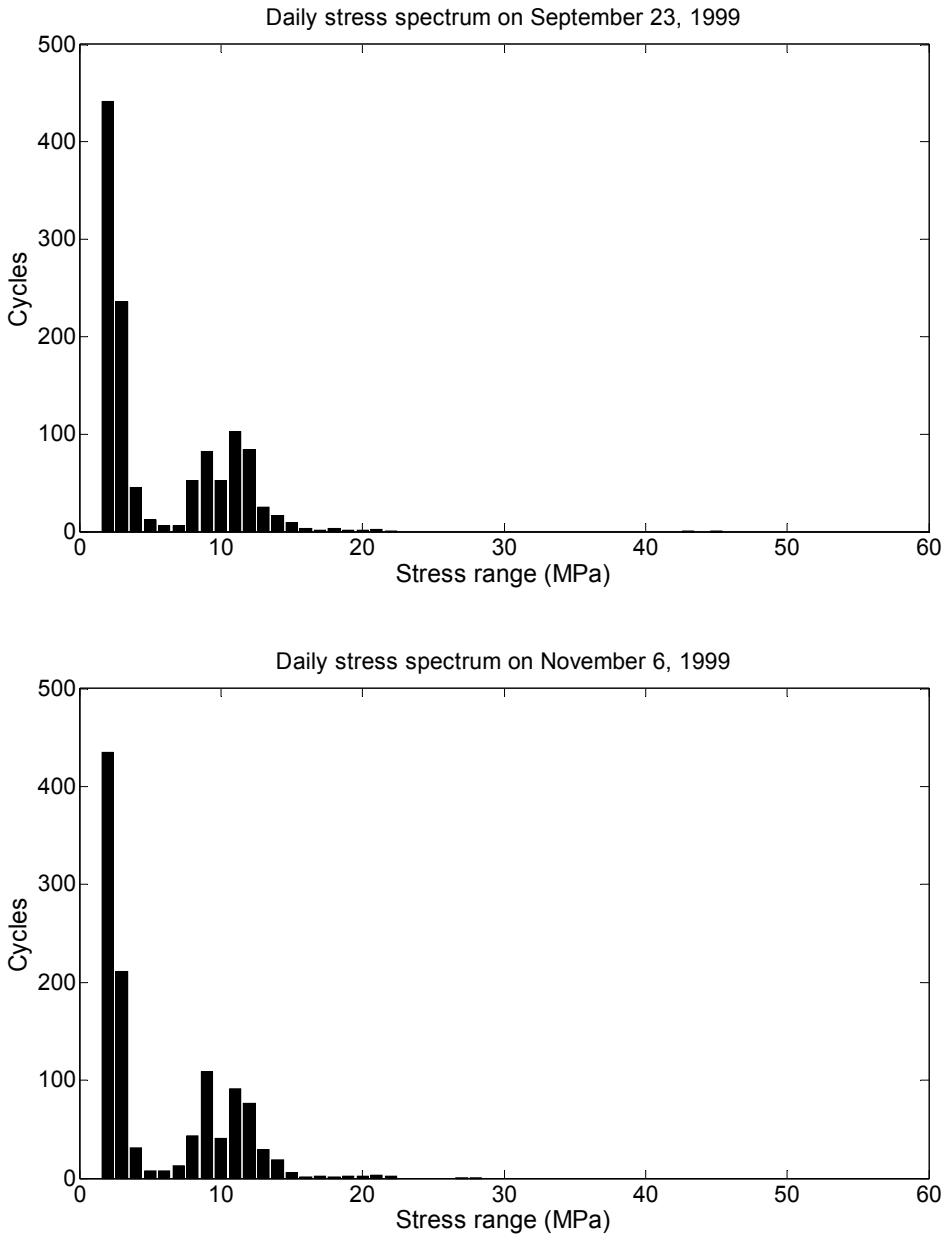

Figure 6.6 Histograms of daily stress spectra

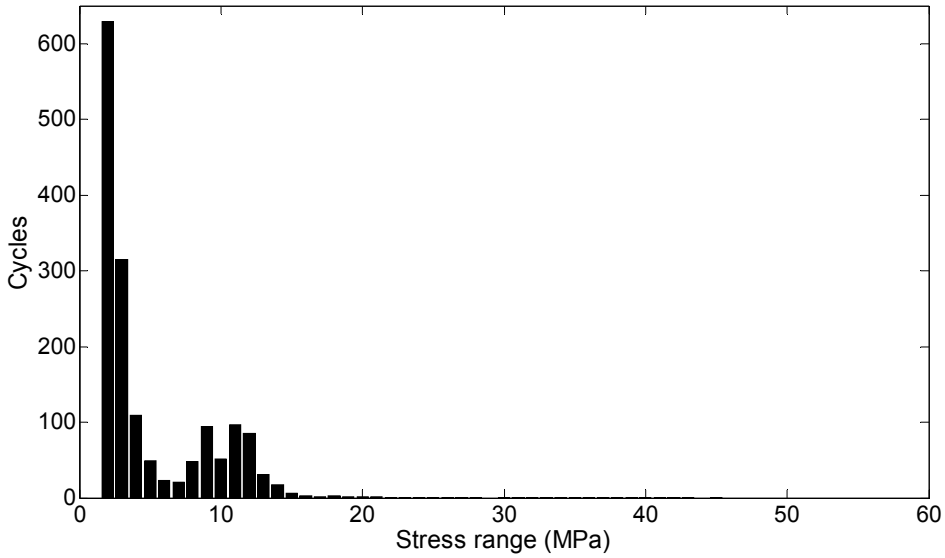

Figure 6.7 Histogram of standard daily stress spectrum

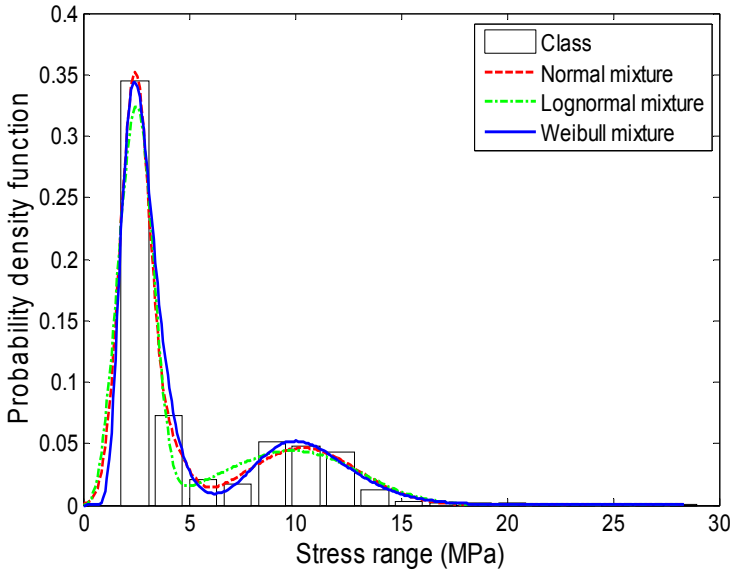

Figure 6.8 Mixed PDFs of 20 days' stress range data

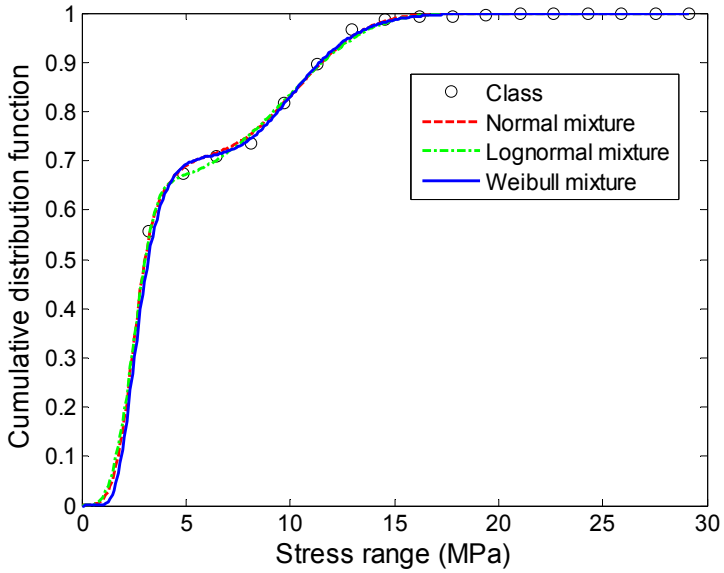

Figure 6.9 Mixed CDFs of 20 days' stress range data

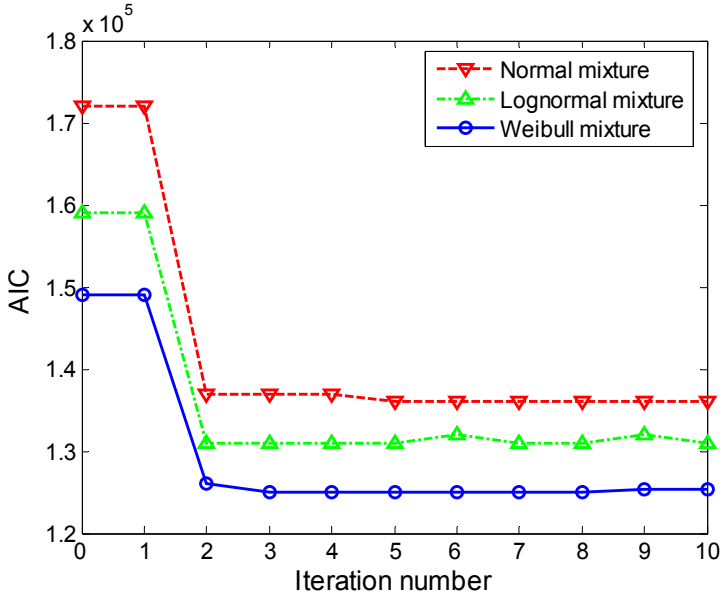

Figure 6.10 AIC values of mixed PDFs of 20 days' stress range data

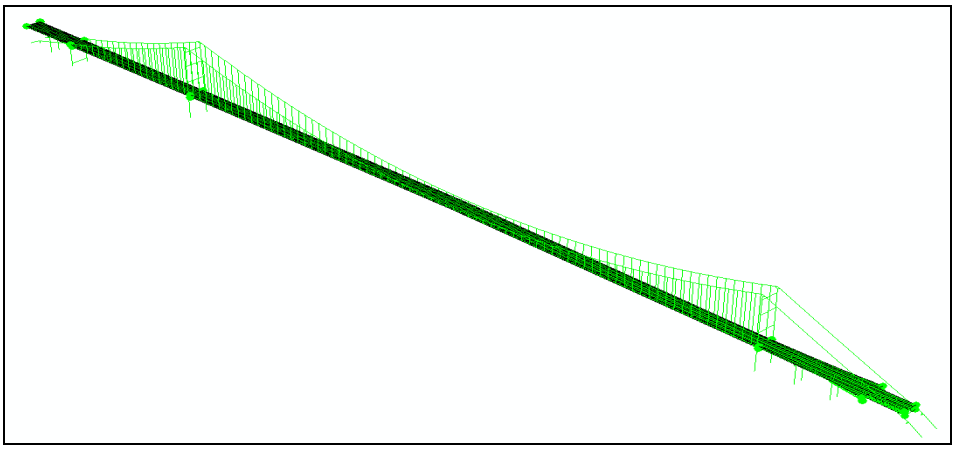

Figure 6.11 Three-dimensional global FEM of TMB

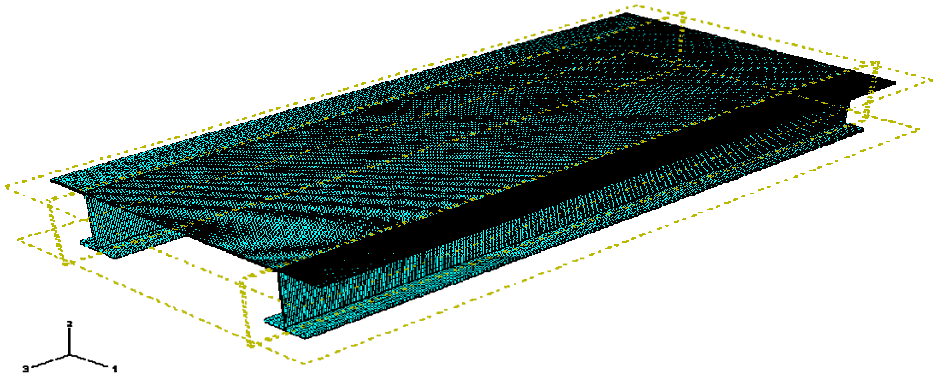

Figure 6.12 Three-dimensional local FEM of welded connections

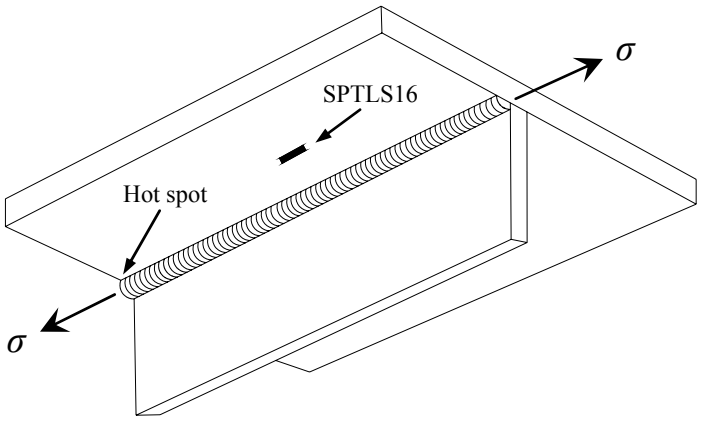

Figure 6.13 Weld stress analysis of welded joint at strain gauge SPTLS16

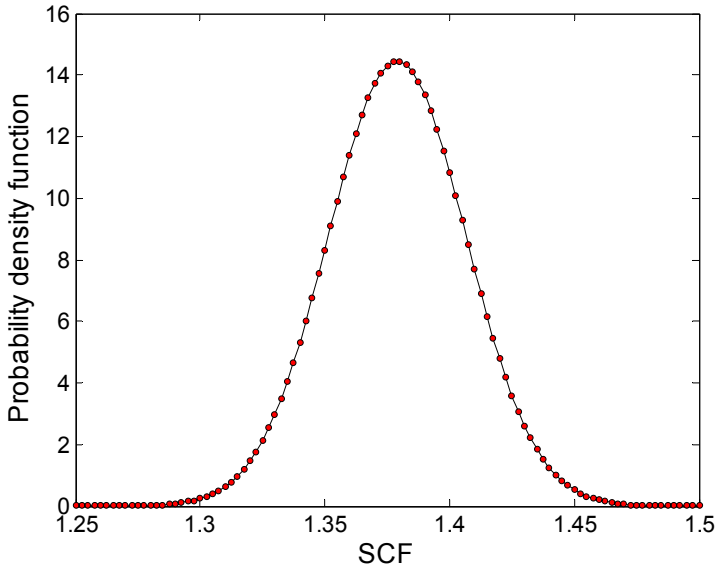

Figure 6.14 PDF of the SCF

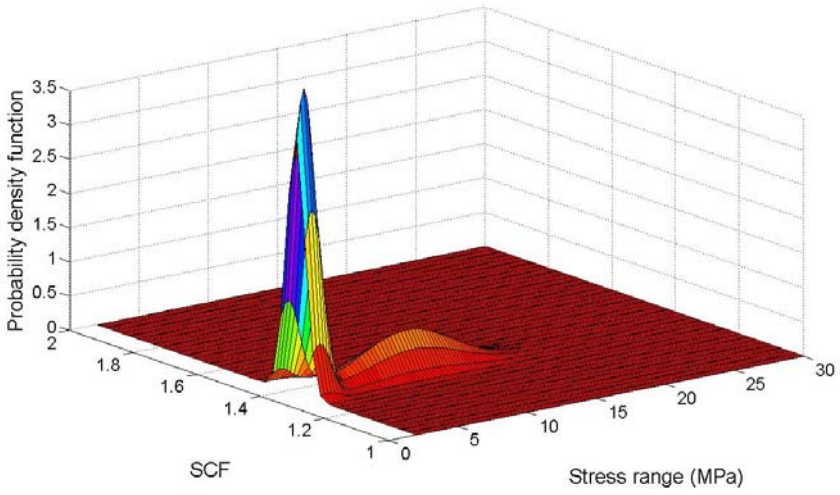

Figure 6.15 Joint PDF of hot spot stress range

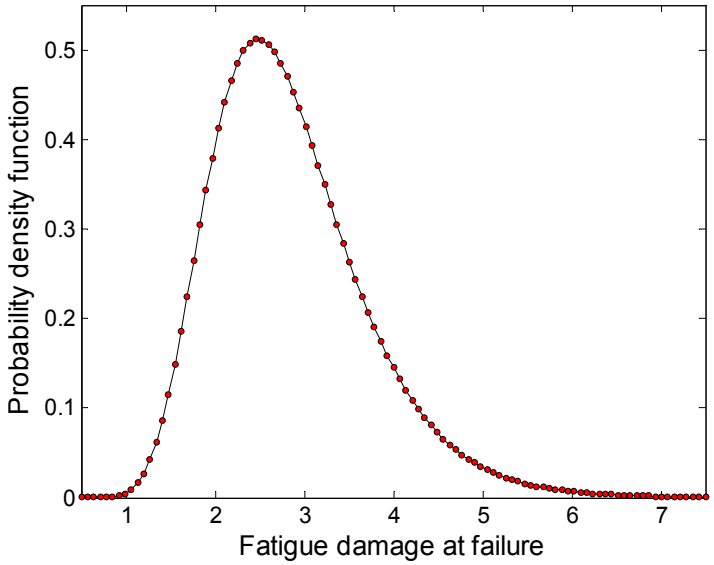

Figure 6.16 PDF of fatigue damage at failure

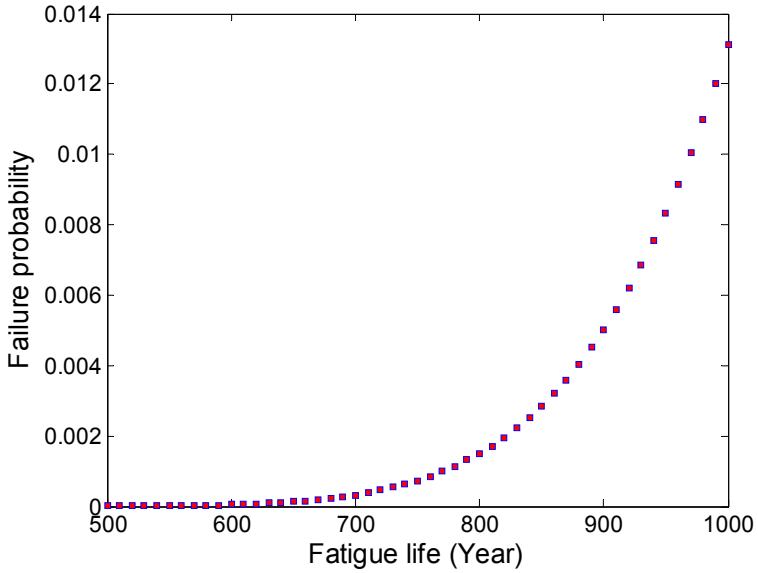

Figure 6.17 Failure probability versus fatigue life

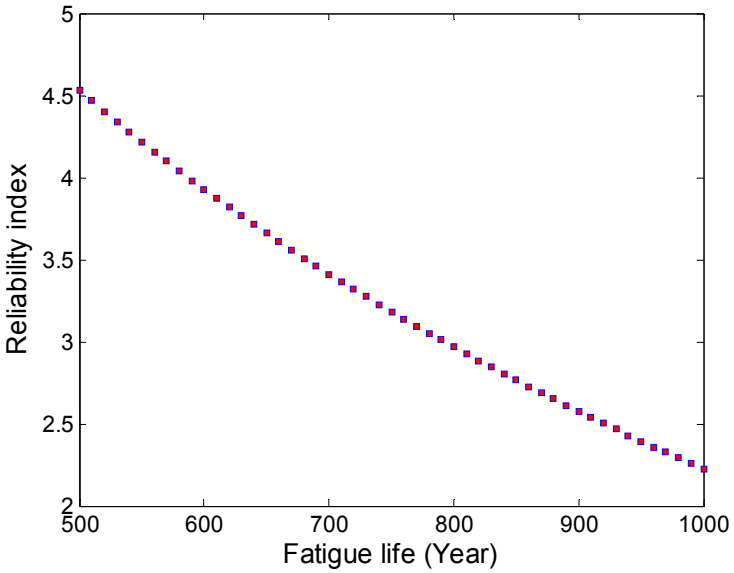

Figure 6.18 Reliability index versus fatigue life

Table 6.1 Reliability index and failure probability versus fatigue life

Expected fatigue life (year)	Reliability index	Failure probability
500	3.565	0.0002
525	3.229	0.0006
550	2.892	0.0019
575	2.556	0.0053
600	2.220	0.0132
625	1.883	0.0299
650	1.547	0.0609
675	1.233	0.1088
700	0.920	0.1788

Table 6.2 Estimated parameters of component distributions from 20 days' stress range data

Parametric family	Weight (w_l)	Mean value (μ_l)	Standard deviation (σ_l)
Normal	0.603	2.428	0.698
	0.304	10.373	2.611
	0.093	4.046	0.842
Lognormal	0.711	0.991	0.322
	0.289	2.351	0.216
Weibull		Shape parameter (θ_l)	Shape parameter (β_l)
	0.651	2.751	3.537
	0.349	10.854	3.584

CHAPTER 7

CONCLUSIONS AND RECOMMENDATIONS

7.1 Conclusions

Long-term SHM technologies have emerged creating an exciting new research field within various branches of engineering such as civil and structural engineering, electrical engineering, computer science, applied physics, and surveying and geo-informatics. Successful implementation and operation of long-term SHM system on large-scale engineering structures such as long-span bridges and high-rise buildings have been widely reported (DeWolf *et al*. 2002; Chong *et al*. 2003; Lynch *et al*. 2006; Ansari 2007; Wang 2008; Katsikeros and Labeas 2009; Ni *et al*. 2009). A crucial issue in the field of SHM is concerning how to effectively excavate feature information from huge amounts of monitoring data for conducting the structural health condition and safety assessment and further resulting in improved operational efficiency of structures, safety or reliability enhancement, and lower maintenance costs. The research efforts in this study have devoted to bridging the gap between SHM technologies and structural condition assessment practices focusing on integrating the strain monitoring data into fatigue life and reliability assessment of

steel bridges instrumented with long-term SHM system.

By adopting diversiform research methodologies in theoretical modeling, numerical simulation, and experimental investigation, this thesis seeks to address the issues of *S-N* approach-based fatigue life assessment, multi-modal stress spectrum modeling, SCF determination and stochastic characterization, and reliability-based fatigue life assessment by making use of long-term monitoring data. The research aims have been to (i) develop a deterministic *S-N* curve-based method for evaluating fatigue life of steel bridges using long-term monitoring data; (ii) propose a procedure for modeling the PDF of stress range and joint PDF of rainflow stress matrix by use of the method of finite mixture distributions in conjunction with a hybrid mixture parameter estimation approach; (iii) experimentally investigate the method of SCF determination for the welded bridge T-joint and the probability distribution and stochastic properties of the SCF for fatigue reliability analysis and assessment, (iv) propose a method for probability-based fatigue life assessment by regarding the daily number of stress cycles of a specified stress range is a random variable with the aid of long-term monitoring data, (v) propose a fatigue reliability model by integrating the probability distribution of hot spot stress range with a continuous probabilistic formulation of the Miner's damage accumulative rule. The major contributions of the work are as follows.

(1) Development of a method for monitoring-based fatigue life assessment

The contribution of this stage of study lies in developing a standard daily stress spectrum method for conducting monitoring-based fatigue life assessment of steel bridges instrumented with long-term SHM system. The specific findings and conclusions are as follows:

(i) It is reasonable to assess the fatigue life of steel bridges with a standard daily stress spectrum obtained by averaging a sufficient number of daily strain data. In the process of creating a standard daily stress spectrum, the measurement data under normal traffic and wind conditions as well as typhoon effects should be taken into consideration; while the optimal number of daily strain data is determined by carefully examining the significant factors that may affect the predicted fatigue life, such as the influence of weekend and workday traffic variations and seasonal changes in traffic patterns; and

(ii) By conducting fatigue life assessment of the TMB with the proposed method, it is concluded that strain data acquired from 20 days including one day under typhoon conditions are adequate for constructing a standard daily stress spectrum. The evaluation results show that the fatigue damage is mainly caused by the traffic loading rather than typhoons, and the predicted fatigue life for the fatigue-prone location is much longer than the design life of the bridge.

(2) Establishment of a procedure for modeling stress spectrum

The contribution of this stage of study is to establish a procedure for generating the

multi-modal PDF of rainflow-counted stress spectrum data from the long-term monitoring data by use of the method of finite mixture distributions in conjunction with a hybrid mixture parameter estimation approach. The specific findings and conclusions are as follows:

(i) The obtained field-data-based stress spectrum exhibits multi-modal behavior due to different load effects, and a conventional parametric distribution model fails to adequately depict the multi-modal behavior. The method of finite mixture distributions in combination with a hybrid mixture parameter estimation algorithm has been adopted to deal with this issue and demonstrated its competence in modeling the stress spectrum derived from the long-term measurement strain data of the TMB; and

(ii) The modeling analysis results show that the Weibull mixture distributions give the best performance in modeling the rainflow-counted stress range, and a fairly good agreement is observed between the obtained distribution functions and the measurement data; while a mixture of multivariate Weibull-normal distributions has been testified to be suitable for modeling the stress matrix that contains the stress range and mean stress. The achieved results provide a powerful tool for fatigue reliability analysis of steel bridges instrumented with long-term SHM system.

(3) Investigation of determination of SCF and its stochastic properties

The contribution of this stage of study is to investigate the method of SCF

determination of typical welded bridge T-joints and stochastic SCF characterization through experiments of full-scale model for a segment of railway beam of the TMB. The specific findings and conclusions are as follows:

(i) In determination of the SCF for typical welded joints through model experiments, considerable effects and sources of uncertainties are involved in geometrical and material properties, weld irregularity and quality, implementation of strain sensors, and load cases and combinations, so that the achieved SCFs exhibit highly scattered. To recognize the stochastic properties of SCF, the use of the theory of probability and statistics as well as the technique of statistical hypothesis test are extremely essential; and

(ii) By conducting full-scale model experiments for a segment of railway beam of the TMB under various weight and velocity combinations of the moving load, the statistical properties and probability distribution of SCF for the typical welded joint are accomplished and attested to conforming to a normal distribution. The results achieved from this study serve as an effective experimental validation of stochastic SCF characterization.

(4) Development of reliability-based fatigue life assessment methods

One contribution of this stage of study is the development of a method for probabilistic assessment of fatigue life by treating the daily number of stress cycles of a specified stress range as a random variable. By use of the Miner's damage accumulative rule and long-term measurement strain data of the TMB, the proposed

method is well applied to predict the mean value, standard deviation, and probability distribution of the fatigue life, and to evaluate the reliability index and failure probability for an expected fatigue life.

Another contribution of this stage of this study is to propose a fatigue reliability model by uniquely integrating the probability distribution of hot spot stress range with a continuous probabilistic formulation of the Miner's rule. The developed probabilistic model is successfully applied to carry out probabilistic fatigue life assessment of the TMB by use of long-term strain monitoring data accounting for highway and railway traffic, typhoons, and stress concentration effects. The achieved results reveal that the service fatigue life significantly affects the probability of failure or reliability index of the welded detail in concern, and the reliability index decreases dramatically when the service life requirement is increased.

7.2 Recommendations

The established methods for fatigue life and reliability assessment of steel bridges are still preliminary and in its infancy, more thorough research is expected to improve the proposed methods for benefiting bridge authorities on fatigue reliability assessment and further actions on fatigue-related inspection, maintenance, and management. The recommendations for future research and exploration are as follows.

(1) Establishment of a linkage between *S-N* approach and fracture mechanics method

The fatigue process is regarded as comprising three phases: crack initiation, crack propagation, and final fracture failure. In general, two different approaches are mainly used to conduct fatigue analysis, namely, the *S-N* approach and the fracture mechanics method. Usually, as can be seen from the majority of references, the two methods are used sequentially and independently, with the *S-N* approach being used at the design or preliminary assessment stage in combination with the Miner's damage accumulation rule and the fracture mechanics method for more refined remaining life prediction or inspection interval and repair schedule estimation based on crack growth models and fracture failure criteria (Chryssanthopoulos and Righiniotis 2006).

The definition of criteria of failure is not always clear when a fatigue analysis is based on the *S-N* approach, usually either initiation of a crack at defined size or complete fracture, in other words for the first and the whole three stages respectively. On the other hand, a fatigue analysis based on the fracture mechanics method is concerned primarily with the second stage, though it can be extended to include final fracture failure through the introduction of appropriate limit state criteria related to fracture resistance which could be expressed in terms of a critical crack size. The majority of engineers are more familiar with the *S-N* approach for fatigue damage and life evaluation rather than the fracture mechanics method which is increasingly

developed. Therefore, it is desirable and essential to develop compatible methodologies to bridge a linkage between the *S-N* approach and the fracture mechanics method. A viable way to deal with this issue is through establishing a relationship between the fatigue crack growth model in the context of fracture mechanics and the fatigue damage model in the *S-N* approach based on the common parameters of stress cycles (Lassen and Sorensen 2002a,b).

(2) Development of methods for time-dependent fatigue reliability assessment using long-term monitoring data and Bayesian theory

Bayesian theory is a powerful and feasible tool to improve the model and parameter distribution as new data are available, and it can combine pre-existing knowledge with subsequent available information and update the prior knowledge of all the uncertainty including mechanical model uncertainty, probability model uncertainty, and statistical uncertainty (Bernardo and Smith 1994). As more and more information becomes available, one tends to get a more accurate model and parameter distribution information for the problem. Several studies have been reported to incorporate the information from field inspection to update fatigue reliability (Madsen 1987; Zhao *et al*. 1994b; Zheng and Ellingwood 1998; Zhang and Mahadevan 2001).

The development and implementation of SHM systems make it possible to collect huge amounts of data from field measurement and create a situation where statistical methods can be increasingly useful and model improvement can be further developed.

It would be interesting to have failure probability at different times as then the time-development of the load/strength model could be established. Time-dependent reliability analyses such as those by Thoft-Christensen (1992), Rajasankar *et al.* (2003) and others can be used as decision-making tools, or to provide additional information on which to enact inspection, maintenance, and repair strategies (Stewart *et al.* 2001). Therefore, in the writer's opinion, it is deserved to make more research efforts on how to update the fatigue damage condition and its reliability based on long-term monitoring data in combination with Bayesian theory.

(3) Investigation of wireless fatigue monitoring system for on-line fatigue life assessment of existing steel bridges

A robust SHM system capable of accurately detecting and localizing damage requires a dense network of sensors installed throughout the structure. For such a system the cost of installing wires to connect the sensors to a centralized monitoring station can run into thousands of dollars per sensing channel (Nagayama and Spencer 2007). Alternatively, replacing tethered sensors with low-cost wireless sensor nodes can substantially reduce system costs to a few hundred dollars or less per sensing channel (Lynch *et al.* 2008); this is a significant saving, especially for systems requiring a large number of nodes. State-of-the-art reviews of the development and research of wireless sensing systems for SHM applications have been made by Spencer *et al.* (2004), Lynch and Loh (2006), Glaser *et al.* (2007), and Lynch (2007).

At present, wireless sensing suites costing only a few hundred dollars per sensing

node and accommodating open-reprogramming functions have been commercially available (Adler *et al*. 2005), and are becoming low-cost alternatives to traditional wired sensing systems. The advanced wireless sensing technologies make it possible to integrate data-driven fatigue life assessment algorithms into the wireless units (microprocessors). Developing such a wireless fatigue monitoring system has a great potential to be commercialized and can be implemented to existing steel bridges for assessing the remaining fatigue life. In the writer's opinion, this issue is promising and should be further studied since lots of aged railway bridges are reaching or have exceeded their original design life.

REFERENCES

AASHTO (1990), *Guide Specifications for Fatigue Evaluation of Existing Steel Bridges*, American Association of State Highway and Transportation Officials, Washington D.C., USA.

Abdou, S., Zhang, W.Z., and Fisher, J.W. (2003), "Orthotropic deck fatigue investigation at Triborough Bridge", *Transportation Research Record 1845*, Transportation Research Board, Washington D.C., USA, 153-162.

Achenbach, J.D. (2000), "Quantitative nondestructive evaluation", *International Journal of Solids and Structures*, Vol. 37, No. 1-2, 13-27.

Adler, R., Flanigan, M., Huang, J., Kling, R., Kushalnagar, N., Nachman, L., Wan, C.-Y., and Yarvis, M. (2005), "Intel Mote 2: an advanced platform for demanding sensor network applications", *Proceedings of the 3rd International Conference on Embedded networked sensor systems*, San Diego, USA, 298-298.

Agerskov, H., and Nielsen, J.A. (1999), "Fatigue in steel highway bridges under random loading", *Journal of Structural Engineering*, ASCE, Vol. 125, No. 2, 152-162.

AISC (1986), *Load and Resistance Factor Design Specifications for Structural Steel Buildings*, American Institute of Steel Construction, Chicago, USA.

Akaike, H. (1974), "A new look at the statistical model identification", *IEEE*

Transactions on Automatic Control, Vol. 19, No. 6, 716-723.

Alampalli, S., and Lund, R. (2006), "Estimating fatigue life of bridge components using measured strains", *Journal of Bridge Engineering*, ASCE, Vol. 11, No. 6, 725-736.

Albrecht, P., and Lenwari, A. (2009), "Variable-amplitude fatigue strength of structural steel bridge details: review and simplified model", *Journal of Bridge Engineering*, ASCE, Vol. 14, No. 4, 226-237.

Al-Emrani, M. (2005), "Fatigue performance of stringer-to-floor-beam connections in riveted railway bridges", *Journal of Bridge Engineering*, ASCE, Vol. 10, No. 2, 179-185.

Al-Rubaie, K.S. (2008), "A general model for stress-life fatigue prediction", *Materialwissenschaft und Werkstofftechnik*, Vol. 39, No. 6, 400-406.

Amanullah, M., Siddiqui, N.A., Umar, A., and Abbas, H. (2002), "Fatigue reliability analysis of welded joints of a TLP tether system", *Steel and Composite Structures*, Vol. 2, No. 5, 331-354.

Ang, A.H.S., Cheung, M.C., Shugar, T.A., and Fernie, J.D. (2001), "Reliability-based fatigue analysis and design of floating structures", *Marine Structures*, Vol. 14, No. 1, 25-36.

Ang, A.H.S., and DeLeon, D. (2005), "Modeling and analysis of uncertainties for risk-informed decisions in infrastructures engineering", *Structure and Infrastructure Engineering*, Vol. 1, No. 1, 19-31.

Ang, A.H.S., and Munse, W.H. (1975), "Practical reliability basis for structural

fatigue", *Proceedings of the ASCE National Structural Engineering Conference*, New York, USA.

Ang, A.H.S., and Tang, W.H. (1975), Probability Concepts in Engineering Planning and Design, Volume I: Basic Principles, Wiley, New York, USA.

Ang, A.H.S., and Tang, W.H. (1984), Probability Concepts in Engineering Planning and Design, Volume II: Decision, Risk, and Reliability, Wiley, New York, USA.

Ansari, F. (2007), "Practical implementation of optical fiber sensors in civil structural health monitoring", *Journal of Intelligent Material Systems and Structures*, Vol. 18, No. 8, 879-889.

API (1993), "Recommended practice for planning, designing, and constructing fixed offshore platforms", *APIRP2A-LRFD*, American Petroleum Institute, Washington D.C., USA.

ASCE Committee on Fatigue and Fracture Reliability (1982a), "Fatigue reliability: introduction", *Journal of the Structural Division*, ASCE, Vol. 108, No. 1, 3-23.

ASCE Committee on Fatigue and Fracture Reliability (1982b), "Fatigue reliability: quality assurance and maintainability", *Journal of the Structural Division*, ASCE, Vol. 108, No. 1, 25-46.

ASCE Committee on Fatigue and Fracture Reliability (1982c), "Fatigue reliability: variable amplitude loading", *Journal of the Structural Division*, ASCE, Vol. 108, No. 1, 47-69.

ASCE Committee on Fatigue and Fracture Reliability (1982d), “Fatigue reliability: development of criteria for design”, *Journal of the Structural Division*, ASCE, Vol. 108, No. 1, 71-88.

AWS (1998), “Structural welding code-steel”, *ANSI/AWS D1.1-98*, American Welding Society, Miami, USA.

Ayyub, B.M., Assakkaf, I.A., Kihl, D.P., and Siev, M.W. (2002), “Reliability-based design guidelines for fatigue of ship structures”, *Naval Engineers Journal*, Vol. 114, No. 2, 113-138.

Ayyub, B.M., and McCuen, R.H. (2003), Probability, Statistics, and Reliability for Engineers and Scientists, 2nd edition, Chapman & Hall/CRC, Boca Raton, USA.

Balageas, D., Fritzen, C.P., and Guemes, A. (2006), Structural Health Monitoring, ISTE, London, England.

Barth, A.S.G., and Bowman, M.D. (2001), “Fatigue behavior of welded diaphragm-to-beam connections”, *Journal of Structural Engineering*, ASCE, Vol. 127, No. 10, 1145-1152.

Basquin, O.H. (1910), “The exponential law of endurance tests”, *Proceedings of American Society for Testing and Materials*, Vol. 10, 625-630.

Benjamin, J.R. (1970), Probability, Statistics and Decision for Civil Engineers, McGraw-Hill, New York, USA.

Bernard, K.J., Culmo, M.P., and DeWolf, J.T. (1997), “Strain monitoring to evaluate steel bridge connections”, *Building to Last: Proceedings of Structures*

Congress XV, edited by L. Kempner, Jr. and C.B. Brown, ASCE, Reston, USA, 919-923.

Bernardo, J.M., and Smith, A.F.M. (1994), Bayesian Theory, Wiley, New York, USA.

Bian, L.C., and Lim, J.K. (2003), "Fatigue strength and stress concentration factors of CHS-to-RHS T-joints", *Journal of Constructional Steel Research*, Vol. 59, No. 5, 627-640.

Bishop, C.M. (1995), Neural Networks for Pattern Recognition, Clarendon Press, Oxford, England.

Brownjohn, J.M.W. (2007), "Structural health monitoring of civil infrastructure", *Philosophical Transactions of the Royal Society A*, Vol. 365, No. 1851, 589-622.

BSI (1980), *BS5400: Steel, Concrete and Composite Bridges, Part 10: Code of Practice for Fatigue*, British Standards Institution, London, England.

BSI (1993), *BS7608: Code of Practice for Fatigue Design and Assessment of Steel Structures*, British Standards Institution, London, England.

Byers, W.G., Marley, M.J., Mohammadi, J., Nielsen, R.J., and Sarkani, S. (1997a), "Fatigue reliability reassessment procedures: state-of-the-art paper", *Journal of Structural Engineering*, ASCE, Vol. 123, No. 3, 271-276.

Byers, W.G., Marley, M.J., Mohammadi, J., Nielsen, R.J., and Sarkani, S. (1997b), "Fatigue reliability reassessment applications: state-of-the-art paper", *Journal of Structural Engineering*, ASCE, Vol. 123, No. 3, 277-285.

Casciati, F. (2003), "An overview of structural health monitoring expertise within the

European Union", *Structural Health Monitoring and Intelligent Infrastructure*, edited by Z.S. Wu and M. Abe, Balkema, Lisse, Netherlands, 31-37.

CEN (1992), *Eurocode 3: Design of Steel Structures, Part 1.1: General Rules and Rules for Buildings, ENV 1993-1-1*, European Committee for Standardization, Brussels, Belgium.

Chajes, M.J., Shenton, H.W., and O'Shea, D. (2000), "Bridge-condition assessment and load rating using nondestructive evaluation methods", *Transportation Research Record 1696*, Transportation Research Board, Washington D.C., USA, 83-91.

Chajes, M.J., and Mertz, D.R. (2003), "Fracture analysis and retrofit design for the I-95 bridge over the Brandywine River", *Recent Developments in Bridge Engineering*, edited by K.M. Mahmoud, Balkema, Lisse, Netherlands, 205-220.

Chakraborty, S., and DeWolf, J.T. (2006), "Development and implementation of a continuous strain monitoring system on a multi-girder composite steel bridge", *Journal of Bridge Engineering*, ASCE, Vol. 11, No. 6, 753-762.

Chan, T.H.T., Li, Z.X., and Ko, J.M. (2001), "Fatigue analysis and life prediction of bridges with structural health monitoring data-part II: application", *International Journal of Fatigue*, Vol. 23, No. 1, 55-64.

Chan, T.H.T., Guo, L., and Li, Z.X. (2003), "Finite element modeling for fatigue stress analysis of large suspension bridges", *Journal of Sound and Vibration*, Vol.

261, No. 3, 443-464.

Chan, T.H.T., Zhou, T.Q., Li, Z.X., and Guo, L. (2005), “Hot spot stress approach for Tsing Ma Bridge fatigue evaluation under traffic using finite element method”, *Structural Engineering and Mechanics*, Vol. 19, No. 3, 261-279.

Chang, P.C., Flatau, A., and Liu, S.C. (2003), “Health monitoring of civil infrastructure”, *Structural Health Monitoring*, Vol. 2, No. 3, 257-267.

Cheung, M.S., Tadros, G.S., Dilger, W.H., Ghali, A., and Lau, D.T. (1997), “Field monitoring and research on performance of Confederation Bridge”, *Canadian Journal of Civil Engineering*, Vol. 24, No. 6, 951-962.

Chiew, S.P., Lie, S.T., Lee, C.K., and Huang, Z.W. (2004), “Fatigue performance of cracked tubular T joints under combined loads. I: experimental”, *Journal of Structural Engineering*, ASCE, Vol. 130, No. 4, 562-571.

Chiew, S.P., Lee, C.K., Lie, S.T., and Ji, H.L. (2007), “Fatigue behaviors of square-to-square hollow section T-joint with corner crack. I: experimental studies”, *Engineering Fracture Mechanics*, Vol. 74, No. 5, 703-720.

Cho, H.N., Lim, J.K., and Choi, H.H. (2001), “Reliability-based fatigue failure analysis for causes assessment of a collapsed steel truss bridge”, *Engineering Failure Analysis*, Vol. 8, No. 4, 311-324.

Chong, K.P., Carino, N.J., and Washer, G. (2003), “Health monitoring of civil infrastructures”, *Smart Materials and Structures*, Vol. 12, No. 3, 483-493.

Chotickai, P., and Bowman, M.D. (2006), “Truck models for improved fatigue life predictions of steel bridges”, *Journal of Bridge Engineering*, ASCE, Vol.

11, No. 1, 71-80.

Chryssanthopoulos, M.K., and Righiniotis, T.D. (2006), “Fatigue reliability of welded steel structures”, *Journal of Constructional Steel Research*, Vol. 62, No. 11, 1199-1209.

Chung, H.Y., Manuel, L., and Frank, K.H. (2003), “Reliability-based optimal inspection for fracture-critical steel bridge members”, *Transportation Research Record 1845*, Transportation Research Board, Washington D.C., USA, 39-47.

Chung, H.Y., Manuel, L., and Frank, K.H. (2006), “Optimal inspection scheduling of steel bridges using nondestructive testing techniques”, *Journal of Bridge Engineering*, ASCE, Vol. 11, No. 3, 305-319.

Connor, R.J. (2004), “Influence of cutout geometry on stresses at welded rib-to-diaphragm connections in steel orthotropic bridge decks”, *Transportation Research Record 1892*, Transportation Research Board, Washington D.C., USA, 78-87.

Connor, R.J., and Fisher, J.W. (2001), “Results of field measurements on the Williamsburg Bridge orthotropic deck”, *ATLSS Report No. 01-01*, Department of Civil and Environmental Engineering, Lehigh University, USA.

Connor, R.J., and Fisher, J.W. (2006), “Consistent approach to calculating stresses for fatigue design of welded rib-to-web connections in steel orthotropic bridge decks”, *Journal of Bridge Engineering*, ASCE, Vol. 11, No. 5, 517-525.

Connor, R.J., Richards, S.O., and Fisher, J.W. (2003), “Long-term remote monitoring of prototype orthotropic deck panels on the Bronx-Whitestone Bridge for fatigue evaluation”, *Recent Developments in Bridge Engineering*, edited by K.M. Mahmoud, Balkema, Lisse, Netherlands, 257-268.

Crespo-Minguillon, C., and Casas, J.R. (1998), “Fatigue reliability analysis of prestressed concrete bridges”, *Journal of Structural Engineering*, ASCE, Vol. 124, No. 12, 1458-1466.

Cui, W. (2002), “A state-of-the-art review on fatigue life prediction methods for metal structures”, *Journal of Marine Science and Technology*, Vol. 7, No. 1, 43-56.

Das, P.C. (1998), “Application of reliability analysis in bridge management”, *Engineering Structures*, Vol. 20, No. 11, 957-959.

Deoliya, R., and Datta, T.K. (2001), “Fatigue reliability analysis of microwave antenna towers due to wind”, *Journal of Structural Engineering*, ASCE, Vol. 127, No. 10, 1221-1230.

Desjardins, S.L., Londono, N.A., Lau, D.T., and Khoo, H (2006), “Real-time data processing, analysis and visualization for structural monitoring of the confederation bridge”, *Advances in Structural Engineering*, Vol. 9, No. 1, 141-157.

DeWolf, J.T., Lindsay, T.R., and Culmo, M.P. (1997), “Fatigue evaluations in steel bridges using field monitoring equipment”, *Building to Last: Proceedings of Structures Congress XV*, edited by L. Kempner, Jr. and C.B. Brown,

ASCE, Reston, USA, 26-30.

DeWolf, J.T., Lauzon, R.G., and Culmo, M.P. (2002), "Monitoring bridge performance", *Structural Health Monitoring*, Vol. 1, No. 2, 129-138.

Ditlevsen, O., and Madsen, H.O. (1996), Structural Reliability Methods, John Wiley & Sons, New York, USA.

Doerk, O., Fricke, W., and Weissenborn, C. (2003), "Comparison of different calculation methods for structural stresses at welded joints", *International Journal of Fatigue*, Vol. 25, No. 5, 359-369.

Dong, P. (2001), "A structural stress definition and numerical implementation for fatigue analysis of welded joints", *International Journal of Fatigue*, Vol. 23, No. 10, 865-876.

Dowling, N.E. (1972), "Fatigue failure predictions for complicated stress-strain histories", *Journal of Materials*, Vol. 7, No. 1, 71-87.

Downing, S.D., and Socie, D.F. (1982), "Simple rainflow counting algorithms", *International Journal of Fatigue*, Vol. 4, No. 1, 31-40.

Duda, R.O., and Hart, P.E. (1973), Pattern Classification and Scene Analysis, Wiley, New York, USA.

ECCS (1985), *Recommendations for the Fatigue Design of Steel Structures*, European Convention for Constructional Steelwork, Brussels, Belgium.

Ellingwood, B.R. (1982), "Fatigue reliability", *Journal of the Structural Division*, ASCE, Vol. 108, No. 1, 3-23.

Engesvik, K.M., and Moan, T. (1983), "Probabilistic analysis of the uncertainty in

the fatigue capacity of welded joints", *Engineering Fracture Mechanics*, Vol. 18, No. 4, 743-762.

Ermopoulos, J., and Spyrakos, C.C. (2006), "Validated analysis and strengthening of a 19th century railway bridge", *Engineering Structures*, Vol. 28, No. 5, 783-792.

Estes, A.C., and Frangopol, D.M. (2005), "Reliability-based condition assessment", *Structural Condition Assessment*, edited by R.T. Ratay, Wiley, New Jersey, USA, 25-66.

Feng, M. Q. (2009), "Application of structural health monitoring in civil infrastructure", *Smart Structures and Systems*, Vol. 5, No. 4, 469-482.

Fisher, J.W. (1984), Fatigue and Fracture in Steel Bridges: Case Studies, Wiley, New York, USA.

Flint and Neil Partnership (1998), *Lantau Fixed Crossing and Ting Kau Bridge, Wind and Structural Health Monitoring System – Criticality and Vulnerability Ratings Review*, Highways Department, Government of Hong Kong Special Administrative Region, Hong Kong, China.

Frangopol, D.M., Ghosn, M., Hearn, G., and Nowak, A.S. (1998), "Structural reliability in bridge engineering", *Journal of Bridge Engineering*, ASCE, Vol. 3, No. 4, 151-154.

Frangopol, D.M., and Imai, K. (2000), "Geometrically nonlinear finite element reliability analysis of structural systems. II: applications", *Computers and Structures*, Vol. 77, No. 6, 693-709.

Freudenthal, A.M. (1947), “Safety of structures”, *Transactions of ASCE*, Vol. 112, 125-180.

Fricke, W. (2003), “Fatigue analysis of welded joints: state of development”, *Marine Structures*, Vol. 16, No. 3, 185-200.

Fujino, Y. (2002), “Vibration, control and monitoring of long-span bridges: recent research, developments and practice in Japan”, *Journal of Constructional Steel Research*, Vol. 58, No. 1, 71-97.

Fung, T.C., Soh, C.K., Chan, T.K., and Erni (2002), “Stress concentration factors of doubler plate reinforced tubular T joints”, *Journal of Structural Engineering*, ASCE, Vol. 128, No. 11, 1399-1412.

Gandhi, P., and Berge, S. (1998), “Fatigue behavior of T-joints: square chords and circular braces”, *Journal of Structural Engineering*, ASCE, Vol. 124, No. 4, 399-404.

Gao, F., Shao, Y.B., and Gho, W.M. (2007), “Stress and strain concentration factors of completely overlapped tubular joints under lap brace IPB load”, *Journal of Constructional Steel Research*, Vol. 63, No. 5, 305-316.

Ghidini, T., and Dalle Donne, C. (2009), “Fatigue life predictions using fracture mechanics methods”, *Engineering Fracture Mechanics*, Vol. 76, No. 1, 134-148.

Gho, W.M., Fung, T.C., and Soh, C.K. (2003), “Stress and strain concentration factors of completely overlapped tubular K(N) joints”, *Journal of Structural Engineering*, ASCE, Vol. 129, No. 1, 21-29.

Glaser, S.D., Li, H., Wang, M.L., Ou, J., and Lynch, J. (2007), "Sensor technology innovation for the advancement of structural health monitoring: a strategic program of US-China research for the next decade", *Smart Structures and Systems*, Vol. 3, No. 2, 221-244.

Goode, J.S., and van de Lindt, J.W. (2007), "Development of a semiprescriptive selection procedure for reliability-based fatigue design of high-mast lighting structural supports", *Journal of Performance of Constructed Facilities*, ASCE, Vol. 21, No. 3, 193-206.

Gurney, T.R. (1979), Fatigue of Welded Structures, 2nd edition, Cambridge University Press, Cambridge, England.

Hahin, C., South, J.M., Mohammadi, J., and Polepeddi, R.K. (1993), "Accurate and rapid determination of fatigue damage in steel bridges", *Journal of Structural Engineering*, ASCE, Vol. 119, No. 1, 150-168.

Haldar, A., and Mahadevan, S. (2000a), Probability, Reliability, and Statistical Methods in Engineering Design, John Wiley & Sons, New York, USA.

Haldar, A., and Mahadevan, S. (2000b), Reliability Assessment Using Stochastic Finite Element Analysis, John Wiley & Sons, New York, USA.

Han, S.H., and Shin, B.C. (2000), "The use of hot spot stress for estimating the fatigue strength of welded components", *Steel Research*, Vol. 71, No. 11, 466-473.

Hobbacher, A. (1996), "Fatigue design of welded joints and components", *IIW Doc. XIII-1539-96/XV-845-96*, Abington Publishing, Cambridge, England.

Hurtado, J.E. (2004), Structural Reliability: Statistical Learning Perspectives, Springer,

New York, USA.

Ibrahim, S.A., El-Dakhakhni, W.W., and Elgaaly, M. (2006a), “Fatigue of corrugated-web plate girders: experimental study”, *Journal of Structural Engineering*, ASCE, Vol. 132, No. 9, 1371-1380.

Ibrahim, S.A., El-Dakhakhni, W.W., and Elgaaly, M. (2006b), “Fatigue of corrugated-web plate girders: analytical study”, *Journal of Structural Engineering*, ASCE, Vol. 132, No. 9, 1381-1392.

Iida, K. (1984), “Application of the hot spot strain concept to fatigue life prediction”, *Welding in the World*, Vol. 22, No. 9-10, 222-247.

IIW (2000), “Fatigue design procedures for welded hollow section joints”, *IIW Doc. XIII-1804-99/XV-1035-99, Recommendations for IIW subcommision XV-E*, Abington Publishing, Cambridge, England.

Imai, K., and Frangopol, D.M. (2000), “Geometrically nonlinear finite element reliability analysis of structural systems. I: theory”, *Computers and Structures*, Vol. 77, No. 6, 677-691.

Imam, B.M., Righiniotis, T.D., Chryssanthopoulos, M.K. (2008), “Probabilistic fatigue evaluation of riveted railway bridges”, *Journal of Bridge Engineering*, ASCE, Vol. 13, No. 3, 237-244.

Jakubczak, H., Sobczykiewicz, W., and Glinka, G. (2006), “Fatigue reliability of structural components”, *International Journal of Materials and Product Technology*, Vol. 25, No. 1-3, 64-83.

Jiao, G., and Moan, T. (1992), “Reliability-based fatigue and fracture design criteria

for welded offshore structures", *Engineering Fracture Mechanics*, Vol. 41, No. 2, 271-282.

Kaczinski, M.R., Stokes, F.E., Lugger, P., and Fisher, J.W. (1997), "Williamsburg Bridge, orthotropic deck fatigue tests", *ATLSS Report No. 97-04*, Department of Civil and Environmental Engineering, Lehigh University, USA.

Karamanos, S.A., Romeijn, A., and Wardenier, J. (2000), "Stress concentrations in tubular DT-joints for fatigue design", *Journal of Structural Engineering*, ASCE, Vol. 126, No. 11, 1320-1330.

Katsikeros, Ch.E., and Labeas, G.N. (2009), "Development and validation of a strain-based structural health monitoring system", *Mechanical Systems and Signal Processing*, Vol. 23, No. 2, 372-383.

Kececioglu, D. (1991a), Reliability Engineering Handbook, Volume 1, Prentice-Hall, Englewood Cliffs, USA.

Kececioglu, D. (1991b), Reliability Engineering Handbook, Volume 2, Prentice-Hall, Englewood Cliffs, USA.

Kim, S.H., Lee, S.W., and Mha, H.S. (2001), "Fatigue reliability assessment of an existing steel railroad bridge", *Engineering Structures*, Vol. 23, No. 10, 1203-1211.

Kiss, K., and Dunai, L. (2002), "Fracture mechanics based fatigue analysis of steel bridge decks by two-level cracked models", *Computers and Structures*, Vol. 80, No. 29, 2321-2331.

Ko, J.M. (2004), “Structural health monitoring of large scale bridge: research and experience”, *Progress in Structural Engineering, Mechanics and Computation*, edited by A. Ziongni, Balkema, Leiden, Netherlands, 20-30.

Ko, J.M., and Ni, Y.Q. (2005), “Technology developments in structural health monitoring of large-scale bridges”, *Engineering Structures*, Vol. 27, No. 12, 1715-1725.

Koh, H.M., Cho, J.F., Kim, S.K., and Kim, C.Y. (2003), “Recent application and development of structural health monitoring systems and intelligent structures in Korea”, *Structural Health Monitoring and Intelligent Infrastructure*, edited by Z.S. Wu and M. Abe, Balkema, Lisse, Netherlands, 99-111.

Kottegoda, N.T., and Rosso, R. (1997), Statistics, Probability, and Reliability for Civil and Environmental Engineers, McGraw-Hill, New York, USA.

Laman, J.A., and Nowak, A.S. (1996), “Fatigue-load models for girder bridges”, *Journal of Structural Engineering*, ASCE, Vol. 122, No. 7, 726-733.

Lassen, T., and Sorensen, J. D. (2002a), “A probabilistic damage tolerance concept for welded joints. part 1: data base and stochastic modelling”, *Marine Structures*, Vol. 15, No. 6, 599-613.

Lassen, T., and Sorensen, J. D. (2002b), “A probabilistic damage tolerance concept for welded joints. part 2: a supplement to the rule based *S-N* approach”, *Marine Structures*, Vol. 15, No. 6, 615-626.

Lee, O.S., Kim, D.H., and Park, Y.C. (2008), “Reliability of structures by using

probability and fatigue theories", *Journal of Mechanical Science and Technology*, Vol. 22, No. 4, 672-682.

Li, Z.X., Chan, T.H.T., and Ko, J.M. (2001), "Fatigue analysis and life prediction of bridges with structural health monitoring data-part I: methodology and strategy", *International Journal of Fatigue*, Vol. 23, No. 1, 45-53.

Li, Z.X., Chan, T.H.T., and Ko, J.M. (2002), "Evaluation of typhoon induced fatigue damage for Tsing Ma Bridge", *Engineering Structures*, Vol. 24, No. 8, 1035-1047.

Li, Z.X., Chan, T.H.T., and Zheng, R. (2003), "Statistical analysis of online strain response and its application in fatigue assessment of a long-span steel bridge", *Engineering Structures*, Vol. 25, No. 14, 1731-1741.

Lie, S.T., Chiew, S.P., Lee, C.K., and Huang, Z.W. (2004), "Fatigue performance of cracked tubular T joints under combined loads. II: numerical", *Journal of Structural Engineering*, ASCE, Vol. 130, No. 4, 572-581.

Liu, P.L., and Der Kiureghian, A. (1991), "Finite element reliability of geometrically nonlinear uncertain structures", *Journal of Engineering Mechanics*, ASCE, Vol. 117, No. 8, 1806-1825.

Liu, Y., Liu, L., Stratman, B., and Mahadevan, S. (2008), "Multiaxial fatigue reliability analysis of railroad wheels", *Reliability Engineering and System Safety*, Vol. 93, No. 3, 456-467.

Loren, S. (2004), "Estimating fatigue limit distributions under inhomogeneous stress conditions", *International Journal of Fatigue*, Vol. 26, No. 11,

1197-1205.

Lotsberg, I. (1998), “Stress concentration factors at circumferential welds in tubulars”, *Marine Structures*, Vol. 11, No. 6, 207-230.

Lotsberg, I., and Landet, E. (2005), “Fatigue capacity of side longitudinals in floating structures”, *Marine Structures*, Vol. 18, No. 1, 25-42.

Lukic, M., and Cremona, C. (2001), “Probabilistic assessment of welded joints versus fatigue and fracture”, *Journal of Structural Engineering*, ASCE, Vol. 127, No. 2, 211-218.

Lund, R., and Alampalli, S. (2004), “Estimation fatigue life of Patroon Island Bridge using strain measurements”, *REPORT FHWA/NY/SR-04/142*, Transportation Research and Development Bureau, New York State Department of Transportation, New York, USA.

Lynch, J.P. (2007), “An overview of wireless structural health monitoring for civil structures”, *Philosophical Transactions of the Royal Society A*, Vol. 365, No. 1851, 345-372.

Lynch, J.P., and Loh, K.J. (2006), “A summary review of wireless sensors and sensor networks for structural health monitoring”, *The Shock and Vibration Digest*, Vol. 38, No. 2, 91-128.

Lynch, J.P., Wang, Y., Loh, K.J., Yi, J.-H., and Yun, C.-B. (2006), “Performance monitoring of the Geumdang Bridge using a dense network of high-resolution wireless sensors”, *Smart Materials and Structures*, Vol. 15, No. 6, 1561-1575.

Lynch, J.P., Swartz, R.A., and Zimmerman, A.T. (2008), "Distributed data processing architectures for structural monitoring systems implemented on wireless sensor networks", *Proceedings of the 4th European Workshop on Structural Health Monitoring*, edited by T. Uhl, W. Ostachowicz and J. Holnicki-Szulc, DEStech Publications, Lancaster, USA, 21-32.

MacDougall, C., Green, M.F., and Shillinglaw, S. (2006), "Fatigue damage of steel bridges due to dynamic vehicle loads", *Journal of Bridge Engineering*, ASCE, Vol. 11, No. 3, 320-328.

Maddox, S.J. (1991), Fatigue Strength of Welded Structures, Abington Publishing, Cambridge, England.

Madsen, H.O. (1984), "Bayesian fatigue life prediction", *Proceedings of International Symposium on Probabilistic Method in the Mechanics of Solids and Structures*, edited by S. Eggwertz and N.C. Lind, Springer-Verlag, Berlin, Germany, 395-406.

Madsen, H.O. (1987), "Model updating in reliability theory", *Proceedings of International Conference on Advances in Solidification Processes-5*, Vancouver, Canada, 564-577.

Malm, R., and Andersson, A. (2006), "Field testing and simulation of dynamic properties of a tied arch railway bridge", *Engineering Structures*, Vol. 28, No. 1, 143-152.

Mann, J.Y. (1970, 1978, 1983, 1990), Bibliography on the Fatigue of Materials, Components and Structures, Volumes 1 to 4, Pergamon Press, Oxford,

England.

Mashiri, F.R., Zhao, X.L., and Grundy, P. (2002), “Fatigue tests and design of welded T connections in thin cold-formed square hollow sections under in-plane bending”, *Journal of Structural Engineering*, ASCE, Vol. 128, No. 11, 1413-1422.

Mashiri, F.R., Zhao, X.L., and Grundy, P. (2004a), “Stress concentration factors and fatigue behaviour of welded thin-walled CHS-SHS T-joints under in-plane bending”, *Engineering Structures*, Vol. 26, No. 13, 1861-1875.

Mashiri, F.R., Zhao, X.L., and Grundy, P. (2004b), “Stress concentration factors and fatigue failure of welded T-connections in circular hollow sections under in-plane bending”, *International Journal of Structural Stability and Dynamics*, Vol. 4, No. 3, 403-422.

Matos, J. C., Garcia, O., Henriques, A.A., Casas, J.R., and Vehi, J. (2009), “Health monitoring system (HMS) for structural assessment”, *Smart Structures and Systems*, Vol. 5, No. 3, 223-240.

Matsuishi, M., and Endo, T. (1968), “Fatigue of metals subjected to varying stress”, *Japan Society of Mechanical Engineers*, 37-40.

McLachlan, G.J., and Peel, D. (2000), Finite Mixture Models, Wiley, New York, USA.

Miki, C., and Tateishi, K. (1997), “Fatigue strength of cope hole details in steel bridges”, *International Journal of Fatigue*, Vol. 19, No. 6, 445-455.

Miner, M.A. (1945), “Cumulative damage in fatigue”, *Journal of Applied Mechanics*, ASME, Vol. 12, No. 3, 159-164.

Mita, A. (1999), “Emerging needs in Japan for health monitoring technologies in civil and building structures”, *Structural Health Monitoring 2000*, edited by F.K. Chang, Technomic, Lancaster, USA, 56-68.

Mohammadi, J. (1995), “Fatigue reliability analysis using field data”, *Restructuring: America and Beyond: Proceedings of Structures Congress XIII*, edited by M. Snayei, ASCE, Reston, USA, 1570-1573.

Mohammadi, J., Guralnick, S.A., and Polepeddi, R. (1998), “Bridge fatigue life estimation from field data”, *Practice Periodical on Structural Design and Construction*, ASCE, Vol. 3, No. 3, 128-133.

Mohammadi, J., and Polepeddi, R. (2000), “Bridge rating with consideration for fatigue damage from overloads”, *Journal of Bridge Engineering*, ASCE, Vol. 5, No. 3, 259-265.

Mohammadi, J. (2001), “Input data requirements for fatigue reliability analysis of aging structures”, *Proceedings of the 2001 Structures Congress and Exposition*, edited by P.C. Chang, ASCE, Reston, USA (CD-ROM).

Morgan, M.R., and Lee, M.M.K. (1997), “New parametric equations for stress concentration factors in tubular K-joints under balanced loading”, *International Journal of Fatigue*, Vol. 19, No. 4, 309-317.

Morgan, M.R., and Lee, M.M.K. (1998a), “Stress concentration factors in tubular K-joints under in-plane moment loading”, *Journal of Structural Engineering*, ASCE, Vol. 124, No. 4, 382-390.

Morgan, M.R., and Lee, M.M.K. (1998b), “Parametric equations for distributions of

stress concentration factors in tubular K-joints under out-of-plane moment loading", *International Journal of Fatigue*, Vol. 20, No. 6, 449-461.

Moses, F., Lebet, J.P., and Bez, R. (1994), "Applications of field testing to bridge evaluation", *Journal of Structural Engineering*, ASCE, Vol. 120, No. 6, 1754-1763.

Moses, F., Schilling, C.G., and Raju, K.S. (1987), "Fatigue evaluation procedures for steel bridges", *NCHRP Report No. 299*, Transportation Research Board, Washington D.C., USA.

Mufti, A.A. (2002), "Structural health monitoring of innovative Canadian civil engineering structures", *Structural Health Monitoring*, Vol. 1, No. 1, 89-103.

Murty, A.S.R., Gupta, U.C., and Krishna, A.R. (1995), "A new approach to fatigue strength distribution for fatigue reliability evaluation", *International Journal of Fatigue*, Vol. 17, No. 2, 85-89.

Nagayama, T., and Spencer Jr., B.F. (2007), "Structural health monitoring using smart sensors", *Report No. NSEL-001*, Newmark Structural Engineering Laboratory, Department of Civil and Environmental Engineering, University of Illinois at Urbana-Champaign, Urbana, USA.

Nagode, M., and Fajdiga, M. (1998), "A general multi-modal probability density function suitable for the rainflow ranges of stationary random processes," *International Journal of Fatigue*, Vol. 20, No. 3, 211-223.

Nagode, M., Klemenc, J., and Fajdiga, M. (2001), "Parametric modeling and scatter

prediction of rainflow matrices", *International Journal of Fatigue*, Vol. 23, No. 6, 525-532.

Nagode, M., Bucar, T., and Fajdiga, M. (2006), "Normal, lognormal and Weibull mixture estimation", *Proceedings of the European Safety and Reliability Conference*, Estoril, Portugal, 935-942.

Nagode, M., and Fajdiga, M. (2006), "An alternative perspective on the mixture estimation problem", *Reliability Engineering and System Safety*, Vol. 91, No. 4, 388-397.

Nazir, M., Khan, F., and Amyotte, P. (2008), "Fatigue reliability analysis of deep water rigid marine risers associated with Morison-type wave loading", *Stochastic Environmental Research and Risk Assessment*, Vol. 22, No. 3, 379-390.

Ni, Y.Q., Chen, G., Ye, X.W., and Ko, J.M. (2006a), "Fatigue life assessment of a suspension bridge using long-term monitoring data", *Proceedings of the 4th World Conference on Structural Control and Monitoring*, San Diego, USA (CD-ROM).

Ni, Y.Q., Xia, H.W., and Ko, J.M. (2008), "Structural performance evaluation of Tsing Ma Bridge deck using long-term monitoring data", *Modern Physics Letters B*, Vol. 22, No. 11, 875-880.

Ni, Y.Q., Xia, Y., Liao, W.Y. and Ko, J.M. (2009), "Technology innovation in developing the structural health monitoring system for Guangzhou New TV Tower", *Structural Control and Health Monitoring*, Vol. 16, No. 1,

73-98.

Ni, Y.Q., Ye, X.W., and Ko, J.M. (2006b), “Fatigue reliability analysis of a suspension bridge using long-term monitoring data”, *Key Engineering Materials*, Vol. 321-323, 223-229.

Niemi, E. (1995), “Stress determination for fatigue analysis of welded components”, *IIS/IIW-1221-93*, Abington Publishing, Cambridge, England.

Niemi, E., Fricke, W., and Maddox, S.J. (2003), “Structural hot-spot stress approach to fatigue analysis of welded components”, *IIW Doc. XIII-1819-00/XV-1090-01/ XIII-WG3-06-99*, International Institute of Welding, Villeurbanne, France.

Nowak, A.S., and Szerszen, M.M. (1999), “Fatigue reliability of steel girder bridges”, *Structural Engineering in the 21st Century: Proceedings of the 1999 Structures Congress*, edited by R.R. Avent and M. Alawady, ASCE, Reston, USA, 255-258.

Ou, J.P. (2004), “The state-of-the-art and application of intelligent health monitoring systems for civil infrastructure in mainland of China”, *Progress in Structural Engineering, Mechanics and Computation*, edited by A. Ziongni, Balkema, Leiden, Netherlands, 599-608.

Pang, N.L., Zhao, X.L., Mashiri, F.R., and Dayawansa, P. (2009), “Full-size testing to determine stress concentration factors of dragline tubular joints”, *Engineering Structures*, Vol. 31, No. 1, 43-56.

Park, Y.H., and Tang, J. (2006), “An efficient methodology for fatigue reliability

analysis for mechanical components", *Journal of Pressure Vessel Technology*, ASME, Vol. 128, No. 3, 293-297.

Park, Y.S., Han, S.Y., and Suh, B.C. (2005), "Fatigue reliability of steel bridge welding member by fracture mechanics method", *Structural Engineering and Mechanics*, Vol. 19, No. 3, 347-359.

Peil, U. (2005), "Assessment of bridges via monitoring", *Structure and Infrastructure Engineering*, Vol. 1, No. 2, 101-117.

Peil, U., and Mehdianpour, M. (2000), "Fatigue prediction of bridges by monitoring and parallel testing", *Bridge Management 4: Inspection, Maintenance, Assessment and Repair*, edited by M.J. Ryall, G.A.R. Parke and J.E. Harding, Thomas Telford, London, England, 145-153.

Peil, U., and Mehdianpour, M. (2000), "Fatigue prediction of bridges by monitoring and parallel testing", *Bridge Management 4: Inspection, Maintenance, Assessment and Repair*, edited by M.J. Ryall, G.A.R. Parke and J.E. Harding, Thomas Telford, London, England, 145-153.

Peil, U., Mehdianpour, M., and Frenz, M. (2001), "Fatigue prediction of steel structures by means of monitoring and testing", *Life-Cycle Cost Analysis and Design of Civil Infrastructure Systems*, edited by D.M. Frangopol and H. Furuta, ASCE, Reston, USA, 222-238.

Pilkey, W.D. (2008), Peterson's Stress Concentration Factors, 3rd edition, Wiley, New York, USA.

Pines, D.J., and Aktan, A.E. (2002), "Status of structural health monitoring of

long-span bridges in the United States", *Progress in Structural Engineering and Materials*, Vol. 4, No. 4, 372-380.

Pourzeynali, S., and Datta, T.K. (2005), "Reliability analysis of suspension bridges against fatigue failure from the gusting of wind", *Journal of Bridge Engineering*, ASCE, Vol. 10, No. 3, 262-271.

Poutiainen, I., Tanskanen, P., and Marquis, G. (2004), "Finite element methods for structural hot spot stress determination – a comparison of procedures", *International Journal of Fatigue*, Vol. 26, No. 11, 1147-1157.

Puthli, R.S., Wardenier, J., de Koning, C.H.M., van Wingerde, A.M., and van Dooren, F.J. (1988), "Numerical and experimental determination of strain (stress) concentration factors of welded joints between square hollow sections", *HERON*, Vol. 33, No. 2, 1-50.

Rackwitz, R., and Fiessler, B. (1978), "Structure reliability under combined random load sequences", *Computers and Structures*, Vol. 9, No. 5, 489-494.

Radaj, D. (1996), "Review of fatigue strength assessment of non-welded and welded structures based on local parameters", *International Journal of Fatigue*, Vol. 18, No. 3, 153-170.

Radaj, D., Sonsino, C.M., and Fricke, W. (2006), Fatigue Assessment of Welded Joints by Local Approaches, 2nd edition, Abington Publishing, Cambridge, England.

Rajasankar, J., Iyer, N.R., and Appa Rao, T.V.S.R. (2003), "Structural integrity assessment of offshore tubular joints based on reliability analysis",

International Journal of Fatigue, Vol. 25, No. 7, 609-619.

Raju, K.S., Moses, F., and Schilling, C.G. (1990), "Reliability calibration of fatigue evaluation and design procedures", *Journal of Structural Engineering*, ASCE, Vol. 116, No. 5, 1356-1369.

Reed, R.P., Smith, J.H., and Christ, B.W. (1983), "The economic effects of fracture in the United States", *Special Publication 647-1*, National Bureau of Standards, U.S. Department of Commerce, Gaithersburg, USA.

Richardson, S., and Green, P.J. (1997), "On Bayesian analysis of mixtures with an unknown number of components", *Journal of the Royal Statistical Society: Series B*, Vol. 59, No. 4, 731-792.

Ricles, J.M., and Leger, P. (1993), "Marine component fatigue reliability", *Journal of Structural Engineering*, ASCE, Vol. 119, No. 7, 2215-2234.

Righiniotis, T.D., and Chryssanthopoulos, M.K. (2003), "Probabilistic fatigue analysis under constant amplitude loading", *Journal of Constructional Steel Research*, Vol. 59, No. 7, 867-886.

Roeder, C.W., MacRae, G., Crocker, P., Arima, K., and Wong, S. (2000), "Dynamic response and fatigue of steel tied-arch bridge", *Journal of Bridge Engineering*, ASCE, Vol. 5, No. 1, 14-21.

Russo, F.M., Wipf, T.J., and Klaiber, F.W. (2000), "Diagnostic load tests of a prestressed concrete bridge damaged by overheight vehicle impact", *Transportation Research Record 1696*, Transportation Research Board, Washington D.C., USA, 103-110.

Sartor, R.R., Culmo, M.P., and Dewolf, J.T. (1999), “Short-term strain monitoring of bridge structures”, *Journal of Bridge Engineering*, ASCE, Vol. 4, No. 3, 157-164.

Savaidis, G., and Vormwald, M. (2000), “Hot-spot stress evaluation of fatigue in welded structural connections supported by finite element analysis”, *International Journal of Fatigue*, Vol. 22, No. 2, 85-91.

Schilling, C.G., Klippstein, K.H., Barson, J.M., and Blake, G.T. (1978), “Fatigue of welded steel bridge members under variable-amplitude loadings”, *NCHRP Report No. 188*, Transportation Research Board, Washington D.C., USA.

Schütz, W. (1996), “A history of fatigue”, *Engineering Fracture Mechanics*, Vol. 54, No. 2, 263-300.

Shenton, H.W., Chajes, M.J., Sivakumar, B., and Finch, W.W. (2003), “Field tests and in-service monitoring of Newburgh-Beacon Bridge”, *Transportation Research Record 1845*, Transportation Research Board, Washington D.C., USA, 163-170.

Snoussi, H., and Mohammad-Djafari, A. (2007), “Estimation of structured Gaussian mixtures: the inverse EM algorithm”, *IEEE Transactions on Signal Processing*, Vol. 55, No. 7, 3185-3191.

Sobczyk, K., and Spencer, B.F. (1992), Random Fatigue: from Data to Theory, Academic Press, Boston, USA.

Spencer Jr., B.F., Ruiz-Sandoval, M.E., and Kurata, N. (2004), “Smart sensing technology: opportunities and challenges”, *Structural Control and Health*

Monitoring, Vol. 11, No. 4, 349-368.

Spyrakos, C.C., Raftoyiannis, I.G., and Ermopoulos, J.C. (2004), "Condition assessment and retrofit of a historic steel-truss railway bridge", *Journal of Constructional Steel Research*, Vol. 60, No. 8, 1213-1225.

Steiner, P.M., and Hudec, M. (2007), "Classification of large data sets with mixture models via sufficient EM", *Journal of Computational Statistics and Data Analysis*, Vol. 51, No. 11, 5416-5428.

Stewart, M.G. (2001), "Reliability-based assessment of ageing bridges using risk ranking and life cycle cost decision analyses", *Reliability Engineering and System Safety*, Vol. 74, No. 3, 263-273.

Stephens, R.I., Fatemi, A., Stephens, R.R., and Fuchs, H.O. (2001), Metal Fatigue in Engineering, John Wiley, New York, USA.

Stromeyer, C.E. (1914), "The determination of fatigue limits under alternating stress conditions", *Proceedings of the Royal Society of London: Series A*, Vol. 90, No. 620, 411-425.

Sturges, H.A. (1926), "The choice of a class interval", *Journal of the American Statistical Association*, Vol. 21, No. 153, 65-66.

Suresh, S. (1998), Fatigue of Materials, Cambridge University Press, New York, USA.

Susmel, L., Tovo, R., and Lazzarin, P. (2005), "The mean stress effect on the high-cycle fatigue strength from a multiaxial fatigue point of view", *International Journal of Fatigue*, Vol. 27, No. 8, 928-943.

Szerszen, M.M., Nowak, A.S., and Laman, J.A. (1999), “Fatigue reliability of steel bridges”, *Journal of Constructional Steel Research*, Vol. 52, No. 1, 83-92.

Tang, J., and Zhao, J. (1995), “A practical approach for predicting fatigue reliability under random cyclic loading”, *Reliability Engineering and System Safety*, Vol. 50, No. 1, 7-15.

Thoft-Christensen, P., and Baker, M.J. (1982), Structural Reliability Theory and Its Applications, Springer-Verlag, Berlin, Germany.

Thoft-Christensen, P. (1992), “Advanced bridge management systems”, *Structural Engineering Review*, Vol. 7, No. 3, 151-163.

Titterington, D., Smith, A., and Makov, U. (1985), Statistical Analysis of Finite Mixture Distributions, Wiley, New York, USA.

Tovo, R. (2001), “On the fatigue reliability evaluation of structural components under service loading”, *International Journal of Fatigue*, Vol. 23, No. 7, 587-598.

Tsakopoulos, P.A., and Fisher, J.W. (2002), “Fatigue resistance investigation for the orthotropic deck on the Bronx-Whitestone Bridge”, *ATLSS Report No. 02-05*, Department of Civil and Environmental Engineering, Lehigh University, USA.

van Delft, D.R.V. (1981), “Two dimensional analyses of stress at the vicinity of weld toes of tubular structures”, *Stevin Report 6-81-8*, Stevin Laboratory, Delft University of Technology, Netherlands.

van Wingerde, A.M., Packer, J.A., and Wardenier, J. (1995), “Criteria for the fatigue

assessment of hollow structural section connections", *Journal of Constructional Steel Research*, Vol. 35, No. 1, 71-115.

van Wingerde, A.M., Packer, J.A., and Wardenier, J. (2001), "Simplified SCF formulae and graphs for CHS and RHS K- and KK-connections", *Journal of Constructional Steel Research*, Vol. 57, No. 3, 221-252.

Walker, E.K. (1970), "The effect of stress ratio during crack propagation and fatigue for 2024-T3 and 7075-T6 aluminum", *Effects of Environment and Complex Load History on Fatigue Life*, *ASTM STP 462*, American Society for Testing and Materials, 1-14.

Walker, W.H. (1978), "An interim report on studies of stress histories in highway bridges, volume I and II", *Structural Research Series No. 448, Report No. UIUC-Eng-80-2005*, University of Illinois at Urbana Champaign, Urbana, USA.

Wang, J.Y., Ko, J.M., and Ni, Y.Q. (2000), "Participation of local modes in seismic response of Tsing Ma Suspension Bridge", *Advances in Structual Dynamics*, edited by J.M. Ko and Y.L. Xu, Elsevier Science Ltd., Oxford, UK, Vol. 2, 963-970.

Wang, T.L., Liu, C.H., Huang, D.Z., and Shahawy, M. (2005), "Truck loading and fatigue damage analysis for girder bridges based on weigh-in-motion data", *Journal of Bridge Engineering*, ASCE, Vol. 10, No. 1, 12-20.

Wang, M.L. (2008), "Long term health monitoring of post-tensioning box girder bridges", *Smart Structures and Systems*, Vol. 4, No. 6, 711-726.

Wirsching, P.H. (1984), “Fatigue reliability for offshore structures”, *Journal of Structural Engineering*, ASCE, Vol. 110, No. 10, 2340-2356.

Wirsching, P.H., and Chen, Y.N. (1987), “Fatigue design criteria for TLP tendons”, *Journal of Structural Engineering*, ASCE, Vol. 113, No. 7, 1398-1414.

Wirsching, P.H., and Chen, Y.N. (1988), “Consideration of probability based fatigue design criteria for marine structures”, *Marine Structures*, Vol. 1, No. 1, 23-45.

Wirsching, P.H., and Yao, J.T.P. (1970), “Statistical methods in structural fatigue”, *Journal of the Structural Division*, ASCE, Vol. 96, No. 6, 1201-1219.

Wong, K.Y. (2004), “Instrumentation and health monitoring of cable-supported bridges”, *Structural Control and Health Monitoring*, Vol. 11, No. 2, 91-124.

Wong, K.Y. (2007), “Design of a structural health monitoring system for long-span bridges”, *Structure and Infrastructure Engineering*, Vol. 3, No. 2, 169-185.

Wong, K.Y., and Ni, Y.Q. (2009), “Structural Health Monitoring of Cable-Supported Bridges in Hong Kong”, *Structural Health Monitoring of Civil Infrastructure Systems*, edited by V.M. Karbhari and F. Ansari, Woodhead Publishing, Abington, Cambridge, UK, 371-411.

Wong, M.P. (2005), “Validation of Tsing Ma Bridge influence line coefficients using measurement data”, *Project Report*, Department of Civil and Structural Engineering, The Hong Kong Polytechnic University, Hong Kong.

Xiang, H.F. (2000), “Health monitoring status of long-span bridges in China”, *Proceedings of the International Workshop on Research and Monitoring of Long Span Bridge*, Hong Kong, China, 24-31.

Xiao, Z.G., and Yamada, K. (2004), “A method of determining geometric stress for fatigue strength evaluation of steel welded joints”, *International Journal of Fatigue*, Vol. 26, No. 12, 1277-1293.

Xiao, Z.G., Yamada, K., Inoue, J., and Yamaguchi, K. (2006), “Fatigue cracks in longitudinal ribs of steel orthotropic deck”, *International Journal of Fatigue*, Vol. 28, No. 4, 409-416.

Xu, Y.L., Liu, T.T., and Zhang, W.S. (2009), “Buffeting-induced fatigue damage assessment of a long suspension bridge”, *International Journal of Fatigue*, Vol. 31, No. 3, 575-586.

Yagi, J., Machida, S., Tomita, Y., Matoba, M., and Kawasaki, T. (1991), “Definition of hot spot stress in welded plate type structure for fatigue assessment”, *IIW Doc. XIII-1414-91*, International Institute of Welding, Villeurbanne, France.

Yamada, K., and Albrecht, P. (1976), “Fatigue design of welded bridge details for service stresses”, *Transportation Research Record No. 607*, Transportation Research Board, Washington D.C., USA, 25-30.

Yan, J.H., Zheng, X.L., and Zhao, K. (2000), “Prediction of fatigue life and its probability distribution of notched friction welded joints under variable-amplitude loading”, *International Journal of Fatigue*, Vol. 22, No.

6, 481-494.

Yun, C.B., Lee, J.J., Kim, S.K., and Kim, J.W. (2003), “Recent R&D activities on structural health monitoring for civil infra-structures in Korea”, *Journal of Civil Engineering*, KSCE, Vol. 7, No. 6, 637-651.

Zhang, Q.W., and Zhou, Y. (2007), “Investigation of the applicability of current bridge health monitoring technology”, *Structure and Infrastructure Engineering*, Vol. 3, No. 2, 159-168.

Zhang, R., and Mahadevan, S. (2001), “Fatigue reliability analysis using nondestructive inspection”, *Journal of Structural Engineering*, ASCE, Vol. 127, No. 8, 957-965.

Zhao, J., Tang, J., and Wu, H.C. (2000), “A generalized random variable approach for strain-based fatigue reliability analysis”, *Journal of Pressure Vessel Technology*, ASME, Vol. 122, No. 2, 156-161.

Zhao, Y.X., Gao, Q., and Wang, J.N. (2000), “An approach for determining an appropriate assumed distribution of fatigue life under limited data”, *Reliability Engineering and System Safety*, Vol. 67, No. 1, 1-7.

Zhao, Z., Haldar, A., and Breen, F.L. (1994a), “Fatigue-reliability evaluation of steel bridges”, *Journal of Structural Engineering*, ASCE, Vol. 120, No.5, 1608-1623.

Zhao, Z., Haldar, A., and Breen, F.L. (1994b), “Fatigue reliability updating through inspections of steel bridges”, *Journal of Structural Engineering*, ASCE, Vol. 120, No. 5, 1624-1643.

Zhao, Z., and Haldar, A. (1996), “Bridge fatigue damage evaluation and updating using non-destructive inspections”, *Engineering Fracture Mechanics*, Vol. 53, No. 5, 775-788.

Zheng, R., and Ellingwood, B.R. (1998), “Role of non-destructive evaluation in time dependent reliability analysis”, *Structural Safety*, Vol. 20, No. 4, 325-339.

Zheng, X.L., Lu, B., and Jiang, H. (1995), “Determination of probability distribution of fatigue strength and expressions of P-S-N curves”, *Engineering Fracture Mechanics*, Vol. 50, No. 4, 483-491.

Zhou, Y.E. (2003), “Assessing remaining fatigue life of existing riveted steel bridges”, *Recent Developments in Bridge Engineering*, edited by K.M. Mahmoud, Balkema, Lisse, Netherlands, 193-204.

Zhou, Y.E. (2004), “Fatigue problems in steel bridge structures”, *Securing the Future: Proceedings of the 2004 Structures Congress-Building on the Past*, Nashville, USA, 397-406.

Zhou, Y.E. (2005), “Assessment of bridge remaining fatigue life through field strain measurement”, *Metropolis and Beyond: Proceedings of the 2005 Structures Congress and the 2005 Forensic Engineering Symposium*, New York, USA, 129-139.

Zhou, Y.E. (2006), “Assessment of bridge remaining fatigue life through field strain measurement”, *Journal of Bridge Engineering*, ASCE, Vol. 11, No. 6, 737-744.